ECONOMICS OF CARBON DIOXIDE SEQUESTRATION IN A MATURE OIL FIELD

A THESIS SUBMITTED TO
THE GRADUATE SCHOOL OF NATURAL AND APPLIED SCIENCES

OF
MIDDLE EAST TECHNICAL UNIVERSITY

BY

ALI SUAD RASHEED

IN PARTIAL FULFILLMENT OF THE REQUIREMENTS
FOR
THE DEGREE OF MASTER OF SCIENCE
IN
PETROLEUM AND NATURAL GAS ENGINEERING

DECEMBER 2008

Approval of the thesis:

ECONOMICS OF CARBON DIOXIDE SEQUESTRATION IN A MATURE OIL FIELD

Submitted by **Ali Suad Rasheed** in partial fulfillment of the requirements for the degree of **Master of Science** in **Petroleum and Natural Gas Engineering, Middle East Technical University, by**

Prof. Dr. Canan ÖZGEN ____________________

Dean, Graduate School of **Natural and Applied Sciences**

Prof. Dr. Mahmut PARLAKTUNA ____________________

Head of Department, **Petroleum and Natural Gas Engineering**

Prof. Dr. Serhat AKIN ____________________

Supervisor, **Petroleum and Natural Gas Engineering, METU**

Examining Committee Members:

Prof. Dr. Mahmut PARLAKTUNA

Petroleum and Natural Gas Engineering, METU ____________________

Prof. Dr. Serhat AKIN

Petroleum and Natural Gas Engineering, METU ____________________

Prof. Dr. Mustafa Versan KÖK

Petroleum and Natural Gas Engineering, METU ____________________

Asst. Prof. Dr. Evren ÖZBAYOGLU

Petroleum and Natural Gas Engineering, METU ____________________

Dr. Tayfun Yener UMUCU

Turkish Petroleum Corporation ____________________

Date: ____________________

I hereby declare that all information in this document has been obtained and presented in accordance with academic rules and ethical conduct. I also declare that, as required by these rules and conduct, I have fully cited and referenced all material and results that are not original to this work.

Name, Surname: Ali Suad Rasheed

Signature:

ABSTRACT

ECONOMICS OF CARBON DIOXIDE SEQUESTRATION IN A MATURE OIL FIELD

Ali Suad Rasheed

M.S., Department of Petroleum and Natural Gas Engineering

Supervisor: Prof. Dr. Serhat AKIN

December 2008

155 pages

To meet the goal of atmospheric stabilization of carbon dioxide (CO_2) levels a technological transformation should occur in the energy sector. One strategy to achieve this is carbon sequestration. Carbon dioxide can be captured from industrial sources and sequestered underground into depleted oil and gas reservoirs. CO_2 injected into geological formations, such as mature oil reservoirs can be effectively trapped by hydrodynamical (structural), solution, residual (capillary) and mineral trapping methods.

In this work, a case study was conducted using CMG-STARS software for CO_2 sequestration in a mature oil field. History matching was done with the available production, bottom hole pressures and water cut data to compare the results obtained from the simulator with the field data.

Next, previously developed optimization methods were modified and used for the case of study. The main object of the optimization was to determine the optimal location, number of injection wells, injection rate, injection depth and pressure of

wells to maximize the total trapped amount of CO_2 while enhancing the amount of oil recovered.

A second round of simulations was carried out to study the factors that affect the total oil recovery and CO_2 storage amount. These include relative permeability end points effect, hysteresis effect, fracture spacing and additives of simultaneous injection of carbon dioxide with CO and H_2S. Optimization runs were carried out on a mildly heterogeneous 3D model for variety of cases. When compared with the base case, the optimized case led to an increase of 20% in the amount of oil that is recovered; and more than 95% of the injected CO_2 was trapped as solution gas on and as an immobile gas.

Finally, an investigation of the economical feasibility was accomplished. NPV values for various cases were obtained, selected and studied yielding in a number of cases that are found to be applicable for the field of concern.

Keywards.: CO_2sequestration, mature oil field, CMG-STARS, history matching, optimization, relative permeability end points , hystersis,CO,H_2S, impurity.

ÖZ

OLGUN PETROL SAHALARINDA KABONDİOKSİT TECRİDİNİN EKONOMİSİ

Ali Suad Rasheed

Yüksek Lisans, Petrol ve Doğal Gaz Mühendisliği Bölümü

Tez Yöneticisi Prof. Dr. Serhat AKIN

Aralık 2008

155 sayfa

Atmosferdeki karbondioksit (CO_2) oranının dengelenmesi için, enerji sektöründe teknolojik dönüşümler olmalıdır. Atmosferdeki CO_2 dengesini sağlayacak yöntemlerden birisi de CO_2 tecridir.

Sanayi kaynaklarından ele geçirilen CO_2 yeraltındaki tükenmiş petrol ve doğal gaz rezervuarlarına tecrid edilebilmektedir. Jeolojik formasyonlara (örneğin : tükenmiş petrol rezervuarlarına) basılan CO_2 etkin bir şekilde hidrodinamik , çözelti ve rezidüel (kapiler) yakalanma ve mineral oluşumu ile depolanabilmektedir.

Bu çalışmada, CMG-STARS programı kullanılarak geliştirilmiş bir petrol sahasına CO_2 depolama seneryoları çalışılmıştır. Depolama senoryolarından önce program sonuçları, sahanın üretim, basınç düşümü ve üretilen su oranı verileri kullanılarak tarihsel çakıştırma yapılmıştır.

Sonra , gelişmiş optimizasyon metodları doğrultusunda saha geliştirilmiş ve bu çalışmada kullanılmıştır. Yapılan bu çalışmanın genel amacı, en uygun enjeksiyon yerinin , optimum enjektör kuyu sayısının, enjeksiyon derinliğinin ve debisinin ve kuyu başınçlarının bulunup depolanabilir CO_2 ve üretilebilir petrol miktarının maksimum dereceye çıkarılmasıdır.

Ardından, toplam üretilebilir petrol ve depolanabilir CO_2 miktarını belirleyen parametreleri bulmak ve bu parametrelerin toplam üretilebilir petrol ve depolanabilir CO_2 miktarını nasıl etkilediğini görmek için ikinci bir simülasyon çalışması yapılmıştır. Bu simülasyon çalışmalarında incelenen parametreler göreli geçirgenlik eğrilerinin son noktaları, histerez etkisi, çatlak yoğunluğu ve H_2S /CO gazlarının CO_2 ile eşzamanlı enjekte edilmesidir. Neredeyse homojen yapıda olan 3D model kullanılarak çeşitli simülasyon çalışmaları yapılmış ve bu simulasyon çalışmaları temel alınan simulasyon çalışması ile karşılaştırılmıştır. Optimium simulasyon çalışmalası sonuçlarına göre, üretilebilir petrol miktarında, %20 artma, enjekte edilen CO_2 gazının %95'den fazlası çözünmüş, gaz olarak ve bazı çalışmalar da ise hareketsiz gaz olarak depolandığı görülmüştür.

Son olarak, tüm simülasyon çalışmaları için ekonomik fizibilite çalışmaları NPV'nin hesaplanmasıyla yapılmış ve ekonomik fizibilite çalışmalarının sonucunda sahaya uygulanabilecek en uygun enjeksiyon yöntemleri belirlenmiştir.

Anahtar kelimeler: Karbondioksit tecridi, Karbon depolanması, geliştirilmiş petrol sahası, CMG-STARS, tarihsel çakıştırma, optimizasyon, göreli geçirgenlik eğrilerinin son noktaları, histerez, H_2S /CO katkıları.

This work is dedicated to my brother Murad and my mother Aziza

ACKNOWLEDGEMENTS

Special thanks to all my colleagues in Petroleum Engineering Department who contributed actively to bring together friendliness and scientific excellence in this school that provides moral, and intellectual support to its lucky members. Thanks for having given me the chance to be a part of this team.

I salute the Petroleum Engineering faculty for all I have learned from their teaching and enthusiasm. I personally would like to express my gratitude to my research and academic advisor Dr. Serhat Akın. His encouragement, intelligence and guidance were deeply appreciated throughout the course of this research. It was his vision and optimism that I admired so much as well as his drive for perfection in our research work. Looking back I was truly lucky to have the opportunity to work with such a world class individual.

I would also like to express my deepest gratitude to Dr.Mahmut Parlaktuna for his valuable contributions to this work; Dr.Engin Küçükkaya and my colleague Sultan Anbar for their suggestions which made this a reality.

My love goes to my mother whose presence by my side, even remotely, was my most precious ally during these years at METU. Finally, I want to extend my love to my family who has always been my life, my inspiration, and every happiness.

TABLE OF CONTENTS

LIST OF TABLES

LIST OF FIGURES

NOMENCLATURE

$R_{v/g}$: Ratio between viscous to gravitational forces

υ : Darcy velocity

L : Distance between wells

K : Gas permeability

G : Gravity force

$\Delta\varrho$: Density difference among fluids

H : Height of the displacement zone

M : Mobility Ratio

k_{rg} : Gas relative permeability

k_{ro} :Oil relative permeability

L : Distance between wells

μ_o : Oil velocity

μ_g : Gas viscosity

ΔSg : Difference in residual gas saturation

$k^d rg(o)$: Bounding drainage curve

$k^i rg(o)$: Bounding imbibition curve

$S_{g,norm}$: Normalized gas saturation

E_i : Root mean square error

P : Predicted value by program

T : Target value (RMSE equation)

S_{omax} : Maximum oil saturation

S_{ocrt} : Trapped oil saturation (STARS)

S_{ohmax} : Historical maximum oil saturation

S_{of} : Free oil saturation

S_o : Grid cell oil saturation

S_{orw} : Residual oil saturation for the drainage curve

S_{ocrt} : Inputted maximum trapped oil saturation

S_{gi} : Initial gas saturation

S_{gmax} : Maximum gas saturation

S_{gtmax} : Maximum trapped gas saturation

ABBRIVIATIONS

BHP : Bottom Hole Pressure

CapEx : Capital Expenditures

CMG : Computer Modeling Group

C_{CO2} : Carbon credit

DST : Drill Stem Test

EOR : Enhanced Oil Recovery

GHG : Green House Gases

GSGI : Gravity Stabilizing Gas Injection

IW : Drilling and completion expenditures

MMP : Minimum Miscibility Pressure

NCF : Net Cash Flow

NPV : Net Present Value

OpEx. : Operating Expenditure

Roy : Royalties

RMSE : Root Mean Square Error

T : Corporate tax (Economical model)

TPAO : Turkish Petroleum Corporation

WAG : Water Alternating Gas

CHAPTER 1

INTRODUCTION

Climate change policies involve an in-depth change in the most powerful sector of developed economies: oil and electricity industries. It is because that climate change is rooted to the very essence of humankind development. The developed and developing economies will involve an in-depth change in the oil electricity industries. For this reason, Kyoto Protocol (1997) has ignited so much discussion, but still, the destabilization of our atmosphere has not been prevented, and even less reverted.

Above all, carbon sequestration (also known as CO_2 sequestration) is the most promising technology that could be adapted in the short term for its application. Carbon sequestration has the potential to remove large amounts of CO_2 from the atmosphere by capturing and storing it away for a long time period. Technology for carbon capture is commercially available for large CO_2 emitters like power plants. CO_2 storage is envisaged either in deep geological formations, deep oceans, or in the form of mineral carbonates.

Capturing massive quantities of CO_2, from flue gases in large stationary sources and storing them in geologic formations is considered technically feasible and ecologically convenient to close the fossil fuels life cycle. There are many geologic formations that can store CO_2, such as oil and gas reservoirs, unmineable coal seams, and deep saline aquifers. These are subsurface structures that have stored crude oil, natural gas, brine, and even CO_2 over millions of years.

This research evaluates the effects of many factors on CO_2 sequestration in a light oil field in B Formation. Due to the presence of high permeability channels in the reservoir, the amount of CO_2 that can be injected varies across the field affecting the overall CO_2 storage goals in the project. Thus, a group of factors and their impacts will be considered. History matching and prediction runs where CO_2 storage by means of hydrodynamcial, solution, capillary and mineral trapping methods will be studied. An evaluation of different well completions and cases will be analyzed. Additionally, economical analysis and future cautions will be dealt with.

CHAPTER 2

LITERATURE REVIEW

2.1 CO_2 sequestration and climate change

2.1.1 Evidence of climate change

It has been said that climate change is indicated by the increase in regional and global temperatures along with the changes in the sea level, precipitation, and weather patterns. Many statistics indicate that the global mean temperature has risen 0.45°C since the middle of the 19^{th} century [1]. Furthermore, long term statistics show that if all countries continue with a 'business as usual', an increase in the global mean temperature of 2.7°C will occur by 2100 [2]. Considering accustomed geological age and previous climate alters of the planet Earth, observations show that global temperatures have raised by roughly 0.6°C over a small period of less than 140 years. (Figure 2.1) refers to the change in temperature that took place in last 140 years.

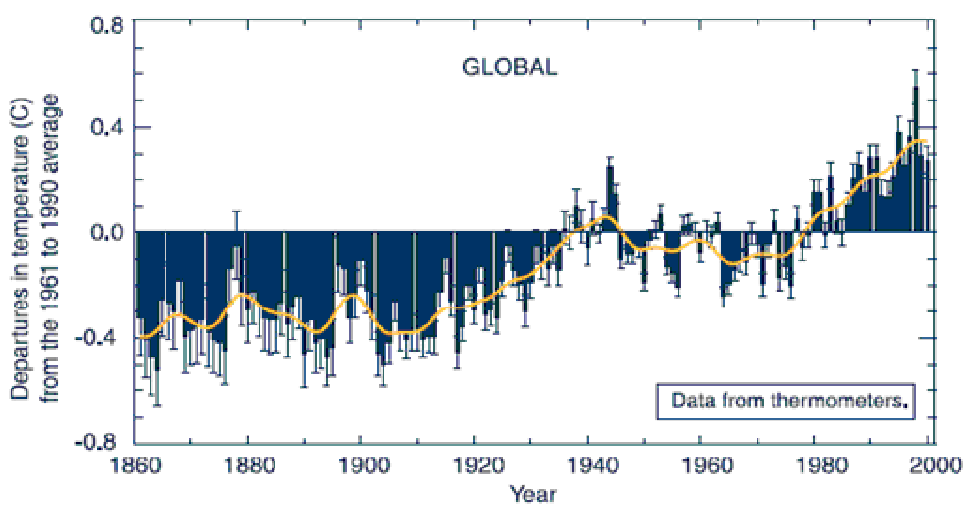

Figure 2.1 Temperature changes [3]

The world today is widely accepting that green houses gases emissions are the major cause of global warming. The importance of finding stabilizing schemes for climate change requires basic knowledge about the behavior of the natural system, as well as the human induced disturbances and the global socioeconomic system that we are all part of. Preliminary knowledge is essential for addressing such issues in a rational way [2, 4, 5, and 6].

2.1.2 CO_2 a cause and an effect

When the reservoir pressure increases, the solubility of carbon dioxide in oil increases. Nevertheless, we detect the opposite when the temperature decreases.
The solubility of carbon dioxide will decrease with a low API gravity. Carbon dioxide solubility depends on the composition of crude oil, reservoir temperature, saturation pressure and in a biased manner on the gravity of oil. [7]

Carbon dioxide has a density close to oil but higher than the density of other gases. At reservoir conditions carbon dioxide has a small compressibility factor. Most importantly the viscosity of 0.1cp which is so small compared to that of oil: the light oils viscosity ranges from 1-3 cp and the viscosity of water is 0.7 [7]. (Figure 2.2) shows how CO_2 behaves at different pressures and temperatures.

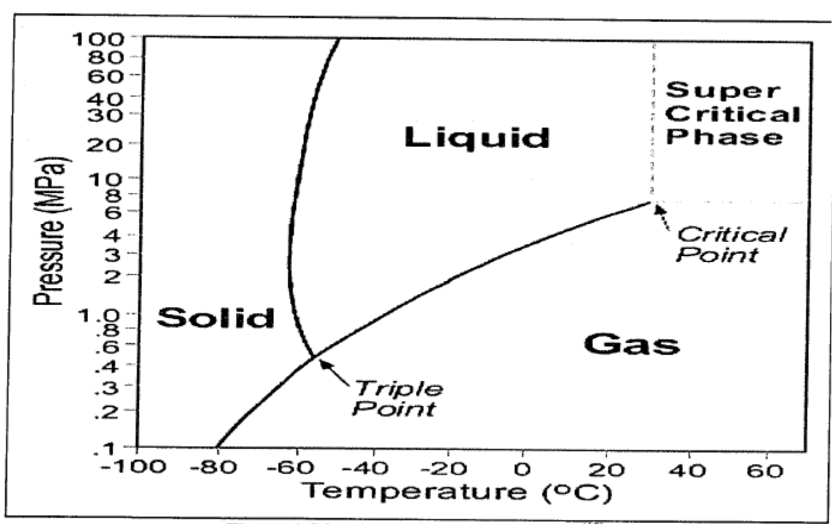

Figure 2.2 CO_2 Phase behavior after Herzog [8]

A dense phase fluid can make full usage of the reservoir capacity. This is a reason why CO_2 should be in the supercritical phase of above 7.4 MPa. Such a condition can be met at depths above 800 m; and about 80% of world's oil fields are at depths greater than 800m and a temperature greater 31°C. When CO_2 is injected it will be stored in the inner granular pores of the reservoir rock. The supercritical phase of CO_2 is still less dense than formation water. The density difference will make the CO_2 migrate to the top of the reservoir where a trap is required to ensure that it does not reach the surface [7].

Perhaps, the best solution to these emissions is to use fossil fuels with an environment friendly energy source. However, the current trend shows, this shift will take much longer than it is expected. Power and industrial sectors are the main contributors to CO_2 emissions. Bearing this in mind, CO_2 sequestration (capturing and storing CO_2 underground) can offer an appealing solution to the problem of CO_2 emissions.

The geological trapping sites of CO_2 can be divided into two types onshore and offshore trapping site. Where both have some advantages and disadvantages as in (Table 2.1) [8]

Table 2.1 Advantages and disadvantages of different CO_2 storage sites [8]

Geological Sites	Advantages	Disadvantages
Coal beds	Large capacity	High costs
Mined salt domes	Custom designs	High costs
Deep saline aquifers	Large capacity	Unknown storage integrity
Depleted oil or gas reservoirs	Proven storage integrity	Limited capacity
Marine Sites	Advantages	Disadvantages
Droplet plume	Minimal environmental effects	Some leakage
Towed pipe	Minimal environmental effects	Some leakage
Dry ice	Simply technology	High costs
Carbon dioxide lake	Carbon dioxide will remain in ocean for thousands of years	Immature technology

It can be seen from (Table 2.1) above that the only proven storage integrity is in depleted oil and gas reservoirs.

2.1.3 CO_2 trapping in oil reservoirs

Trapping CO_2 in geologic formations has four forms. The first one of these is solution trapping, when we trap CO_2 by dissolving it in oil. The dissolved CO_2 in oil will make it denser and will sink down. Next, hydrodynamical (structural) trapping. This kind of trapping takes place when CO_2 is present as a gas or a supercritical fluid under none or low permeability cap rock. The third one of these trapping methods involves trapping CO_2 due to the hysteresis in relative permeability curves and residual gas saturation. This leads a significant amount of CO_2 to be trapped as immobile phase. Finally, CO_2's reaction to minerals present in the rocks will result in a trapping mechanism [9].

Solution trapping occurs during the injection of CO_2. It is caused by the dissolved portion of CO_2 in oil. This will lower the viscosity of residual oil ending in swelling and having an oil that is more ready to flow. The process will make the CO_2 less likely to retaliate back to the atmosphere [10]. However, a typical solution will last from 10-100 years [9].

After that hydrodynamical(Structural) trapping occurs. This kind of trapping is conducted after injection has stopped. It is due to the difference in the densities of CO_2 and oil which will lead the CO_2 to migrate upward to the top of the geologic structure. This type of trapping has a potential risk of leakage. When the congruity of the cap rock is lost such leakage may cause the CO_2 to return to the atmosphere [9].

Moreover, as in structural trapping, residual trapping occurs after the injection when CO_2 migrates upward. When CO_2 migrates upward, it replaces water at the front edge. But in the meanwhile water displaces CO_2 at the back edge of the elongated CO_2 plume. Thus, imbibitions and drainage takes place contemporarily. By the relative permeability curves and residual gas saturation hystereses, CO_2 gets trapped in large amounts as an immobile phase [11, 12].

Mineral trapping on the other hand, will give fruitful results after longer periods of time [13, 14]. It happens when CO_2 reacts with the minerals present in rocks. The dissolution and chemical reactions will need longer periods of time i.e. 10-15 thousand years [15].

Juanes [16] has compared an approximate time scale for all trapping mechanisms and found that hydro dynamical trapping and residual (capillary trapping) have a smaller time scale than dissolution trapping. Dissolution trapping in return will require less time than mineral trapping.

2.1.4 CO_2 injection techniques

The methods that often dictate the injection of carbon dioxide can be divided into two methods. When gravity forces are superior, gravity stabilizing gas injection (GSGI) is used [17]. On the contrary, when viscous forces are dominating, water alternating gas (WAG) is used.

Gravity stabilizing gas injection (GSGI)

Compared to the upward water flooding the expected incremental oil recovery is usually in a range of 15-40% [17].This process is put into practice in anticline reservoirs, pinnacle reefs and high relief angles. The gas is injected from the top of the reservoir and the production of oil is from a deeper moving oil bank. The vertical sweep efficiency is affected by both viscous and gravitational forces as in the Equation 2.1.1.

$$\mathrm{R}v/g = \left(\frac{\nu\ \mu\mathrm{o}}{\mathrm{kg}\Delta\rho}\right) * \left(\frac{\mathrm{L}}{H}\right) \qquad (2.1.1)$$

Where υ is the Darcy velocity, R v/g is the ratio of viscous to gravitational forces μ_o is oil velocity, L is the distance between wells, k is the permeability, g is the gravity force, $\Delta\varrho$ is the density difference between the fluids and H is the height of the displacement zone.

Factors that influence the vertical sweep efficiency are: Horizontal shale barriers, reservoir dip angle, vertical permeability and injection and production rates which have the control over the shape of the oil bank and the oil drainage.

Water alternating gas injection (WAG)

This process has an expected incremental oil recovery of 5-15% of the original oil in place. It is applied in horizontal oil reservoirs where the reservoir slope is almost zero. The main purposes of this technique are: to reduce gravity affects, eradicate the dominant viscous forces in the reservoir and stabilize the front [18]. The mobility ratio (M) is the defining factor of the front. Thus, it can influence the horizontal sweep efficiency to a great extent. Equation 2.1.2 will provide a definition from the mobility ratio:

$$M = \left(\frac{K_{rg}}{\mu_g}\right) * \left(\frac{K_{ro}}{\mu_o}\right) \qquad (2.1.2)$$

Where K_{rg} and K_{ro} are the relative permebilities and μ_o and μ_g are the viscosities of the oil and gas, respectively.

Water alternating gas can have problems with viscous fingering, inability to control injection profiles and gravity override [19].

2.2 CO_2 sequestration: parameters and problems

2.2.1 The parameters that affect oil recovery and CO_2 sequestration.

Nine parameters are thought to have a real effect on the reliability of any sequestration project [10].These are, pressure, temperature, reservoir structure, heterogeneity, CO_2 impurity and well configuration and completions.

2.2.1.1 Reservoir pressure

Operating below the minimum miscible contact pressure (MMP), (the pressure at which reservoir oil and the CO_2 become a single phase) can result in low recovery, whereas operating at high pressures than MMP will demand additional CO_2. This is needed because a denser CO_2 will occupy less volume in the reservoir. Therefore,

CO_2 gained is expected to be large. However the reservoir parting pressure which is the pressure at which fractures may be induced will be the upper limit of CO_2 injection. Otherwise, when such fractures are formed CO_2 will eventually migrate back to the atmosphere [19].

Since a pressure of less MMP is the problem. Studies and field applications have shown that this can be solved by one or more of the following suggestions:

Over injecting water in order to increase pressure to the MMP i.e. Lost Soldier tertiary project [20] in which within a period of 4 months the over injecting of 3 million water barrels, made it possible to raise the pressure by 1200psi.

According to Hadlow [21], Shell concluded that the injection of CO_2 both below and above the MMP has brought good reservoir response. Additionally, CO_2 injection has caused a raise in reservoir pressure that achieved miscibility in Dollarhide [22]. Therefore, these studies conclude that reservoir pressure can be increased by continuous CO_2 injection. Furthermore, this can increase the possibility of injecting and keeping higher volumes of CO_2.

2.2.1.2 Reservoir temperature

The minimum miscibility contact pressure (MMP) required for the oil will increase with higher temperatures. Solubility of CO_2 decreases with increasing temperature [23]. At an increasing temperature and a constant pressure the density of CO_2 decreases.

2.2.1.3 The structure of the reservoir

To determine whether a gravity stabilizing gas injection (GSGI) or a water alternating gas (WAG) should be used, the important role of reservoir structure and shape can be seen.

In gravity stabilizing gas injection (GSGI) technique, to fill up the reservoir with large quantities of gas that is injected from the top of the reservoir. This technique is applied in high dipping reservoirs, a significant vertical thickness and in pinnacle reefs that have a comparably small area extent. High dip reservoirs are good candidates for gravity stabilizing gas injection (GSGI), the higher the slope the better the overall performance of the technique [24]. Both oil recovery and CO_2 storage will be large in a homogenous reservoir and/or a reservoir with no horizontal barriers. But if that is not the case, producing from the bottom of the reservoir, will necessitate asserting a stable flood front to maximize the oil recovery. As the flood moves downward, in order to reduce the composite layers loss, drilling new wells and recompilation, may be required.

In water alternating gas (WAG) process, to overcome viscous forces by decreasing the mobility ratio contrasted with the gas injection. Water in slugs is frequently injected in an alternate mode with gas. The residual oil that is blocked and the disturbed formation of the solvent bank are mainly due to the introduction of water into the reservoir. This can reduce the ultimate recovery. This technique takes a shorter time to recover more oil, compared to gravity stabilizing gas injection (GSGI) [24]. But, it also can recover less oil and has a lower gas storage potential than the gravity stabilizing gas injection (GSGI). In addition, the technique requires less accomplishing costs. The possibility of circulating a gas is high, and a gas cap cannot be formed. Finally, frequent well completions are not necessary, since the wells used previously in water injection can be used for CO_2 injection.

2.2.1.4 The heterogeneity of the reservoir

Using numerical simulations, Laieb and Tiab [25] have studied the effect of random heterogeneities. Heterogeneity is the most important factor that affects the performance of miscible flood. Poor sweep efficiency and early breakthroughs were caused by the tendency that high permeability channels have to circulate gas. Gas access prevention to un-swept regions was caused by the horizontal no flow barriers in vertical flooding. Moreover, if the vertical to horizontal permeability ratio are low it may slow the proceeding displacement.

These will result in low CO_2 intake capacity as well as lower oil recovery. In fact reservoir heterogeneity is detrimental for both CO_2 storage and oil recovery.The characterization of a reservoir to evaluate the impact of shale barriers for the vertical miscible flood and the effects of stratification for the horizontal miscible flood. Sweep problems involve, directional permeability, high permeability channels, fractures and faults, shale barriers and vertical to horizontal permeability ratio. In field miscible floods, for the purpose of improving sweep efficiency, gel and foam injections are used [21]. While polymers and gels were used to improve vertical and areal sweep efficiency, foams are used to improve the ratio between reservoir crude and CO_2.

2.2.1.5 Influences of the aquifer that underlies the reservoir.

Aquifers differ in properties, some act from the bottom and others from the edge of the reservoir, some are strong and others are weak. Identifying the strength of an aquifer in oil reservoirs can be accomplished by Cambell diagnostic plots and material balance [24]. When a significant portion of volumetric withdrawals of reservoirs fluids are replaced by water movement of during the producing life of the reservoir, such reservoirs are played down by aquifers. However, the pressure time behavior along the original reservoir /aquifer contact together with the aquifers characteristics are the governing agents of the influx rates and total influxes of the such as water movements. The influence of such aquifers on CO_2 storage capacity and oil recovery was studied by Malik and Islam [26]. As a result of their studies a threefold solution is suggested to obtain the maximum oil recovery; If there is no aquifer support or if CO_2 was injected into the producing formation for reservoirs with bottom aquifers after water flooding; or that with the presence of bottom aquifers CO_2 flooding was developed in the early life of the reservoir. Additionally, they concluded that in the presence of bottom aquifers a peak storage is reachable if utilizing high reservoir pressure the CO_2 is injected into the producing formation in the early life of the reservoir.

Bachu and Shaw [27] suggested that if the cumulative net water oil ratio (WOR) is larger than 0.25, the aquifer is strong and weak if the WOR was less than 0.15. However, if the WOR was between 0.15-0.25 and the gas oil ratio (GOR) should be less than 5600 scf/bbl; otherwise, the aquifer support is weak. They studied the effect of aquifer strength on the reduction in CO_2 sequestration capacity using material balance. The reduction in CO_2 capacity varied between 17-41% (Average 28%) for gas reservoirs and between 25-80% (average 60%) for oil reservoirs. The reason why the reduction in oil reservoirs was greater was due to the longer time needed to produce the oil which permits greater aquifer influx [28]. On the other hand, for weak aquifers, by the time the reservoir builds back up to its initial pressure the water is expelled.

2.2.1.6 Oil production and CO_2 injection rates

The important role in regulating the shape of oil-gas front, formation of oil bank and in preventing viscous fingers is more obvious when gravity assisted CO_2 injection process (vertical injection) is applied. Demure [29] explained two rates: stable and critical rate in gravity drainage process. At rates greater than the critical rate, the displacement is unstable and the viscous fingers will develop strongly, while at rates between the stable and critical rates, the displacement is only partially stable and viscous fingers will develop less strongly. He then reported that viscous fingering is more severe in downward displacement in sloping layers than in pinnacle reefs.

Lee et al [30] reported that since greater volumes of water can be flushed through the reservoir before the economic limit was reached. In carbonate reservoirs increased overall recovery will be obtained at increased production rates. So, Asgarpour [17] has claimed that when increasing the fluid velocity in CO_2 horizontal flooding, vertical sweep efficiency can be partially improved, which in due will increases the ratio for viscous to gravity forces.

2.2.1.7 CO_2 injection time

It is theorized that starting with CO_2 injection in earlier stages of a reservoir life could improve oil production and also result in CO_2 storage. That is because during secondary recovery introducing water into the reservoir can reduce the space available for gas. However, a disadvantage is that when characterizing a reservoir, it is expensive to do it with CO_2.Because the CO_2 is more mobile. That is why early water injections are often more convincing for the characterization process. Possible water blocking problems can be eradicated in water wet formations by injecting CO_2 directly after the primary solution. Also, for the sake of reducing the risk of dilution by methane and nitrogen that could migrate from a secondary gas cap during the primary depletion, continues CO_2 injection can be started in dipping reservoirs as early as primary production [6].

2.2.1.8 CO_2 impurities

Contamination of the CO_2 injection stream may have both advantages and disadvantages. The presence of intermediate carbons like (C3 or C4) and H_2S reduces the MMP [12]. However adulterating the CO_2 with N_2 and CH_4 could increase the MMP. Zhang et al [31] found that the swelling in oil caused by carbon dioxide can be reduced if the diffusivity and solubility of CO_2 into oil was decreased by the presence of N_2. When miscibility is not achieved at sufficiently high pressures, the composition of the injected fluid should be changed [32]. Producers can be much cautious in the case of H_2S-CO_2 mixtures; it is because of the high corrosiveness and toxicity of hydrogen sulphide. To avoid hydrate formation and corrosion, Bachu [33] reported that when injecting sour gas, the reservoir temperature should be greater than 35°C in order to prevent hydrate formation and with water content lower than the saturation limit. A minimum miscibility experiment should be repeated by increasing the mole fraction of the CO_2 in the injected fluid and the appropriate quantity of increase is called the minimum enrichment for miscibility [MME]. This happens when at high pressures miscibility was not achieved. Then if the injected CO_2 was pure, we will need to add more or contaminate it with some additives. Some reinject the produced CO_2 without removing the impurities, while others were satisfied with the extracting the NGLs from the produced CO_2 [34].

2.2.1.9 Well configurations and completions

To distribute the gas in to all reservoir regions completion and injection wells are to be drilled. For the sake of minimizing the gas coning problems injection wells need to be completed in the lower zone while production wells are perforated at all zones of the formation [10].

In horizontal reservoirs, completing injection wells low in the formation rather than over the entire reservoir column improves the contact of gas with reservoir columns due to gravity effect. The tendency of gas channeling between the producer and injector is increased when perforation happens in a region with a high permeability [10].

2.2.2 CO_2 flooding problems

These can be divided into two parts, leakage and operational problems.

2.2.2.1 CO_2 leakage

Potential leakage sources include faults, fractures, reservoir cap rock and abandoned or poorly cemented wells. Reservoirs that are exposed to CO_2 injection will change the in-situ effective stresses [34]. Geo-material's permeability is highly dependent on the mechanical behavior of such stresses. These changes will affect the hydraulic integrity of the caprock. This will bring us to point of discussing the reservoir fracture (parting) pressure. CO_2 sequestration can become ineffective if pressurizing the reservoir exceeded parting pressure. This can break the seal and allow large amounts of CO_2 to migrate up to underground water and back to the atmosphere [10].

2.2.2.2 Operational problems

The phase behavior of the reservoir; heterogeneities and properties of injected gas mixtures should be understood. Some of problems that happen during a sequestration process involve: early breakthrough in production wells, reduced injectivity, corrosion, scale formation and asphalting precipitation [10].

Early breakthrough in production well

Early gas breakthrough is a result of an inadequate reservoir description or poor understanding of reservoir and unresolved design strategies.

Reduced injectivity

The factors that influence the reduced injectivity include: change in relative permeability owing to three phase flow. Wellbore heating and thereby reduced effects of thermal fractures during gas injection or precipitates (hydrates and asphaltanees) formed in near well bore zone.

Corrosion

CO_2 as injection gas may result in reports severe corrosion problem. These can be due to an additive (i.e. H_2S), that are sometimes added for different reasons. Solutions to the problem include using high quality steel and equipment treatment.

2.3 Field applications

Carbon dioxide injection is a commercially proven technology that is applied as an EOR technique in different types and parts in the world.

CO_2 flooding in Batı Raman field

Heavy oil was first produced from Batı Raman (south east Turkey)in 1961. The pay zone's name is Garzan: A carbonate reservoir mainly composed of limestone. Immiscible CO_2 injection has started in 1987. The estimated reserve is 1.850MMM barrels of heavy oil. Due to low API gravity of 12 and high viscosity, primary recovery produced only 1.5%of original oil in place by 1986 ,while with immiscible CO_2 injection starting in 1986 and as of 2003 5% of OOIP was produced. To increase the sweep efficiency polymer and gel treatments are started [35].

Sleipner project

The Sleipner oil and gas field operated by Statoil, is located in the North Sea about 240 Km off the coast of Norway. To meet commercial specifications the natural gas from this field needs to reduce its CO_2 concentration from about 9% to 2.5% .This is a common practice at gas fields worldwide in which the CO_2 captured from natural gas is vented the atmosphere [36].

It is standard practice natural gas production for the byproduct CO_2 to be vented to the atmosphere at Sleipner. However, CO_2 is compressed and pumped into a 250 - m – thick brine saturated sandstone layer, the Utsira formation which lies about 1000 m below the seabed. About 1 Million metric tons of CO_2 (equivalent to about 3% of Norway's total annual CO_2 emissions) have been sequestered annually at Sleipner since October 1996, with a total of 20 Mt of CO_2 expected to be sequestered over the lifetime of the project.

Evolution of the CO_2 plumb was monitored by time lapsed 3D seismic, well logging and geochemical analysis. Both simulation modeling and field data indicated a safe and reliable, storage of CO_2 in Ustira formation.

A second scheme is planned that would involve about 0.7 Mt per year of CO_2 production at the Snohvit gas field in the Barents Sea off northern Norway being injected into a deep sub – sea formation[36].

Weyburn project

The Weyburn CO_2 monitoring and Storage Project is an extensive research program investigating long – term geological storage of CO_2 within the Weyburn Midale pool of southeastern Saskatchewan.

The CO_2 used in the project is piped from the Great Plains Synfuels Plant near Beulah , N.D. , and is by product of the plant's coal gasification process .Before the Weyburn Project much of the CO_2 used in similar U.S. EOR projects has been taken at considerable expense from naturally occurring reservoirs[36] . Using an industrial source of CO_2 sequesters this emission that would normally be vented into the atmosphere.

In the first phase, carbon dioxide was injected into Mississippian carbonates of the Midale Beds in the Wayburn Oilfield in Saskatchewann, Canada. The CO_2 increased the underground pressure of the field to bring more oil to the surface. The project increased the field's oil production by an additional 10,000 barrels per day (2005) and demonstrated the technical and economic feasibility of permanent carbon sequestration – the capture band permanent storage of carbon dioxide in geologic formations Weyburn Project successfully sequestered five Million tons of CO_2 in to the Weyburn Oilfield in Saskatchewan, Canada, while doubling the field's oil recovery rate If the methodology used in the Weyburn Project was successfully applied on a world wide scale, one –third to one – half of CO_2 emissions could be eliminated in the next 100 years and billions of barrels of oil could recovered [36].

EOR technique used in the project, has a potential to increase an oil field's ultimate oil recovery up to 60 percent and extend the oilfield's life by decades. Scientists project that , by using knowledge gained from the Wayburn Project , the Weyburn Oilfield will remain viable for another 20 years , produce an additional 130 million barrels of oil , and sequester as mach as 30 million tons of CO_2 . The first stage involved the injection of more than 110 billion cubic feet of 95 per cent pure CO_2 into the Weyburn Oilfield in Saskatchewan, Canada.

Now the Weyburn Project will move in to Phase II where researchers will compile a best practices manual to serve as a world – class industrial reference in the design and implementation of CO_2 sequestration in conjunction with enhanced oil recovery projects. They will also expand their efforts to the neighboring Midale Unit , develop more rigorous risk – assessment modeling techniques , and improve injection efficiencies , and monitor CO_2 flooding and storage with a variety of methods , including seismic wave technologies and geochemical surveys[36].

In Salah project

In Salah CO_2 injection started in June 2004 injecting CO_2 into the Krechba Carboniferous sandstone reservoir in the Algerian Central Sahara The operation is a joint venture between BP, Sonatrach and Statoil. The natural gas from the Krechba reservoir, together with the neighboring Teguentour and Rag reservoirs, contains CO_2 concentrations ranging between 1 to 9% while the gas has to have a maximum of 0.3 % when delivered to the customer The excess CO_2 , expected to peak at approximately 1.2 million tones a year , is then injected . Total predicted injection over the life of the field is 17 million tones. The field is particularly interesting since it is an analogue to several potential storage in the North sea and North America.

Key challenges are to insure the sustainability of 9 billion cubic meters for 13 years minimum in one of the most hostile environments, to put in place the requirement is that the CO_2 concentration in the gas stream should be less than 0.3 %, significantly below the concentration present in the Salah Gas fields, which ranges between 1% and 9%. The most important aspect of the project is the commitment to non – atmospheric disposal of the 0.66 billion cubic meters per year of extracted CO_2 stream that results form the fields ' production to meet the contracted sales gas volumes. This means that an alternative solution to simply venting would be required.

Storage and sequestration of the extracted CO_2 stream is planned with in the aquifer region of the hydrocarbon bearing carboniferous formation adjacent to the Krechba field, the most northerly of the gas field currently in production since July 2004. Three CO_2 injection wells have been drilled with results as prognoses from seismic, providing access into the east and north aquifer reservoir region for storage and sequestration of CO_2 .The project is now one of the largest sequestration and storage schemes in the world [36].

Frio brine pilot project

A research project involving a small-scale CO_2 injection test conducted at the South Liberty field, in Dayton, Texas (USA), as a case study to illustrate the concept of an iterative sequence in which traditional site characterization is used to prepare for CO_2 injection and then CO_2 injection itself is used to further site-characterization efforts, constrain geologic storage potential, and validate the understanding of geochemical and hydrological processes [37]. The techniques used included: Traditional site characterization techniques such as geological mapping, geophysical imaging, well logging, core analyses, and hydraulic well testing provide the basis for judging whether or not a site is suitable for CO_2 storage. 1,600 metric tons of CO_2 was injected over a period of 10 days into a steeply dipping brine-saturated sand layer at a depth of 1,500 m [38]. At this depth, free-phase CO_2 is supercritical. The pilot employed one injection well and one observation well.

However, it was proved that only through the injection and monitoring of CO_2 itself can the coupling between buoyancy flow, geologic heterogeneity, and history-dependent multi-phase flow effects be observed and quantified. CO_2 injection and monitoring can therefore provide a valuable addition to the site-characterization process. Additionally, careful monitoring and verification of CO_2 plume development during the early stages of commercial operation should be performed to assess storage potential and demonstrate permanence.

CHAPTER 3

THEORY

3.1 Trapping mechanisms in geological media

The trapping mechanisms for CO_2 sequestration in geological media (geosphere) can be divided fundamentally into two categories: Physical and chemical mechanisms. The physical mechanisms involve trapping of CO_2 s a free-phase substance within a volume of a geological medium in its gaseous, liquid or supercritical state. The following fall in this category: geological trapping, hydrodynamic trapping and cavern trapping. Chemical mechanisms involve trapping of CO_2 as a result of various chemical processes between the fluids and/or rocks and CO_2 in the geosphere. In this case, CO_2 generally loses its state as free CO_2 and transforms into or becomes attached to another substance. The following fall into this category: solubility trapping in formation water or reservoir oil, ionic trapping by which CO_2 decomposes into its ionic components, adsorption trapping and mineral trapping as CO_2 may precipitate into a stable mineral phase[39].

Trapping means

Trapping may happen using the following means:

1. Volumetric, whereby pure-phase CO_2 is trapped in a rock volume and cannot rise to the surface due to physical and/or hydrodynamic barriers. The storage volume can be provided by:

a) The pore space present in geological media. If trapped in the pore space, CO_2 can be at saturations greater or less than the irreducible saturation. If the latter is the case, the interfacial tension keeps the residual gas in place. If the former is valid, pure CO_2 can be trapped: in stratigraphic and structural traps in depleted oil and gas reservoirs and in aquifers (static accumulations); or as a migrating plume in large-scale flow systems (hydrodynamic trapping).

b) Large, man-made cavities, such as caverns and mines;

2. Solution trapping, whereby CO_2 is dissolved into fluids that saturate the pore space in geological media, such as formation water and reservoir oil.

3. Adsorbed onto coal matrix. Adsorption trapping is achieved by preferential adsorption of gaseous CO_2 onto the coal matrix because of its higher affinity to coal than that of the methane that is usually found in coal beds.

4. Chemically bound as a mineral precipitate. These means of CO_2 storage are found in the following geological media: oil and gas reservoirs, either at depletion or for enhanced oil, and possibly gas, recovery; uneconomic coal beds, with the possibility of producing coal bed methane; deep aquifers saturated with brackish water or brine; and salt caverns[39].

3.2 Pressure effect on CO_2 sequestration

The average pressure increases with injection into a finite space. This increase in pressure reciprocal to the available space. The average pressure from the injection pressure must be distinguished; a local pressure increase is needed for injecting fluid into a well area. Another factor, still local, is the reservoir pressure, which will show a distribution over the reservoir. With respect to CO_2 injection and the integrity of the cap rock, the injection pressures applied are of great importance. In general, these depend on several factors: the local reservoir permeability, the length and quality of perforations, the injection rate and the size and degree of heterogeneity of the storage system [40].

3.3 Hysteresis effect on CO_2 sequestration

Dependence of the wetting or non wetting phase relative permeabilities and capillary pressures on the amount of trapped and flowing saturations that are unique to drainage or imbibitions process is multiphase flow hysteresis.

The first trapping model we investigate was proposed by Land [41], and is the most widely used empirical trapping model published by Carlson S. Land [39] in 1968. His model was developed for trapped gas saturation as a function of the initial saturation based on published experimental data from water-wet sandstone cores He also developed an analytical model for imbibition gas relative permeability based on his trapping model that will be discussed later in this thesis.

Most relative permeability models that incorporate hysteresis [41] are based on the trapping model proposed by Land [41]. In this model, the trapped non wetting phase saturation is computed as:

$$Sgt(sgi) = \frac{Sgi}{1 + CSgi} \tag{3.1}$$

Where Sgi equals the initial gas saturation or the saturation at the flow reversal, and *C* is the Land trapping parameter. The Land coefficient is computed from the bounding drainage and imbibition curves as follows:

$$C = \left(\frac{1}{Sgt, \max} - \frac{1}{Sg, \max} \right) \tag{3.2}$$

where Sgmax is the maximum gas saturation, and Sgtmax is the maximum trapped gas saturation, associated with the bounding imbibition curve. All these quantities are illustrated in (Figure 3.1). The value of the Land trapping parameter is dependent on the type of rock and fluids.

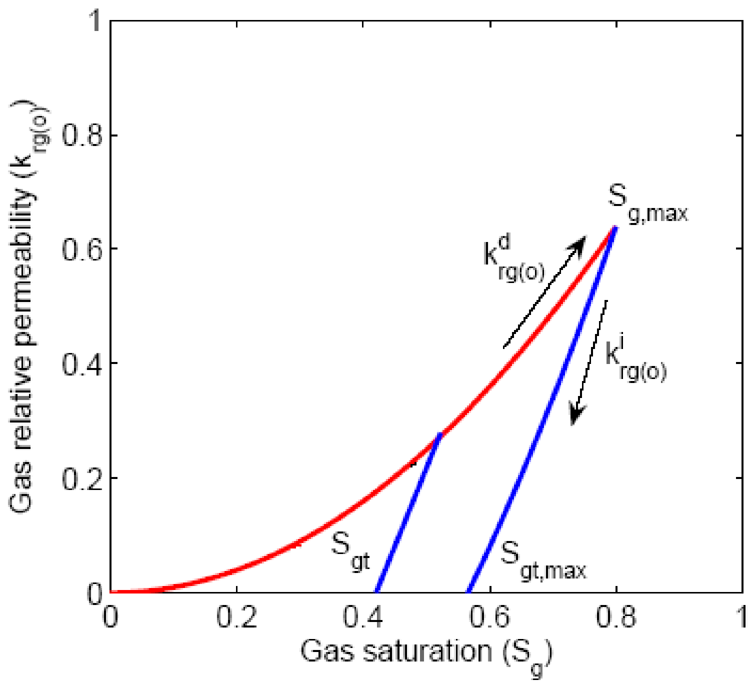

Figure 3.1 Parameters required in the relative permeability hysteresis models

Carlson trapping model

Shifting the bounding imbibitions curve to intersect will determine the trapped gas saturation; the idea behind Carlson's interpretation is to use the model of the imbibitions relative permeability scanning curves as being parallel to each other [13]. This geometric extrapolation procedure is illustrated in Figure 3.1. The trapped wetting-phase saturation is computed as:

$$Sgt = Sgr - \Delta Sg \tag{3.3}$$

Where Sgt is residually trapped saturation minus the difference in residual gas saturations

Killough trapping model

Killough [42], used Land's trapping model to derive a relative permeability hysteresis model; an interpolative scheme for defining the intermediate scanning curves, inter- mediate imbibition relative permeability curves between the bounding drainage $k^d rg(o)$ and imbibition $k^i rg(o)$ relative permeability curves (Figure 3.1). This allowed for the use of empirical or analytical curves if experimental data were not available [40]. In Killough's method, the non-wetting phase relative permeability along a scanning curve is computed as:

$$k^i{}_{rg}(S_g) = \frac{k^i{}_{rg}(o)(S_{g,norm})K^i{}_{rg}(o)(S_{gi})}{k^i{}_{rg}(o)(S_{g,\max})} \tag{3.4}$$

Where *Sgi* is the initial gas saturation, Sg, max is the maximum gas saturation from the bounding imbibition curve, and Sg,norm is the normalized gas saturation computed as:

$$S_{g,norm} = S_g - \frac{(S_g - S_{gt,norm})(S_{gt,\max} - S_g)}{S_{gi} - S_{gt,\max}} \tag{3.5}$$

In Equation (3.5), $k^i rg(o)$ and $k^d rg(o)$ represent the relative permeability values on the bounding imbibition and drainage curves, respectively. Each of these variables is illustrated in Figure 3.1.

3.4 Impurity's effect on CO_2 sequestration

In this work we investigate the additive of H_2S and CO:

Injecting an acid gas (H_2S) impurity

The acid gas may also contain 1-3% hydrocarbon gases obtained after the removal of H_2S and CO_2 from the sour gas, and is saturated with water vapor in the range of 2-6%. The solubility of water in both H_2S and CO_2, hence in acid gas, decreases as pressure increases up to 3-8M. Unlike the case of hydrocarbon gases, for which water solubility decreases with increasing pressure, depending on temperature, after which it increases dramatically (see.Figure.3.2). The solubility minimum reflects the pressure at which the acid gas mixture passes into the dense liquid phase form, where the solubility of water can increase substantially with between these polar compounds. The ability of acid-gas to hold water increases with temperature and decreases with the addition of small amounts of methane

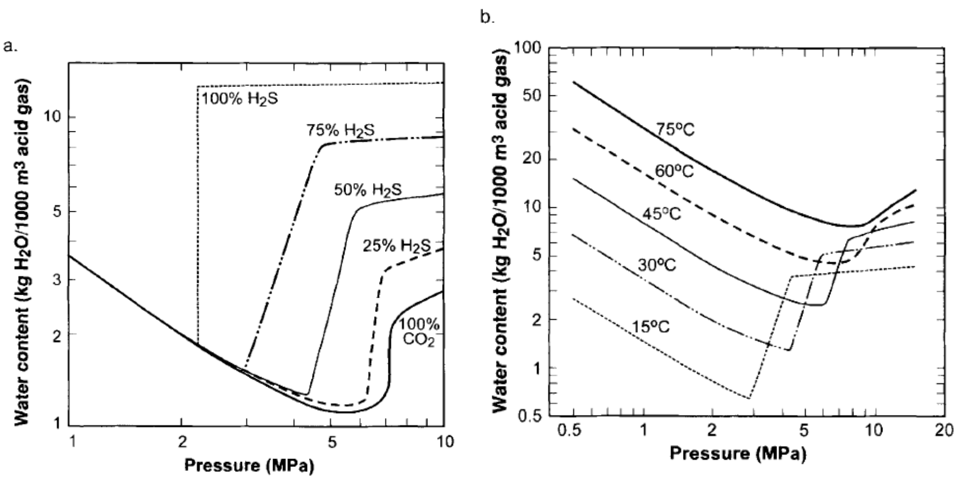

Figure 3.2 Water content's effect on sour gas after Bachu [43]

This property of the acid gas mixture is used in dewatering the acid-gas to avoid pipe and well corrosion [43]. The acid gas is usually compressed from about 100kPa to around 8-10MPa for injection and the water content is generally reduced to less than half a mole %. Although there are not many published properties of the acid-gas mixture, the properties of pure CO_2 and H_2S have been thoroughly examined and reported. In their pure state, CO_2 and H_2S have similar phase equilibrium, but at different pressures and temperatures. They exhibit the normal vapor/liquid behavior with pressure and temperature, with CO_2 condensing at lower temperatures than H_2S. Methane (CH_4) also exhibits this behavior, but at much lower temperatures. The phase behavior of the acid-gas binary optimize storage and minimize risk, the acid gas needs to be injected: (1) in a dense-fluid phase, to increase storage capacity and decrease buoyancy; (2) at bottom-hole pressures greater than the formation pressure, for injectivity; (3) at temperatures in the system generally greater than 35 ~ to avoid hydrate forming, which could plug the pipelines and well; and (4) with water content lower than the saturation limit, to avoid corrosion [43].

Injecting a Carbon monoxide (CO) impurity

By coming out of solution when pressure drawdowns to assist in the pressure drive during the production cycle is how gaseous additives such as carbon dioxide are believed to enhance oil recovery. The carbon monoxide is said to react with water to produce CO_2 and additional hydrogen in the reservoir. These gases will lower oil viscosity making the oil more ready to recovery. The conversion of Carbon monoxide to Carbon dioxide and steam is termed as (water gas equation):

$$CO + H_2O \leftrightarrow CO_2 + H_2 \tag{3.6}$$

The disadvantageous thing about this reaction is that it takes place in temperatures higher than 400 C◦. Such a temperature will cause significant gasification and polymerization that will reduce the amount of oil recovery. At 400 C◦ temperature a significant gasification and polymerization will take place in the oil.

The process is defined by reduction in viscosity, both from the possible upgrading effect of the hydrogen reacting with reservoir oil and from the carbon dioxide being dissolved in oil.

3.5 Economical analysis of CO_2 sequestration

A simple economic model is developed. The main assumption is the free delivery of CO_2. Neither corporate tax nor transportation cost (<1km) was calculated.

The net present value is calculated by discounting the future net cash flow.

$$NPV = \sum_{J=0}^{L} \frac{NCF_j}{(1+i)j} \tag{3.7}$$

$$NCF = (R + C_{CO2} - Roy - OPEX - IW - D) * (1 - T) + D - CAPEX \tag{3.8}$$

Where NCF[45] is net cash flow. C_{CO2} is the assumed carbon credit, royalties is 8% and Operating expenditure can be divided into four parts that are mentioned above. IW is drilling and completion expenditures. Since it will have a positive effect, the depreciation factor was not considered.

CHAPTER 4

PROBLEM STATEMENT

The sequestration process depends on many factors. The proposed ways to optimize both oil recovery and CO_2 storage in a way that it will remain immobile are examined. When CO_2 sequestration is applied, factors are set to get a positive and realistic response from the whole process. Some of these are controlling the production, injection, well location (when group of wells), injection rate, pressure, and depth. However, others are describing the rock and fluid properties (i.e., relative permeability curves and hysteresis, CO_2 impurities). The main purpose of this thesis is to evaluate the chances of getting a successful CO_2 sequestration and oil recovery from the hypothetical field B wells in the Southeastern part of Turkey. This was done by utilizing a model in a commercial simulation tool CMG-STARS developed by Computer Modeling Group of Canada. Then, sensitivity analyses are applied to each of the above factors and their combinations as well. By selecting an optimum case from the first group of properties, this optimum case was used for study of different rock and fluid properties. These properties are found to have an important effect on both EOR and carbon storage. Finally, impurities are added to the gas stream to study their effect in enhancing the oil recovery. In the economical analysis, Net present values for 50 prediction runs was calculated .oil recovery has improved for some of the cases yielding two economically profitable cases. However, when carbon credits was added more than nineteen of the cases have exceeded the base case in terms of the net present values associated.

CHAPTER 5

METHOD OF SOLUTION

5.1 Introduction [15]

STARS are a three-phase multi-component thermal and steam additive simulator. Grid systems may be Cartesian, cylindrical, or variable depth/variable thickness. Two-dimensional and three-dimensional configurations are possible with any of these grid systems.

STARS uses the data set that you create initially and then creates three other files. Each STARS run creates a text output file, an SR2 index file (IRF), and a SR2 main file (MRF). If a restart run is desired, then several existing files are needed and another three are generated.

Naturally fractured reservoirs

The flow in naturally fractured reservoirs can be simulated by using four different models - dual porosity (DP), dual permeability (DK), multiple interacting continua (MINC), or vertical refinement (VR) - depending on the process or mechanisms to be studied.The basic approach idealizes the fractured reservoir as consisting of two parts: fracture and matrix. The fractures, having small storativities, are the primary conduits of fluid flow, whereas the rock matrices have low fluid conductivities but larger storativities [46].

MATRIX solution method

STARS uses a state-of-the-art solution package AIMSOL based on incomplete Gaussian Elimination as a preconditioning step to GMRES acceleration. AIMSOL has been developed especially for adaptive implicit Jacobian matrices. For most applications the defaults control values selected by STARS will enable AIMSOL to perform efficiently. Thus, users do not require detailed knowledge of matrix solution methods [46].

5.1.1 Data Groups

The groups must follow a certain input order: Input/Output Control, Reservoir Description, Other Reservoir Properties, Component Properties, Rock-fluid Data, Initial Conditions, Numerical Methods Control, Geomechanical Model, Well and Recurrent Data.

Restart files

A restart file contains information that allows the simulation to continue from another run. Restarts are done for the following reasons: history matching or sensitivity studies, well specifications that need to be changed, To perform a short simulation run to see if the results are satisfactory, before running bigger, longer jobs, and To save execution time in subsequent runs. For instance, you have completed a simulation run and the preliminary results look good. Now you want to do prediction runs [46].

Because you have created a restart file with the initial run, you may select a time step from the middle of your run and 'restart' the simulation. The simulator does not need to start at the beginning; it continues execution from the time step you have chosen [46].

Matrix

*MATRIX is used immediately after a grid property keyword to indicate that a matrix property is being in .

*FRACTURE is used immediately after a grid property keyword in a dual porosity system to indicate that a fracture property is being input.

J and K Direction Data from I Direction

*EQUALSI indicates that values in the J and K directions are the same as those in I direction, or that the values given for the I direction may be modified by division, multiplication, etc.

Modifying Array Data

*MOD indicates the modification of an input grid property.

Interpolating Table Data

The *INT keyword may be used in table input. This keyword enables the calculation of the table entry by interpolation. Essentially the table entry corresponding to *INT is replaced by a linearly interpolated value. This option is useful when not all table entries are known. This feature is explained in further detail with the help of an example [46].

Suppose that it is required to enter a water-oil relative permeability table into the simulator. Also assume that the water and oil relative- permeabilities are known at different saturations [46].

5.1.2 Reservoir description

Dual Porosity

*DUALPOR indicates the use of a dual porosity model in some or all of the simulator's grid blocks.

This keyword indicates that a dual porosity option will be used in the simulator. This option allows each simulator block to have up to two porosity systems; one called the matrix porosity and the other called the fracture porosity. Each porosity can have its own porosity value and its own permeabilities, as well as other distinct properties. Matrix properties are described using the *MATRIX qualifier while fracture properties are described using the *FRACTURE qualifier.

Inter-block flows are calculated in much the same manner as they would be in the standard (no *DUALPOR keyword) model. These flows are governed by the fracture properties. However, an additional set of matrix-fracture flows is calculated when *DUALPOR is specified. These flows are governed either by the matrix or matrix-fracture properties depending on the choice of the shape factor calculation.

Thus, *DUALPOR allows one matrix porosity and one fracture porosity per grid block, where the matrix is connected only to the fracture in the same grid block. Fracture porosities are connected to other neighboring fracture porosities in the usual manner. The presence of both fracture and matrix porosities in a block, or just a fracture porosity or a matrix porosity, is under user control (see the *POR and *NULL keywords). Property definition for *DUALPOR systems usually requires the use of pairs of definitions for most items, one carrying a *MATRIX qualifier and the other a *FRACTURE qualifier.

Permeabilities

*PERMI indicates input of I direction permeability.

*PERMJ indicates input of J direction permeability.

*PERMK indicates input of K direction permeability

Matrix/Fracture and *EQUALSI Operators [46]

Keywords *PERMJ and *PERMK are able to use the *EQUALSI facility for entering grid array data, even for the *MATRIX and *FRACTURE portions of the array. However, use of *EQUALSI with *MATRIX and *FRACTURE has this additional restriction: the *MATRIX and *FRACTURE instances of the keyword must use the same numerical operator if an operator is used. For example, the following data fragment will not work as expected

Fracture Spacing

*DIFRAC indicates the input of the fracture spacing in the I direction.

*DJFRAC indicates the input of the fracture spacing in the J direction.

*DKFRAC indicates the input of the fracture spacing in the K direction.

5.4 Rocks-Fluid Data [46]

Water-Oil Relative Permeability Table

At least one *SWT table must be entered, and it must appear before *SLT.Entries must be in order of increasing water saturation. The maximum number of rows allowed in this table is 100.For the size of the mobile region 1-S_{wcrit}-S_{orw}, the minimum allowed value is 0.02 and the minimum recommended value is 0.3. These conditions are applied for all temperatures, all interpolation sets and all per-block end-point values.

This table must have either 3 columns (S_w k_{rw} k_{row}), 4 columns (S_w k_{rw} k_{row} P_{cow}) or 5 columns (S_w k_{rw} k_{row} P_{cow} P_{cowi}).

The *LININTERP Option

This option requires that the wetting phase relative permeability entries in the *SWT table be equal to the corresponding liquid relative permeability entries in the *SLT table, between the critical saturations. If they are not, entries are inserted by interpolation to satisfy the condition. The expanded tables must fit within the allowed table dimensions.

Liquid-Gas Relative Permeability Table

If *NOSWC is absent, it is assumed that liquid saturation S_l does contain S_{wc}.

If *WATERGAS is absent, it is assumed that the k_{rwg} table is identical to the k_{rog} table. Thus, you can use *SLT without *WATERGAS to define k_{rwg} when using *OILWET, etc. This table must be entered at least once, even if gas is never present, and it must occur after *SWT, since an endpoint check uses information from *SWT.

For the size of the mobile region 1-S_{gcrit}-S_{lrg}, the minimum allowed value is 0.02 and the minimum recommended value is 0.3. These conditions are applied for all temperatures, all interpolation sets and all per-block end-point values.

When *NOSWC option is not used, k_{row} entries of *SWT before S_{wc} must be equal to k_{row} (S_{wc}), since Stone's models assumes that the endpoint value is k_{row} (S_{wc}). In this case, the only reason to have table entries for $S_w < S_{wc}$ is for P_{cow}. When *NOSWC is used, this restriction is lifted [46].

5.1.3 Component Properties

Solid or Trapped Components

These are components numy+1 to n comp, and appear only in the solid or immobile phase state. These components require only basic data such as density and heat capacity. Examples of such components are:

a) coke fuel created by cracking reaction, b) a component in the adsorbed or trapped state due to non-equilibrium mass transfer, c) rock that will dissolve, such as carbonate.

If there is at least one solid component then there must be at least one reaction, otherwise that component's moles will not be conserved.

5.1.4 Non wetting phase relative permeability hysteresis:

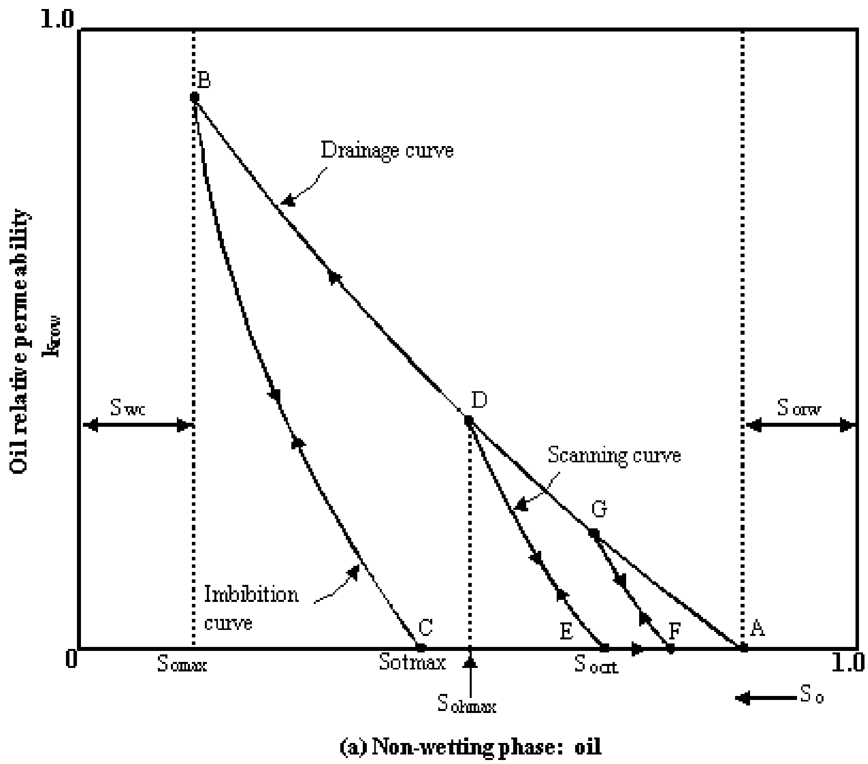

Fig 5.1 Hysteresis effect on non wetting phase relative permeability

If oil saturation increases monotonically from S_{orw} (point A) to the maximum oil saturation $S_{omax} = 1.0 - S_{wc}$ (point B), the drainage curve AB will be followed (see Figure 5.1). If oil saturation then decreases from B all the way to C, the imbibition curve is used. If the drainage or imbibition process is reversed at some point between, the relative permeability will be obtained from a scanning curve [46].

If a drainage process is reversed at some intermediate oil saturation S_{ohmax} (point D), a scanning curve DE is created. The end points of a scanning curve are the trapped oil saturation (S_{ocrt}) and the historical maximum oil saturation reached in the run (S_{ohmax}).

For any state on the scanning curve DE, change back to drainage will stay on the same scanning curve until S_{ohmax} is reached. When the state returns to the drainage curve at D, if drainage continues, the state will follow DB, until imbibitions again succeeds [46].

Another situation may arise when oil saturation decreases at the state of point E. This could happen if oil phase is burnt or dissolved. Then at a point F to the right of E, a subsequent drainage process would result in a scan upward to the drainage curve at point G.

The Carlson method

(*CARLSON) method needs to update the historical maximum oil saturation (S_{ohmax}) for each grid cell during the simulation. If the oil saturation equals or exceeds the historical maximum, S_{ohmax}, the drainage curve will be used to determine the value of the oil relative permeability. On the other hand, if the oil saturation in a grid cell falls below S_{ohmax}, a scanning curve will be employed. In constructing the scanning curve, the approach is based on the assumption that the scanning relative permeability is equal to the drainage relative permeability evaluated at the free oil saturation, S_{of}, that is:

$$k_{row}^{scan}(S_o) = k_{row}^{drian}(S_{of}) \,.. \tag{5.1}$$

Where the free oil saturation S_{of} is obtained from the following equation:

$$S_{of} = S_{orw} + 0.5\left[(S_o - S_{ocrt}) + \sqrt{(S_o - S_{ocrt})^2 + \frac{4(S_o - S_{ocrt})}{c}}\right] \tag{5.2}$$

In (5.2),

S_o: Grid cell oil saturation;

S_{orw}: Residual oil saturation for the drainage curve;

S_{ocrt}:

Trapped oil saturation calculated from

$$S_{ocrt} = S_{orw} + \frac{S_{oh\max} - S_{orw}}{1 + c(S_{oh\max} - S_{orw})} \tag{5.3}$$

C:

Land constant calculated from

$$C = \frac{(S_{o\max} - S_{ot\max})}{(S_{o\max} - S_{orw})(S_{ot\max} - S_{otrw})} \tag{5.4}$$

S_{ohmax}: Historical maximum oil saturation;

Sotmax: Inputted maximum trapped oil saturation of the imbibition curve.

The scanning curves constructed by the Carlson method retain a geometrical simplicity since the only hysteretic parameter inputted is sotmax.

The Killough method

(*KILLOUGH) method renders more user control on the formation of the scanning curves. Similar to the Carlson's, it uses the same formula, (4.3) to compute the trapped saturation S_{ocrt}, but the relative permeability on the scanning curve is calculated by either a relative permeability interpolation

$$k_{row}^{scan}(S_o) = k_{row}^{drian}(S_{oh\max}) * \frac{k_{row}^{imbib}(\overline{S_o})}{k_{row}^{drian}(S_{o\max})} \tag{5.5}$$

Or a saturation interpolation

$$k_{row}^{scan}(S_o) = k_{row}^{drian}(S_{oh\max}) * \left(\frac{(S_o) - (S_{ocrt})}{(S_{oh\max}) - (S_{ocrt})} \right)^{hyexo} \tag{5.6}$$

Where are the relative permeability values on the drainage and imbibition curve and the normalized oil saturation in (5.5) is computed from

$$\overline{S_o} = \frac{(S_o - S_{ocrt}) * (S_{o\max} - S_{ot\max})}{S_{oh\max} - S_{ocrt}} + S_{ot\max} \tag{5.7}$$

5.1.5 Chemical reactions

Chemical reactions have traditionally been used almost exclusively in combustion processes. However, reactions may be used in any thermal or isothermal simulation if desired. Since reactions are treated as source/sink terms for each component and energy, they may be thought of as another way in which to link together the different components of a problem when rate is important. In particular, interphase mass transfer rates can be modeled, involving either well defined components or "dispersed phase" components such as emulsion droplets.

The general heterogeneous mass transfer reaction no. k is represented symbolically as

$$\sum_{i=1}^{n_c} s_{ki} A_i \rightarrow \sum_{i=1}^{n_c} s_{ki} A_i + H_{rk} \tag{5.8}$$

Which proceeds at the rate of rk moles per day per reservoir volume? As expressed above, this relationship has one degree of freedom, which is a proportionality factor. The quantities ski, s'ki and Hrk can be multiplied by an arbitrary factor a, but rk must be divided by a so that the source/sink terms remain.

$$\left(s_{ki} - s_{ki}\right) * r_k and H_{rk} r_k \tag{5.9}$$

Usually the factor is chosen such that ski = 1 for the main reacting component.

Kinetic Model [46]

The kinetic model, also known as reaction kinetics, determines the speed of reaction rk. The general expression is

$$r_k = r_{rk} * \exp\left(\frac{-E_{ak}}{RT}\right) * \prod_{i=1}^{n_c} C_i^{ek} \tag{5.10}$$

The activation energy Eak determines the temperature dependence of rk. While the enthalpies of reaction can be characterized between well defined limits (and can even be calculated from first principles); the observed activation energies can vary dramatically. This is because certain components in the rock surface can act as catalysts. The concentration factor for reacting component i is

$$C_i = \varphi_f \rho_j S_j x_{ji} \tag{5.11}$$

Where j is the phase in which component i is reacting, and xji represents water, oil or gas mole fractions. For the solid component

$$Ci = \varphi_v c_i \tag{5.12}$$

The partial pressure form Ci = yi pg is available also.

The factor rrk is the constant part of rk. Its unit can be quite complex, and must account for the units of the various Ci, which are moles per pore volume or pressure, raised to the power of eik and then multiplied together.

The kinetic model can represent a reacting component in only one phase at a time. If a component reacts in more than one phase, it must be modeled in two separate reactions.

Mass and Volume Conservation

Because the component conservation equations have mole units and the reactions are treated as source/sink terms, moles of each component and energy will be conserved. However, the reaction stoichiometry should be mass conserving as well in order for the reaction to make sense physically. This is important especially when the molecular weight of a pseudo-oil component is not well-defined or is arbitrary.Mass-conserving stoichiometry satisfies the following

$$\sum_{t}^{n} = 1skiMi = \sum_{t}^{n} = 1skiMi \qquad (5.13)$$

Even though a molecular weight is not required by the STARS model for the solid component, a reasonable value should be chosen for the above calculation.

If mass is not conserved in a reaction, the effect probably will not show up in the simulation until the final results are analyzed or compared with a laboratory report.

On the other hand, conservation of volume during reaction is not required in general. However, there is one condition under which large volume changes caused by reactions should be avoided. It is when Sg = 0 and there are reactions between liquids, or between liquids and solids.

5.2 Field description

Reservoir model

The Reservoir is a heterogeneous carbonate reservoir. The original oil in place is 31.7 MMbbl. A number of group B wells are assumed to have been drilled. The reservoir has three layers as shown in (Figure 5.2).

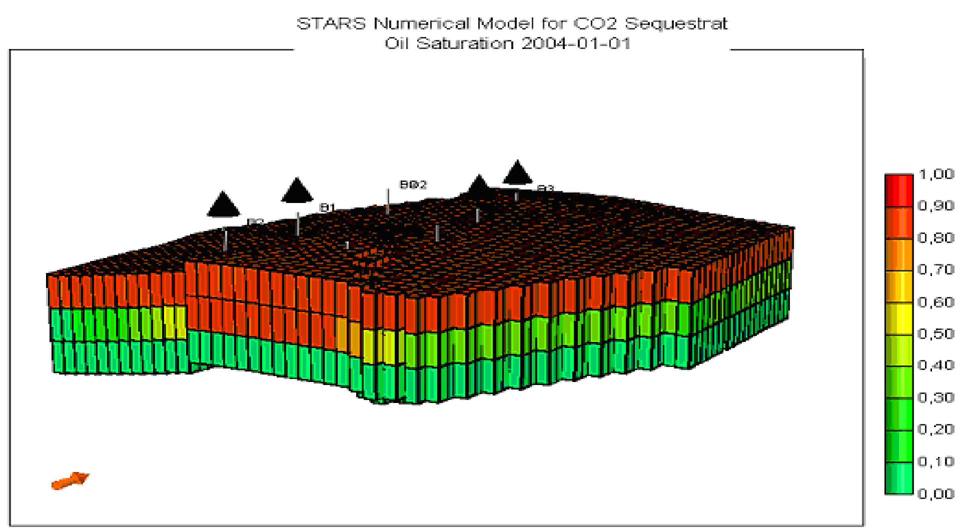

Figure 5.2 a 3-D description of the structure

The average depth is 1400 m and the initial pressure is 18044kpa with average temperature of 143.1 F°. The number of the grids used is 40*40*3 (4800).With a Cartesian grid dimension of 40*40*67 meters(see Figure 5.3).

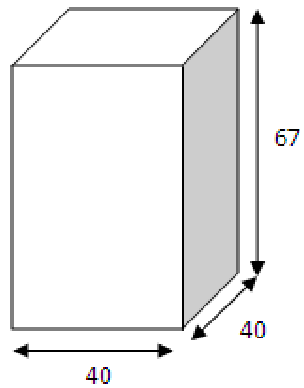

Figure 5.3 Element size (meters)

Production and injection wells

Wells are drilled from the location of well and their perforation locations are taken from a proposed field history. (Table 5.1) shows the wells and their depth and perforations.

Table 5.1 Well locations and depths as proclaimed in the model

	B1	B2	B3	B7	B8	B9or (CO_2)	CO_2-2
Grid location (Perf)	10.23.1	9.31.1	20.7.1	22.23.1	21.15.1	10.10.1	closed
	closed	9.31.2	20.7.2	22.23.2	21.15.2	10.10.2	closed
	closed	9.31.3	20.7.3	22.23.3	21.15.3	10.10.3	26.37.3
Max Depth(m)	1297	1432	1395	1436	1371	1435	1428

The mobility ratios around wells

One of the main characteristics to decide whether a layer is appropriate for CO_2 injection is mobility ratio. STARS-CMG has three options for defining the wells: without mobility consideration, when mobility was calculated implicitly(more realistic) and mobility implicitly calculated when connected to other layers. When the"MOBWEIGHT" option is used (the third case which is our case) the mobility for well is calculated internally. The layer rate for the injected phase at reservoir conditions is

$$q = wi * (Phasemobility) * (Pblock - Pwell) \tag{5.14}$$

Which relies on mobility weighting for each layer. The total mobility is that of the fluid phases in the grid block into which the well is injecting.

A) Rock properties

The represented properties in this section are two of the most important properties namely, porosity and permeability distributions.

Porosity distribution

In order to be able to know the reservoir storage capacity, having an idea about the porosity which is an important factor in the CO_2 sequestration process must be known. Well logging was used for determining and evaluating the porosity distribution. (Figures 5.4-5) show the distribution of porosity in the pay zone.

The available gamma ray and sonic logs from well B1 were used to gather information about the formations of B field. The gamma ray logs are used to find the boundaries and clay type of each zone. (Figure 5.6) explains a sample gamma ray log of well B1.

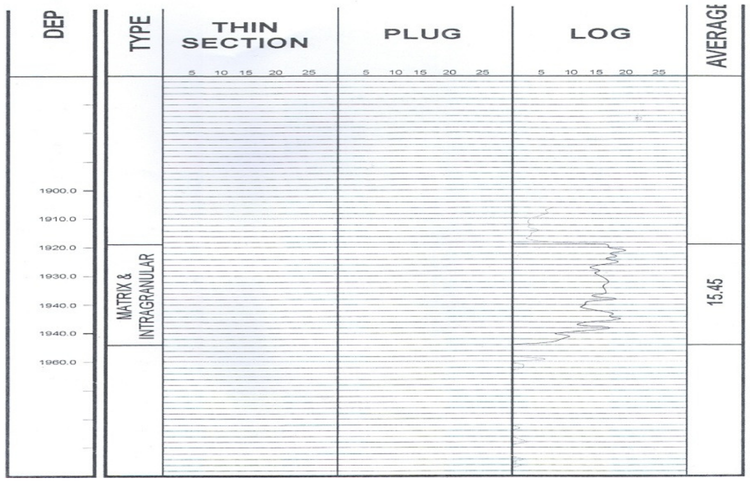

Figure 5.4 Porosity log for well B1 [48]

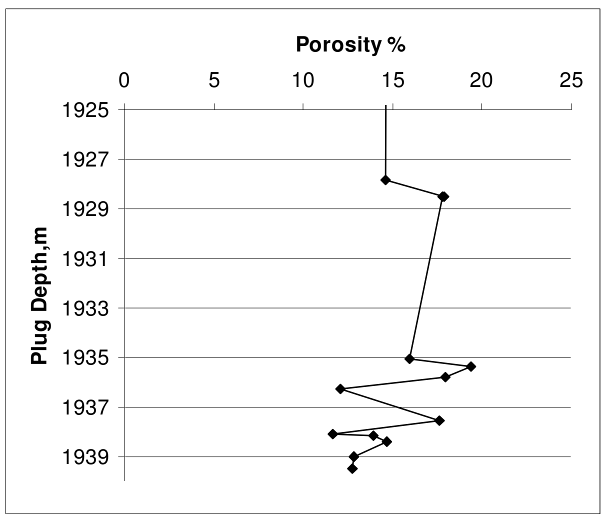

Figure 5.5porosity of the pay zone for well B1

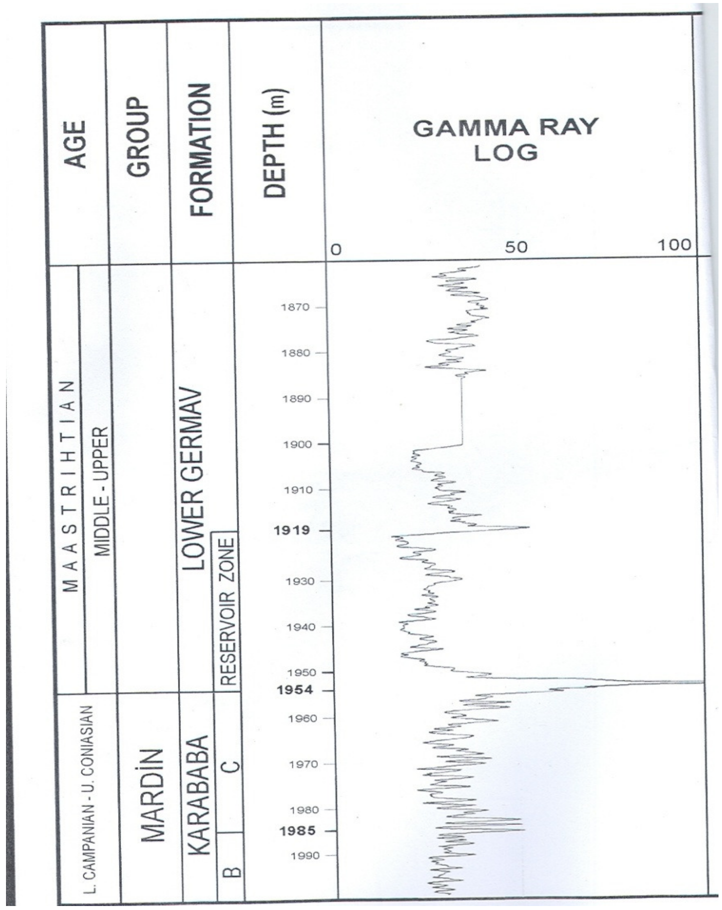

Figure 5.6 Gamma ray log for well B1 [48]

In addition, the sonic log (Figure 5.7) together with density log was used to find the porosities and then from the graph of permeability and porosity the effective porosities and lithology of the formation was found.

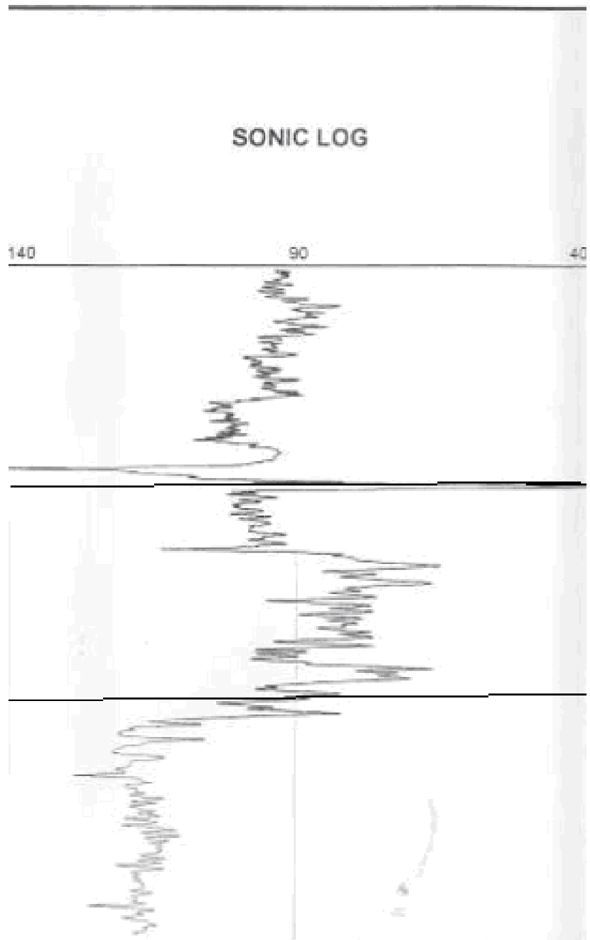

Figure 5.7 sonic log [48]

It was found that the formation is composed of three zones in which the second zone is the main reservoir or pay zone. The lithology of the reservoir is limestone in the upper layer, dolomite and dolomitic limestone in the second and third layers, respectively [48].

These obtained values are assumed to be the same for wells B2, B3 and B8.The porosity distribution, is represented in (Figure 5.8).

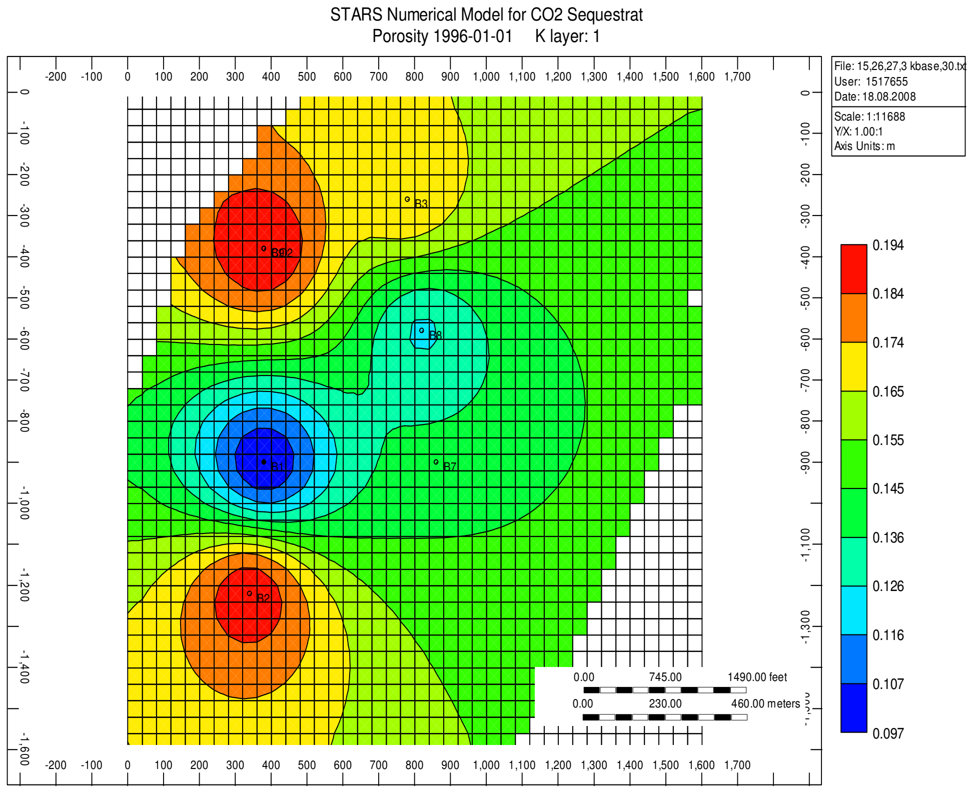

Figure 5.8 porosity distribution of zone 2

Permeability distribution

Permeability distribution will determine the fluid dynamics in most reservoirs. High permeability values will provide the chance of a higher injection rate as well as higher flux within the reservoir.

DST results are used for obtaining the permeability distribution in the reservoir. (see Table 5.2) and (Figures 5.9-5.11).

Table 5.2 Drill stem results for the different wells in B group

B1	Well bottom hole pressures (psi)
07.11.1995	2580
09.11.1995	2619
B2	
01.01.1997	2322
03.01.1997	2380
B3	
20.12.1996	2578
B8	
25.05.1998	2153
B9	
16.12.1998	2246

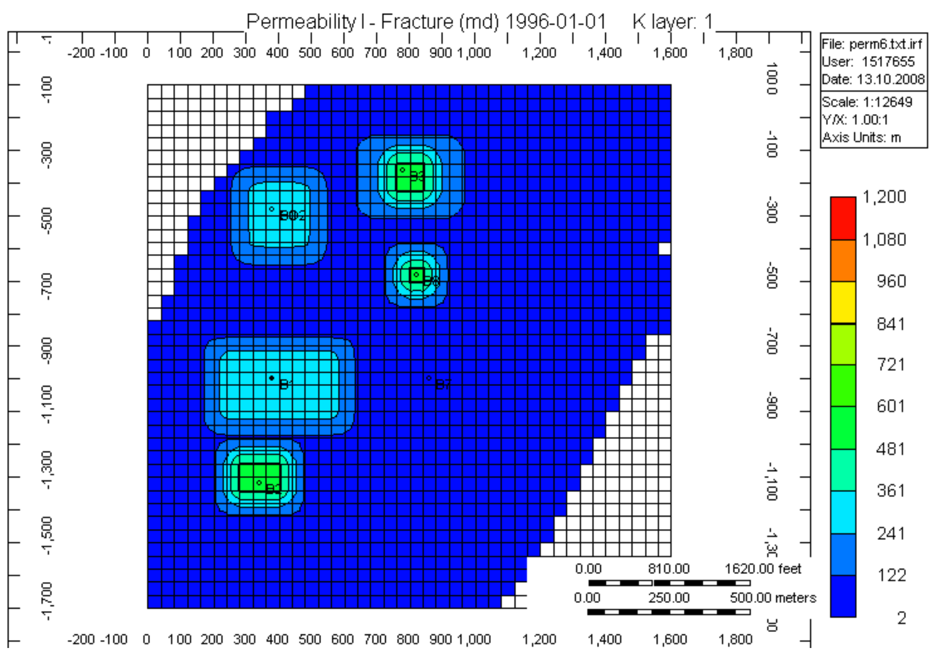

Figure 5.9 Permeability distributions in B well group for Layer 1

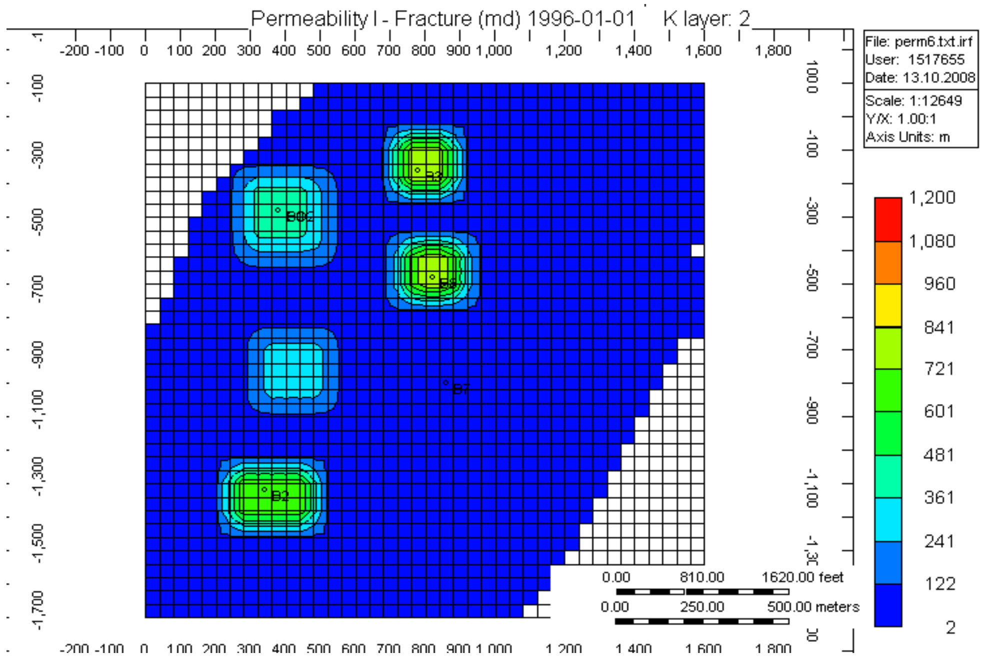

Figure 5.10 Permeability distributions in B well group for Layer2

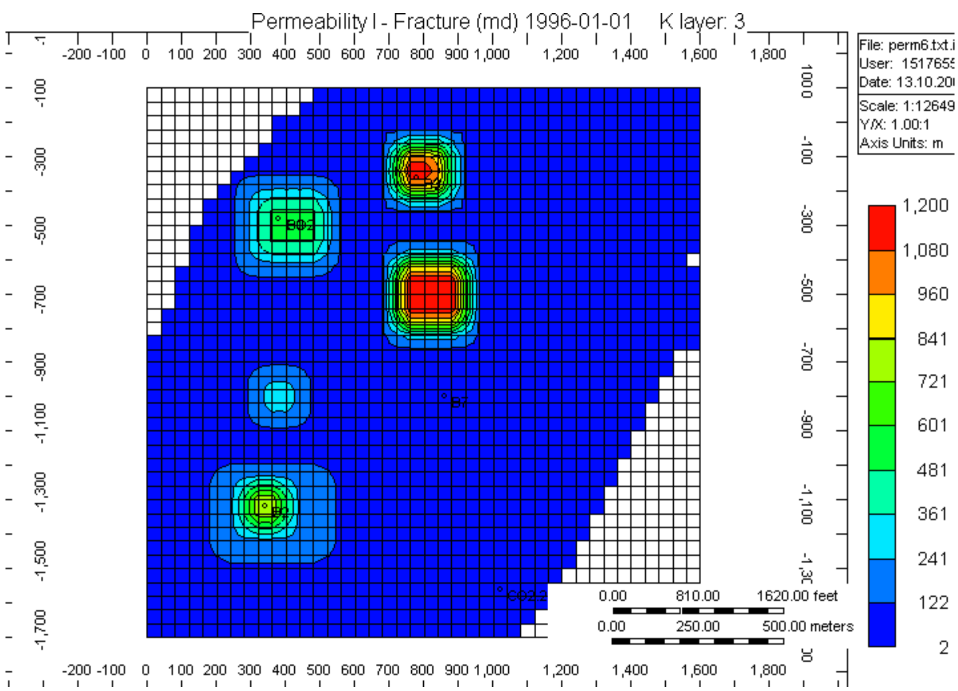

Figure 5.11 Permeability distributions in B well group for Layer3

B) Relative permeability representation

Since the relative permeability is an important factor in determining the mobility ratio and the injectivity of CO_2, for a good representation of the reservoir, it is crucial to carefully examine each and every region.

Thus, oil and water permeability were obtained from core analysis; and were changed during history matching by trial and error. And since, gas relative permeability was not available, the gas –oil relative permeability curves were generated by CMG –STARS.

STONE 2 method is used. STONE 2 is utilizing the two phase relative permeability measurement as a correlation of the three phase relative permeability curves. The porosity spans on a wide range 0.09-0.19, which indicates the possibility of channels and fractures. (Figures 5.12-13) show the relative permeabilities that were used in history matching.

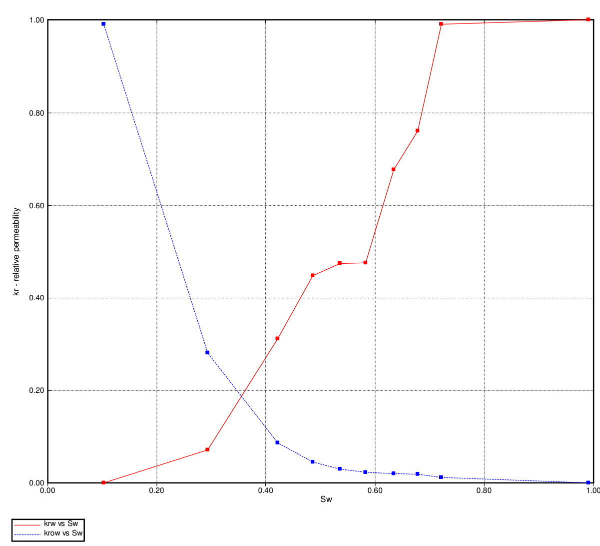

Figure 5.12 relative permeability curves for oil and water

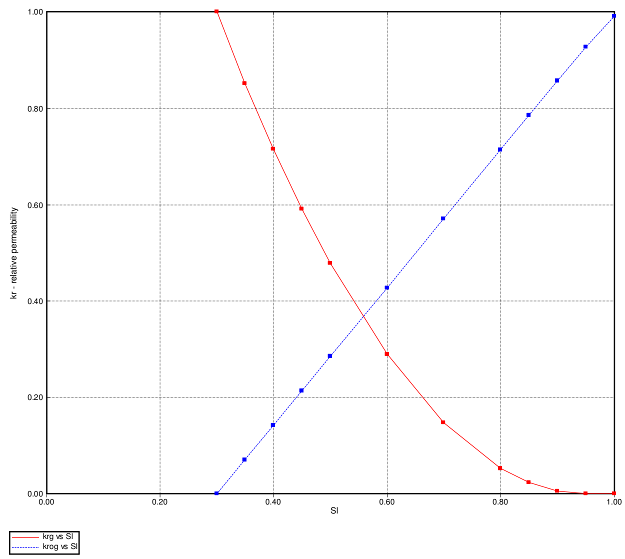

Figure 5.13 relative permeability curves for oil and gas

C) Fluid properties

Initial reservoir pressure was 2616.3 psi, but after 8 years of producing oil the pressure dropped to 2032.4 psi. CO_2 is available of 350M scf/day to be injected at the beginning of 2008 and continue for 20 years. Twenty years later the sequestration will be monitored for another 17 years. The maximum injection pressure was assumed to be 10% higher than the initial reservoir pressure. However, a safety factor of 50 psi was considered when the gas was injected. In other words maximum injection pressure was 2740.5 where the initial pressure was 2790.

To know the amount of injectable gas, we need to know the total emission amount accompanied with the practical limitations associated with our reservoir. The source of emission is a thermal power plant with two units A and B, located in the South Eastern part of Turkey. The highest injection rate in the world is of 40000 rbbl/day; and the typical injection rate of 3000 rbbl/day[49]. unit B emission equivalent to the yearly emission amount times formation volume factor (FVF)for pure CO_2. FVF was found by applying (Equation 6.2):

$$Bg = \frac{Pstp}{Zstp * Tstp} * \frac{ZT}{P} \quad (5.15)$$

Where:

stp= standard conditions of 60F

P stp= 14.7 psia ,Zstp = 1 for ideal gases

T stp= 60F

T = reservoir temperature F

P= reservoir pressure at the time of injection

Z= compressibility factor for pure CO_2, From [42] the z factor chart yields in Figure 5.14.

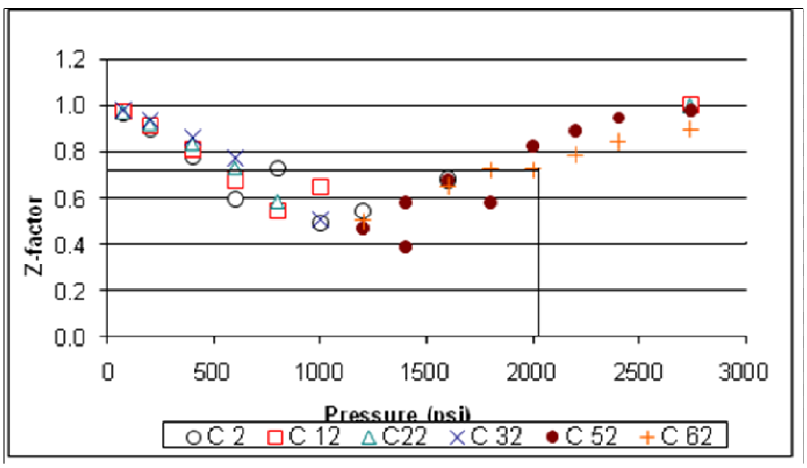

Figure 5.14 Z factor for pure CO_2 at different pressures and temperatures after Parlaktuna [49]

From the amount of total emissions, it was found that the daily obtainable free CO_2 is equal to 350Mscf/day. From (Equation 5.14) Bg is calculated to be 0.0067rcuft/cuft[49].The software used to estimate the compressibility factor was previously, proved to have an error of less than 1% [49]. Therefore, many injection wells are needed to treat the pollution launching from the power plant.

The oil in place is the reciprocal of molar density of oil at the reservoir conditions. Hence, the original oil in place in place is 31.7MMbbl of oil.

Total volume injected = 347886scf /day *365* 20 years

= $2*10^9$ scf (standard conditions)

= 17118500 rcf (reservoir conditions)

D) Determining the minimum miscibility pressure (MMP)

Since the MMP (Minimum Miscibilty Pressure) is highly dependent on oil composition, it was estimated by finding the molecular weight and correlating the result with the results proposed by(Mungan and Johansson) [32]:

$$MW = \left[\frac{7864.9}{API^{o}}\right]^{\frac{1}{1.0386}} \tag{5.16}$$

Where MW is the molecular weight of oil, API is the API gravity. From the specific gravity of the light oil the API gravity was calculated. The well known equation of converting the specific gravity to API gravity at 60 F°:

Where Sg is the specific gravity of oil.The obtained API gravity is 26°API. From (Equation 5.16) the molecular weight was found to be 243.47. According to Mungan and Johansson [32] the API gravity with reservoir temperature is sufficient for the calculation of MMP (Figure 5.15). The reservoir has a temperature of 143.6 °F which will lead to a MMP approximated as 2200 psi.

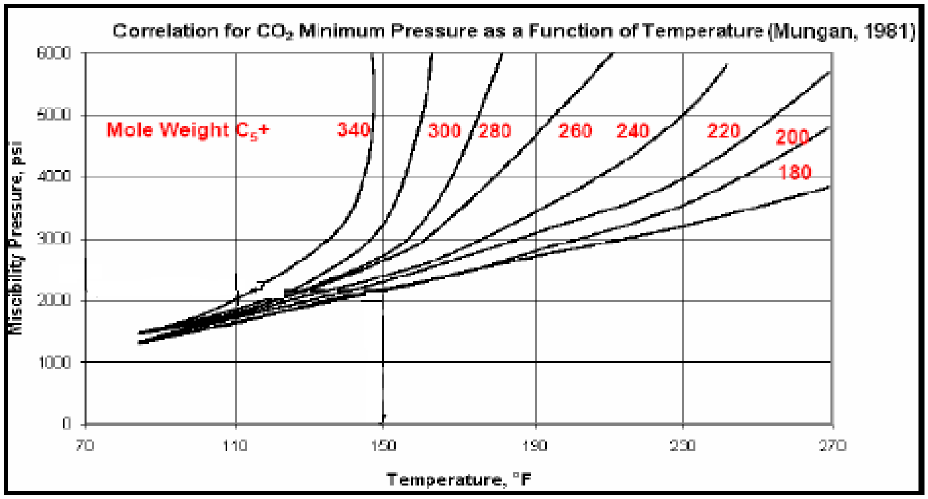

Figure 5.15 Determining MMP after Mungan and Johansson [32]

E) Properties of injected CO_2

The second thermal plant unit (B) emits ≈ 52.5 MMMscf of CO_2 annually, assuming that CO_2 is captured as a 70% percent equivalent to 37.6 MMM scf/year.

Reservoir pore volume = $6.65*10^7$meters

Formation volume factor (FVF) was calculated and equal to 0.0067 rft^3 /ft^3.

CHAPTER 6

RESULTS AND DISCUSSION

6.1 History matching

The Field

The well B1 has started production in February 1996, B2 in April 1997, B3 in March 1997, B8 in November, 1998 and B9 in March 1999. Aside from B8 and B9 no well was shut in during the eight years of history matching period. The oil production from the field started in January 1996. There were no gas production during the production history; and the bottom well pressures declined rapidly without gas breakthroughs. However, water cuts have also increased dramatically. By the end of the 8 year period 12.5 MMSTB of oil and 22.3 MMbbl of water was produced. The history matching was carried out using cumulative oil production, water cuts and bottom hole pressure data.

6.1.1 Production matching

Production data of B. field between the years 1996-2004 was provided.

The production was defined in a rate control and then matched as it was expected (see Figures 6.1-5).

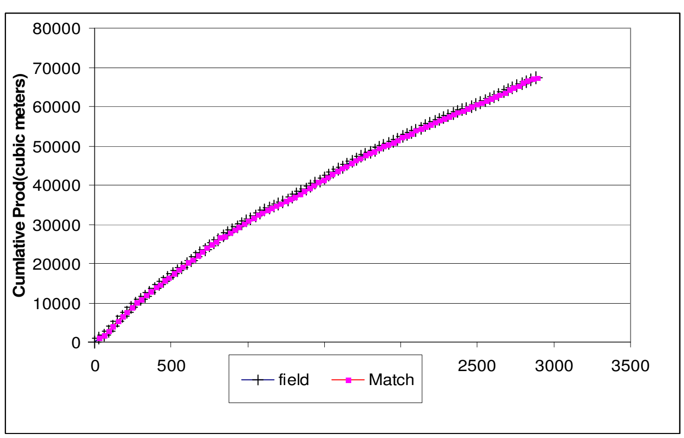

Figure 6.1 B1 production match

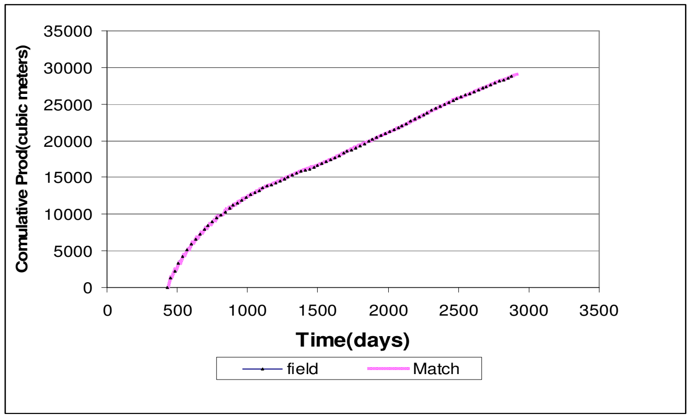

Figure6.2 B2 production match

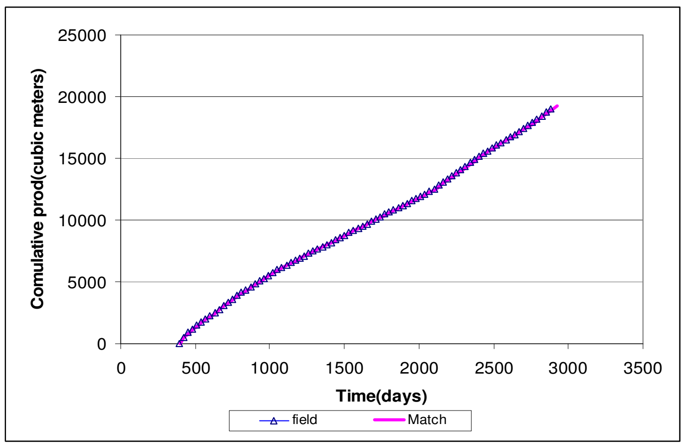

Figure 6.3 B3 Production match

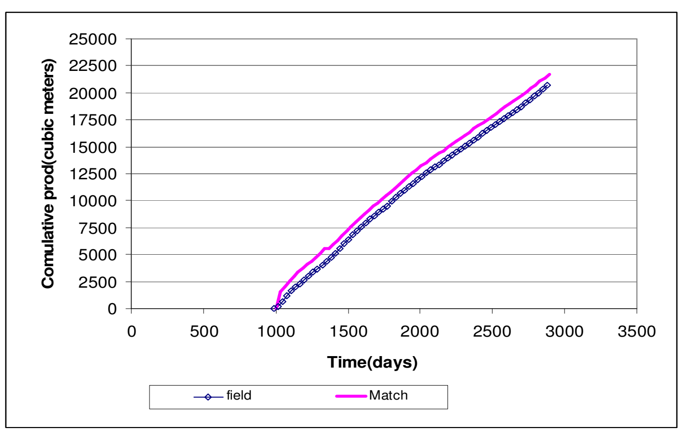

Figure 6.4 B8 Production match

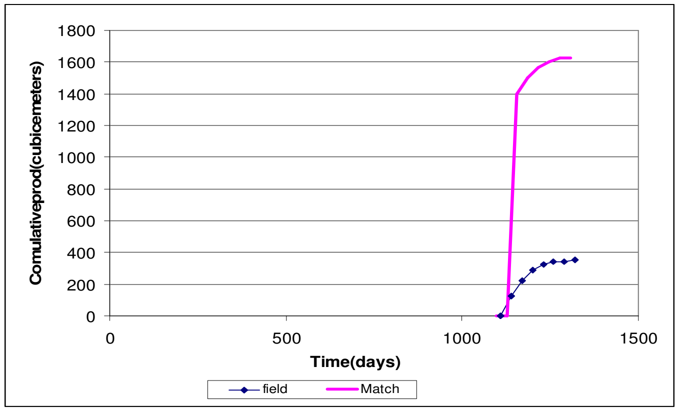

Figure 6.5 B9 Production match

The results show a good match for B1, B2, B3 and B8. Except for B9 a higher error margin was noticed and was ignored for that B9 has produced for a short period (three months).

6.1.2 Well Bottom hole pressure matches

Pressure data from drill stem test were matched using the trial and error procedure. Then the results were compared to field data. Since, for each well the pressure of a single or at most two dates were available, the matches were a rough guess. However, the matching was acceptable. (Figures 6.6-10) compare the results that were obtained from CMG-STARS simulations to these from the field.

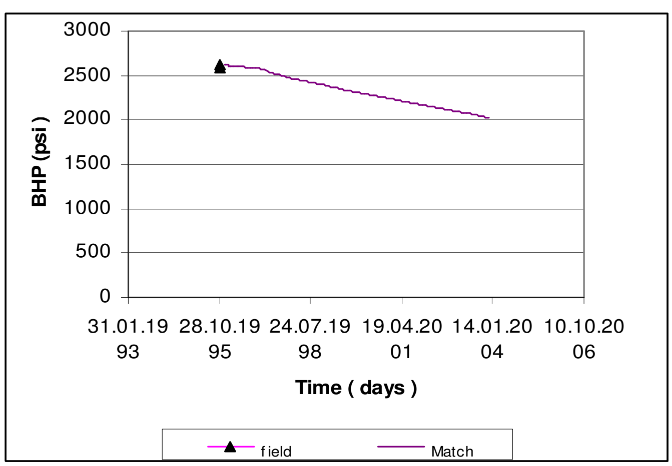

Figure 6.6 Comparison of field &Simulation data of BHP for B1

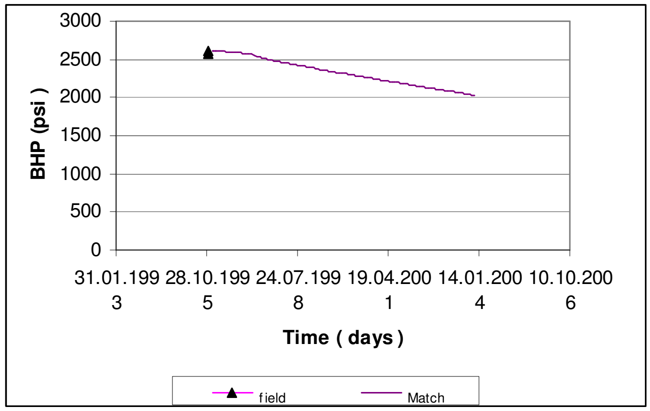

Figure 6.7 Comparison of field &Simulation data of BHP for B2

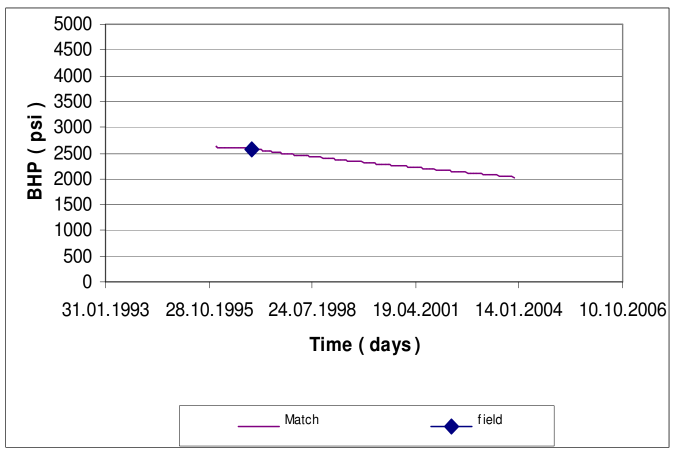

Figure 6.8 Comparison of field &Simulation data of BHP for B3

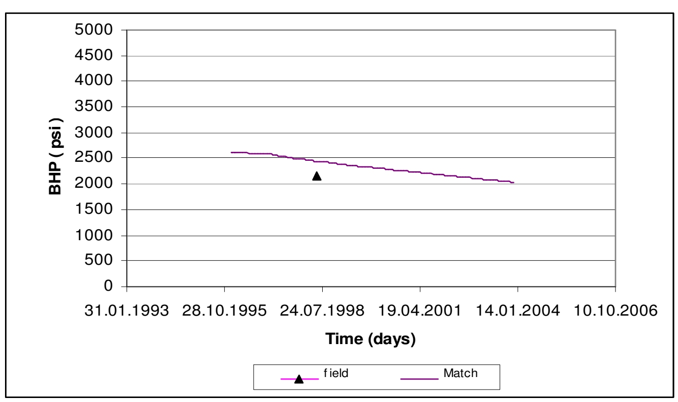

Figure 6.9 Comparison of field &Simulation data of BHP for B8

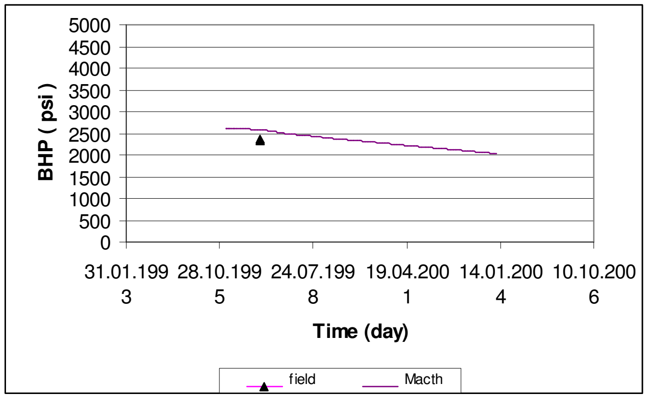

Figure 6.10Comparison of field &Simulation data of BHP for B9

(Figures 6.6-10) show a good match for B1, B3 and B8. But, wells B2 and B8 have an error margin in their match, still having a single point we could not improve the match more and chose to continue with last data type of history matching which is water cut data.

6.1.3 Water cut matching

When checking the water cuts, finding a match was a case sensitive. At first, the data that were obtained from the initial permeability distribution was used. Then, these data modified using the permeability multiplier option. Cases from one to eleven show different terms with different permeability multipliers. Meanwhile different solid concentration values, bicarbonate deposition frequency, temperature dependence on history matching and some handful numerical assumptions were used. Next, In order to evaluate the goodness of the match, the Root Mean Square Error (RMSE) Method was applied. High water cut values suggest the presence of a strong water drive aquifer.

Attempts were made to match field's water cut. This was done by assigning high permeability values around the wells as shown in cases 12-20. A traditional method to find the least erroneous approach to a problem was applied. Since the flow is mainly through fractures, this relied mainly on the changing values of fracture permeability. Equation 6.1 is the defining equation for Root mean square error (RMSE) method.

$$E_i = \sqrt{\frac{1}{n}\sum_{j=1}^{n}(P_{ij} - T_j)^2} \tag{6.1}$$

P is the value predicted by the individual program *i* for sample case *j* out of n sample cases; and *T* is the target value for sample case *j*.

A number of time steps were chosen and (Equation 6.1) was applied. Then the error summation was taken into account.

Applying the Root Mean Square Error (RMSE) Method

Water cuts obtained from different runs were compared by their RMSE, in other words, according to (Equation 6.3) . Eight water cut values are selected to include at least 3-8 points from each well and then (Equation 6.3) was used to obtain the residual analysis value for each model. The model data for the field is listed in, as in (Table A-1) and (Table A-2)[see Appendix A].

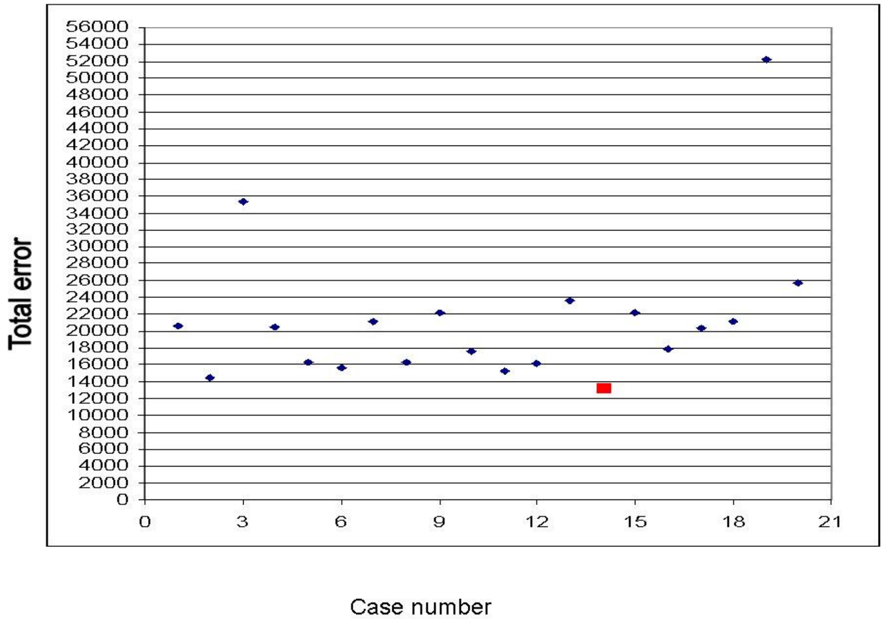

Figure 6.11 water cut error squares for different cases

Water cut match for best case scenario

It was found that a case numbered 14 was the most accurate case for water cut matches (see Appendix A). Twenty simulations were tried to obtain water cut matches (see Tables A.1). The cases started by modifying the permeability that was previously proposed and then the permeability around wells, reaction frequencies, solid concentration, isothermality and tolerance assumptions were changed in a trail and error approach until reaching the best accuracy margin possible.

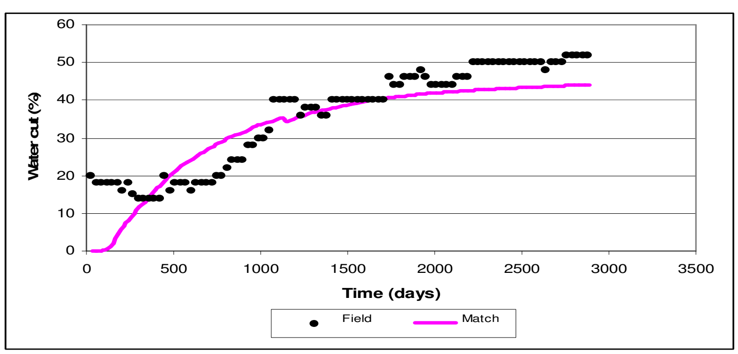

Figure 6.12 water cut match for B1

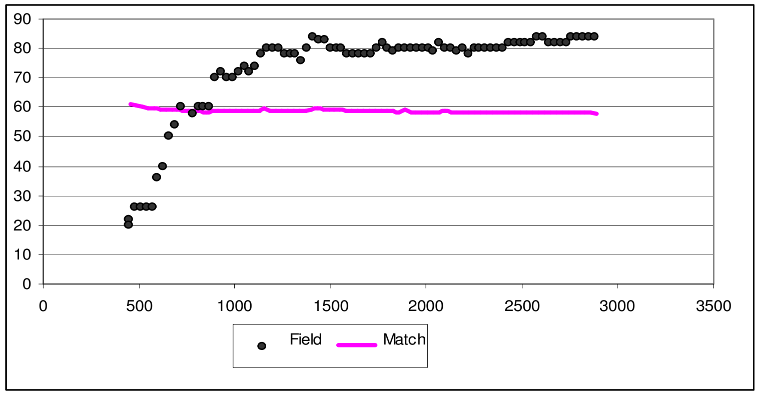

Figure 6.13 water cut match for B2

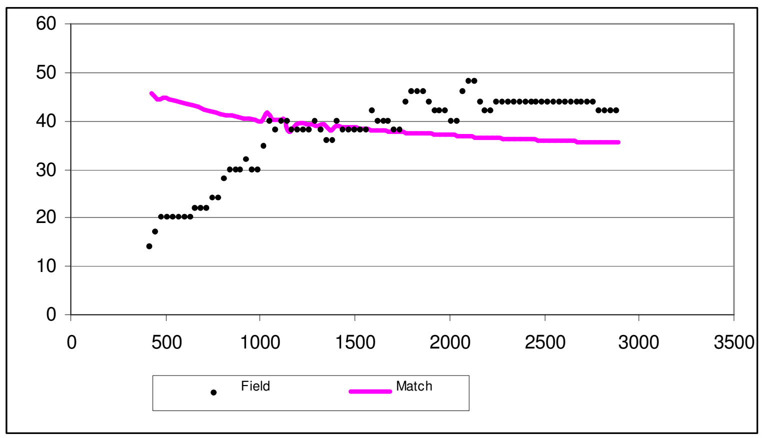

Figure 6.14water cut match for B3

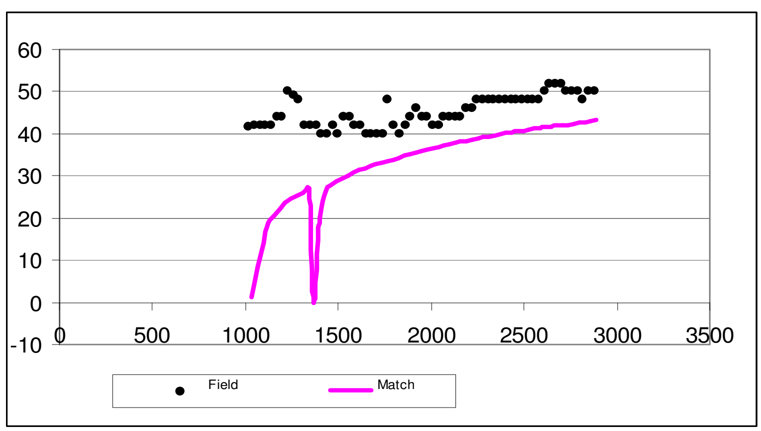

Figure 6.15 water cut match for B8

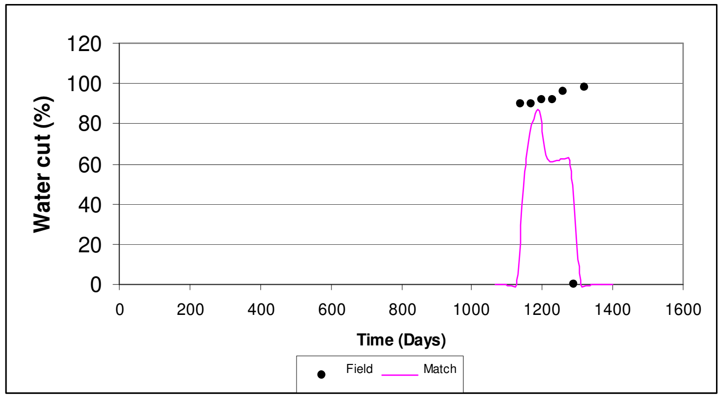

Figure 6.16water cut match for B9

Relying on the least amount obtained and when that changes between different wells, is becomes an arduous job. We have obtained an acceptable match for B1, B2 (thought partially) and B8. B3 and B9 did have neither an accurate match nor a trend that matches the field.

However, this was the best possible match one could get for the field.

6.2 CO_2 sequestration scenarios

Unlike conventional enhanced oil recovery methods, CO_2 sequestration aims at injecting a maximum amount of CO_2 with the ultimate goal of obtaining the maximum amount of oil recovery. The study of the simulation run period is limited to a 20 year injection of CO_2 and 37years of monitoring the storage process. As $Ca(HCO_3)_2$ is solid it will deposit at the bottom of the reservoir but the free CO_2 will segregate due to gravity to upper layer. Overall, the main purpose of the process is examining a successful and economical sequestration. It is attempted to magnify the amount of oil produced. Additionally, we will try to get the highest amount possible of gas trapped inside the reservoir.

6.2.1Constraints

Well head pressures had to be kept above 500kpa to assure surface equipments work and the bottom hole pressures had to be above 7300 Kpa(1070psi) to maintain a supercritical state of CO_2.

The corresponding bottom hole pressure for production wells are considered to be acceptable for the prediction phase. For overall check of the bottom hole pressure match.

The reservoir conditions prior to the sequestration process are listed in (Table 6.1).

Table 6.1Initial reservoir conditions

Current reservoir pressure	2032.45psi
Available gas for injection	≅350M scf /day
Starting date for gas injection	01.01.2008
Injection period, Monitoring period	20 years,17years
Max injection pressure	2740.5 psi
Reservoir fracture pressure	2790.5 psi

6.2.2 Prediction cases

Different factors are attempted to find an optimum case and many of which were successful. However, as in all gas injection for EOR methods, the pressure increased to a point that showed warnings of possible accession of the parting pressure which eventually stopped many of these runs. For a full list of the cases tried (see Table 6.2) and (Appendix B).

Table 6.2
Simulation run results

Case #	Factors	Duration	Oil (mmbbl)	CO2 (mmscf)	Gas Saturation - Average	Final pressure (psi)	Recovery %
Case 1	Base Case	7300	7.34	-	-	63.51	23.15
Case 2	3 injection wells	1752	1.95	561.15	0.00241	1197.584	6.15
Case 3	2 injection wells	1547.6	1.57	367.2	0.102699	1350.534	4.95
Case 4	2 injection wells	1752	1.29	345.00	0.0013	1633.992	4.07
Case 5	2 injection wells	1241	1.20	214.	3.84E-21	1750.985	3.79
Case 6	3 injection wells	2190	1.63	803.73	0.008167	1786.146	5.14
Case 7	3 injection wells	3036.8	2.16	409.0	0.0027	1440.407	6.81
Case 8	3 injection wells	730	1.27	260.5	0.00105	1513.536	4.01
Case 9	3 injection wells-2nd layer injection	4015	4.0	1449.6	0.002	1935.14	12.62
Case 10	2 injection wells	2555	2.55	844.7	0.0026	1994.687	8.04

Table 6.2
Continued

Case #	Factors	Duration	Oil (mmbbl)	CO_2 (mmscf)	Gas Saturation - Average	Final pressure (psi)	Recovery factor %
Case 11	2 injection wells-2nd layer injection	5475	4.75	1580.7	0.0064	1867.113	14.98
Case 12	1injection wells- 2nd layer injection	1547.6	1.92	791.28	0.0007	1801.135	6.06
Case 13	3 injection wells- 2nd layer injection	2058.6	1.6	672.7	0.0032	1513.182	5.05
Case 14	3injection wells- 2nd layer injection	1460	1.42	521.8	0.0051	1339.801	4.48
Case 15	3 injection wells- 2nd layer injection	328.5	0.32	122.03	0	2032.714	1.01
Case 16	1injection wells- 2nd & 3rd layer injection	1182.6	1.16	479.0	0.00012	1271.313	3.66
Case 17	3injection wells- 2nd & 3rd layer injection	846.8	0.87	216.58	0.0019	1668.206	2.74
Case 18	Single Injection well location optimization	13505	13.8	2630	0.0115	1995.306	43.53

Table 6.2
Continued

Case #	Factors	Duration	Oil (mmbbl)	CO_2 (mmscf)	Gas Saturation - Average	Final pressure (psi)	Recovery factor %
Case 11	2 injection wells-2nd layer injection	5475	4.75	1580.7	0.0064	1867.113	14.98
Case 12	1injection wells- 2nd layer injection	1547.6	1.92	791.28	0.0007	1801.135	6.06
Case 13	3 injection wells- 2nd layer injection	2058.6	1.6	672.7	0.0032	1513.182	5.05
Case 14	3injection wells- 2nd layer injection	1460	1.42	521.8	0.0051	1339.801	4.48
Case 15	3 injection wells- 2nd layer injection	328.5	0.32	122.03	0	2032.714	1.01
Case 16	1injection wells- 2nd & 3rd layer injection	1182.6	1.16	479.0	0.00012	1271.313	3.66
Case 17	3injection wells- 2nd & 3rd layer injection	846.8	0.87	216.58	0.0019	1668.206	2.74
Case 18	Single Injection well location optimization	13505	13.8	2630	0.0115	1995.306	43.53

Table 6.2
Continued

Case #	Factors	Duration	Oil (mmbbl)	CO2 (mmscf)	Gas Saturation - Average	Final pressure (psi)	Recovery factor %
Case 19	Single Injection well location optimization	11680	11.8	2550	0.0029	1289.797	37.22
Case 20	Single Injection well location optimization	3650	3.84	1337.6	0.0069	1934.049	12.11
Case 21	Single Injection well location optimization	3285	3.48	1211.7	0.0046	2144.853	10.98
Case 22	Optimum location –layer optimization	6073.6	6.10	2122.5	0.0052	1688.328	19.24
Case 23	Optimum location –layer optimization	6570	6.57	2834.2	0.0061	1826.759	20.73
Case 24	Optimum location –layer optimization	116.8	0.089	30.9	0.0001	2580.088	0.28
Case 25	Optimum location –layer optimization	481.8	0.48	170.0	0.0021	2309.902	1.51
Case 26	Optimum location –layer optimization	146	0.1357	46.85	0.0001	2580.088	0.43

Table 6.2
Continued

Case #	Factors	Duration	Oil (mmbbl)	CO_2 (mmscf)	Gas Saturation - Average	Final pressure (psi)	Recovery factor %
Case 27	Optimum location – pressure	8760	9.1	2550	0.004	1481.46	28.71
Case 28	Optimum location – pressure optimization	13140	13.5	2550	0.007	1705.06	42.59
Case 29	Optimum location – pressure optimization	7081	7.11	2472.4	0.0046	1658.46	22.43
Case 30	Optimum location – pressure optimization	7081	7.126	2476.1	0.0045	1700.79	22.48
Case 31	Optimum location – pressure optimization	7358.4	7.40	2553.61	0.005	1811.28	23.34
Case 32	Optimum location – pressure optimization	6467.8	6.51	2265.40	0.0034	1481.12	20.54
Case 33	Optimum location – pressure optimization	7329.2	7.72	2553.66	0.00467	1751.01	24.35
Case 34	Rel perm optimization-Firo	13505	13.6	2400	0.0032	1935.14	42.90
Case 35	Rel perm optimization-Generic	4745	4.74	794.71	0.002	1898.91	14.95

Table 6.2
Continued

Case #	Factors	Duration	Oil (mmbbl)	CO2 (mmscf)	Gas Saturation - Average	Final pressure (psi)	Recovery factor %
Case 36	Fracture spacing Vertical	9855	10.2	1230	0.01	2073.68	32.18
Case 37	Fracture spacing horizontal	6205	6.02	1021	0.006	1549.87	18.99
Case 38	Fracture spacing higher homogenou	13500	13.6	1230	0.0018	933.72	42.90
Case 39	hys Hystersis Carlson – max trap of 0.4	1460	1.936	568.8	0.0007	1165.00	6.11
Case 40	Hysteresis Killough – max curve of 1.5	1460	1.93	568.8	0.0007	1165.00	6.09
Case 41	Hystersis – Carlson hys Stgmax 0.2	1460	1.92	561.6	0.0012	1249.26	6.06
Case 42	hys Hystersis Carlson – max trap of 0.2	1460	1.92	561.6	0.0007	1165.00	6.06
Case 43	Hysteresiss Killough – max curve of 0,75	1460	1.93	568.84	0.0007	1165.00	6.09
Case 44	Hysteresis Carlson – max trap of 0.1	1518	2.7	368.8	0.0031	1470.41	8.52

Table 6.2
Continued

Case #	Factors	Duration	Oil (mmbbl)	CO_2 (mmscf)	Gas Saturation - Average	Final pressure (psi)	Recovery factor %
Case 45	Hystersis Killough – max curve of 0.375	1095	1.69	468.41	0.003	1455.35	5.33
Case 46	Impurity injection 0.2CO	1825	1.84	225.9	0.001	1957.34	5.80
Case 47	Impurity injection 0.2H2S	1095	0.94	114.2	0.0008	1780.62	2.97
Case 48	Impurity injection 0.1H2S	1182.6	0.79	99.21	0.00069	2295.24	2.49
Case 49	Impurity injection 0.05H2S	1182.6	1.14	398.4	0.0009	2423.53	3.60
Case 50	Impurity injection 0.1CO	1503.8	1.48	185.9	0.0016	2153.98	4.67
Case 51	Impurity injection 0.05CO	1576.8	1.53	533.3	0.0007	2505.06	4.83

6.2.2.1 Injection well locations

The location into which a well can be drilled varies from project to another. Therefore, we have divided this process into two basic stems:

Regional injection

The total amount of carbon emissions was injected from a single well in two different cases. Injection wells are obtained by shutting in a production well and reopening it as an injection well.

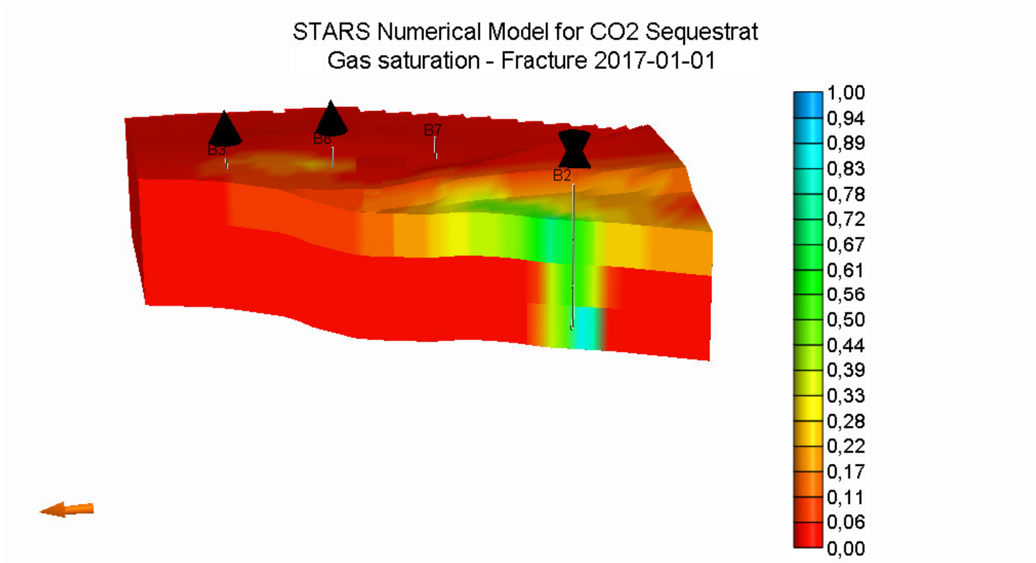

Figure 6.17Gas saturation at the end of shut in period for single well injection in B2

The first case has resulted in the production of 3.48 MMbbl of oil and 1211.7 MM cubic feets of CO_2 sequestered before reaching the fracture pressure after 9 years (Figure 6.17). This is less than the base case (without CO_2 injection) which produced 7.34 MMbbls of oil and lasted for 7300(20years).

The second case includes injection from a less permeable region. In which B7 is opened as an injection well where the production wells are B1, B2, B3 and B8. In this case the gas has a better sweep efficiency in the middle layer (i.e, a longer travel time to the upper layer)(see Figure6.18).

The results of injecting in well B7, are 11.8MMbbl of oil and 2550MMscf of CO_2 being, for 11680 days. Compared to base case, this case has a greater value both in oil recovery and stored CO_2 amount (see Figure6.18).

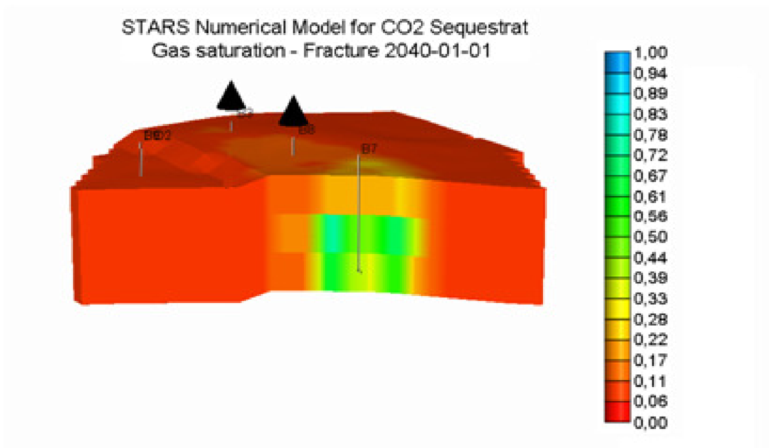

Figure 6.18Gas saturation at the end of shut in period for single well injection in B7 Injection well.

Next, two different cases at (CO2 and CO2.2) are considered to find the best possible well location. Studies suggested injecting in a scattered form. This is done to know if it is scattered or peripheral type of injection to be taken into account. These cases also reveal permeability distribution difference and exhibit the validity of injecting in an area that has a higher permeability.

Thus the followings are some of the characteristics of the following two cases:

Firstly, a case is injecting in well (CO2) after converting the well from a producer (B9) to an injector with production wells are B1, B2, B3 and B8. This case yielded to a recovery better than injecting in B2 (3.84mmbbl) and higher than the base case; and finally, a higher capacity of storing 1337.62 MMscf of supercritical CO_2 (see Figure6.19).

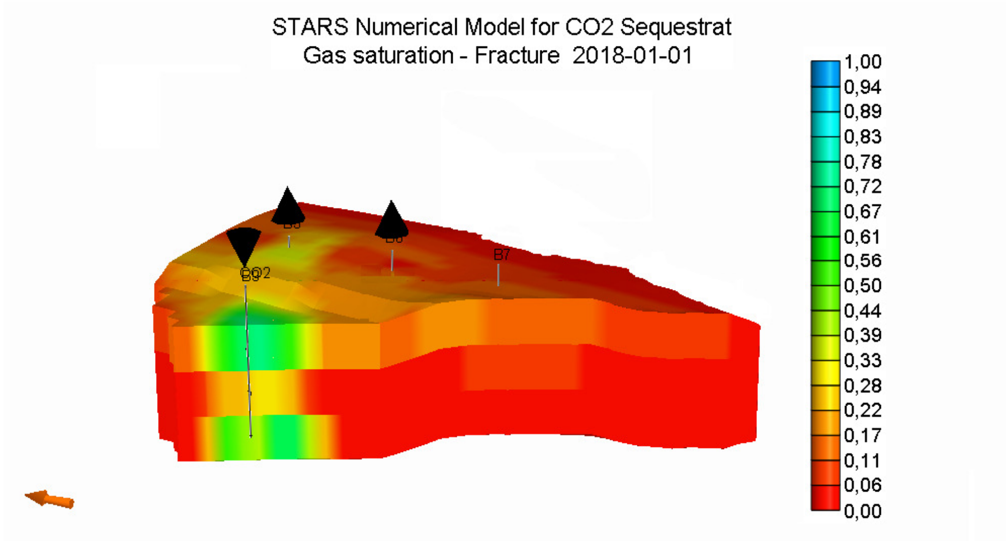

Figure 6.19Gas saturation at the end of shut in period for single well injection in CO2

Compared to injection from (CO2), in the fourth case the sweep efficiency in injecting from well (CO2.2) is better compare (Figures 6.19 and 6.20). However, the mildly permeable region increases the distance from the production wells which results in better residence time and late breakthrough times. Finally, injection well location from the reservoir boundary (spill points) are among the other reasons why (CO2.2) is the optimum well location (see Table 6.3).

Table 6.3 Distance between per wells (feet)

	B2	B9 or CO2	B7	CO2.2
B1	1057.7428	1574.8031	1443.5696	946.19423
B2	-	2755.9055	2002.9528	1950.7874
B3	3464.5669	1370.0787	1531.8241	1530.1837
B7	2002.9528	2321.5223	-	1312.336
B8	2624.6719	1673.2283	927.82152	955.38058
B9	2758.8583	-	2321.5223	1057.7428

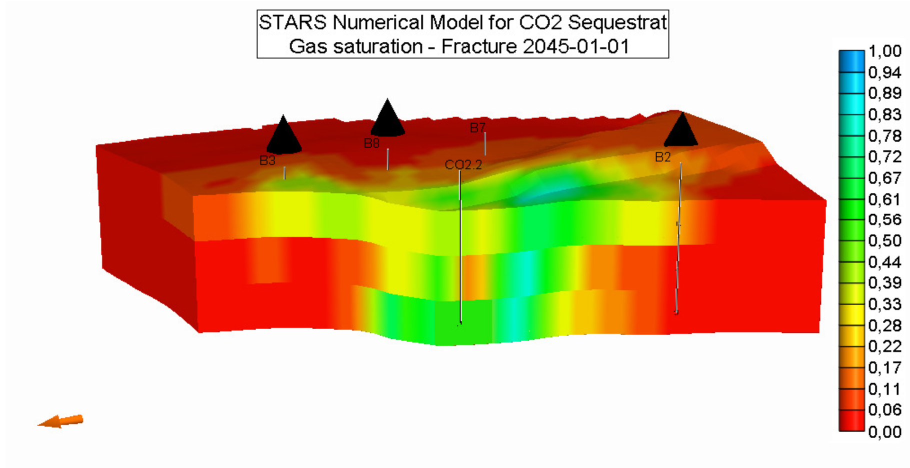

Figure 6.20Gas saturation at the end of shut in period for single well injection in CO2-2

Oil recovery by injecting from (CO2.2) reveals a chance of recovering 13.8 MMbbl of oil and the injection of CO_2 from group B wells. These cases are included as cases numbered (18, 19, 20, and 21) in (Table 6.2) and Appendix B.

6.2.2.2 Impact of Injection rates

Injection rates are studied using the maximum emission released from the plant of 9900 rbbl/day or 347M scf/day, for single well cases. Then two and three injections points are used with the rate of 174Mscf/day and 116Mscf/day respectively. Gravitational effects can be resisted when injection rates are high [16]. The factors that play a role in the deposition process are the characteristics of the porous media and injection fluid properties [13]. A better transfer rate and a larger residence time in the porous medium is obtained when gas injection rate is low. Apart from that, deposition reactions are better completed when the flow rate is low. Thus this will lead to precipitation in a higher rate. Paradoxically, Juanes and MacMinn [16] concluded that high injection rates are better for residual trapping (a highly important case when the study scope is of less than a century) and ultimately for overall CO_2 storage.

To verify which case is applicable for this field, we have used many injection rates for different depths and locations providing a constant injection pressure.

Factors that are included when discussing injection rates can be listed as: injection well location, number of injection wells, injection rates. As injection rate increased oil recovery and CO_2 stored amount increased leading to a better recovery and storage capacity (Table 6.4). Only two cases (case 18 and 19) have a higher oil recovery and longer production period (high recovery factor) than the base case. When the base case (without gas injection) has a 7.32mmbbl of oil produced, cases (18and 19) produce (12.4 and 11.8) MMbbl of oil respectively. It is worth noting here from the petroleum industry point of view that our main goal is to produce as much oil as possible. Therefore when comparing cases we prioritized high oil recovery case to high storage case.

The results are similar for simulation runs conducted at each injection rate. High rate cases are in single injection points where the injection is from the bottom of the reservoir and the assumed carbon emissions are being completely injected. As opposed to injection rate divided in two or three points results in gravity segregation dominated flow. Hence, less oil recovery can be achieved.

It was found that numerical instabilities in some simulation runs prohibit the simulation from progressing. Thus, only two viable cases were found to be comparable: case 18 and case 19. It was found that the oil rate of case 18 is 1020 bbl/day while that of 19 is 1010 bbl/day. Therefore, case 18 was decided to be the optimum case for well location and injection well number.

Table 6.4 Injection rate

Case #	Injection wells locations	# of Inject points	Inject Rate (sm^3/day)	Oil rcovered (mmbbl)	CO_2 stored (mmscf)	Duration (days)	Top Layer	Middle Layer	Bottom Layer
Case 25	CO_2.2	1	9900	0.48	170.07	481.8	-	x	x
Case 19	B7	1	9900	11.8	2250	11680	-	-	x
Case 20	CO2	1	9900	3.84	1337.62	3650	-	-	x
Case 21	B2	1	9900	3.48	1211.74	3285	-	-	x
Case 22	CO_2.2	1	9900	5.98	2440	5110	x	-	-
Case 23	CO_2.2	1	9900	6.57	2834.2	6570	-	x	-
Case 24	CO_2.2	1	9900	0.08	30.98	116.8	x	-	x
Case 18	CO_2.2	1	9900	13.8	2630	13505	-	-	x
Case 26	CO_2.2	1	9900	0.13	46.85	146	x	x	x
Case 4	CO2 &B7	2	4950	1.57	367.29	1547.6	-	-	x
Case 10	CO_2.2& B7	2	4950	2.55	844.74	2555	-	-	x
Case 3	B1 & B2	2	4950	1.29	345	1752	-	-	x
Case 5	B1 & B3	2	4950	1.2	214	1241	-	-	x
Case 6	B7 &B1 &B8	3	3300	1.63	803.73	2190	-	-	x
Case 7	B2 & B3& CO_2.2	3	3300	2.16	409	3036.8	-	-	x
Case 2	CO_2.2 & B7& B1	3	3300	1.95	561.15	1752	-	-	x
Case 8	co2.2&B7&CO2	3	3300	1.27	260.54	730	-	-	x
Case 13	B6 &B7 &B1	3	3300	1.6	672.77	2058.6	-	x	x
Case 14	B7 &B1 &B8	3	3300	1.42	521.8	1460	-	x	x
Case 15	Co2&B7&Co2-2	3	3300	0.32	122.03	328.5	-	x	x
Case 17	B2&B3&Co2-2	3	3300	0.87	216.58	846.8	-	x	x

6.2.2.3 Injection depth optimization

The reservoir is consisted of three layers denoted as layers 1, 2&3. From the injection rate and location information obtained at the previous step, we are more confident about injecting through a single well in (CO2.2).

Optimizations were carried out using the aforementioned case, but at different depths of the top completion interval. A better recovery and higher storage capacity was obtained when all of the gas is injected from the bottommost interval. Since all the gas was injected from the bottom completion, this nullifies the idea of injecting in other layers. As the gas in the rest of the reservoir moves upward under gravity, a greater amount gets trapped as an immobile phase, resulting in lower gas saturation in the top layer of the reservoir. This is a favorable point to avoid leakage through cap rock.

Cases other than injecting in the bottom layer resulted in a lower oil recovery, due to the mobility difference. Mobility difference can be due to permeability difference as the permeability is different in different layers; or due to the difference in layer thickness in each layer and even each grid (where the lowest thickness is in layer 1).

These results underscore the need to complete the wells as far as possible from the top of the reservoir. Similar results were obtained by Kumar [12] who recommended completing the well in the bottom half of the reservoir. Janssen and Bossie [50] too concluded that injecting far from the top of the reservoir was an important step towards optimizing a CO_2 injection strategy.

(Table 6.5) and (Figure 6.2); explain the effect of injection depth. The only feasible gas saturation scenarios can be seen, as case 18 where the injection was solely from the bottom layer.

Table 6.5 Injection layer optimization

Case #	Layer	Oil recovered (mmbbl)	CO2 stored (mmscf)	Duration (day)
Case 1 Base Case	-	7.34	-	7300
Case 22	1	6.1	2122.5	6073.6
Case 23	2	6.57	2834.23	6570
Case 18	3	13.8	2630	13505
Case 24	1 &3	0.089	30.98	116.8
Case 25	2 & 3	0.48	170.07	481.8
Case 26	all layers (1&2&3)	0.135	46.85	146
constraints	Maximum gas injection rate 9900 rbbl/day. Maximum gas injection pressure 2741psi Minimum bottom hole pressure is 1000psi for production wells			

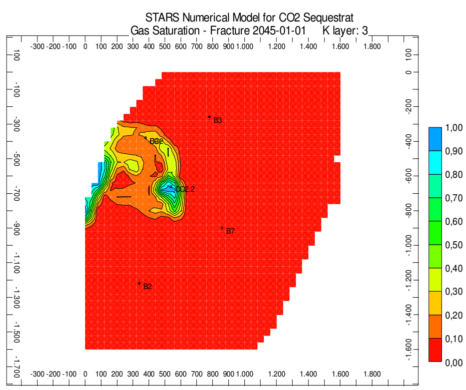

Layer 3-case18

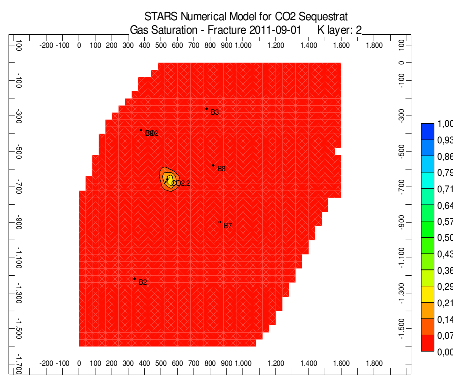

Layer 2 -case23

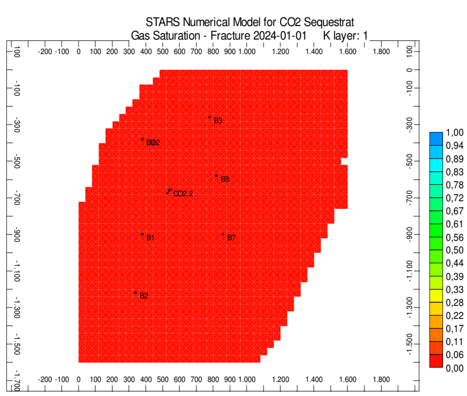

Layer 3-case 22

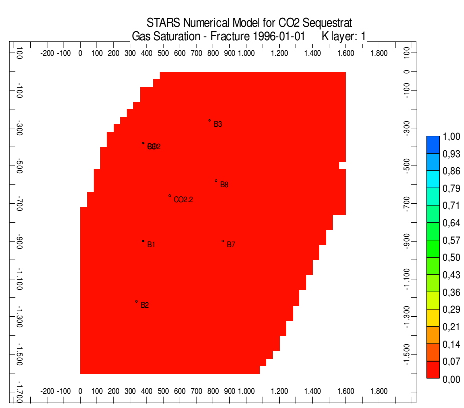

Layer 2-case 24

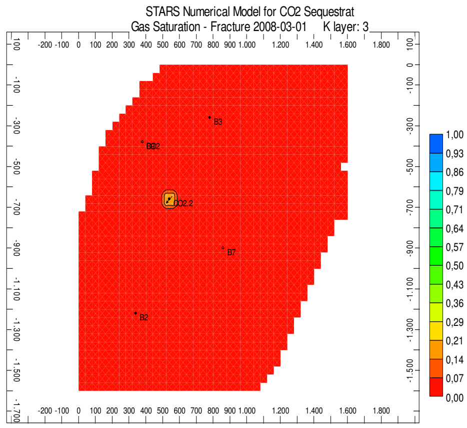

Layer 3-case 24

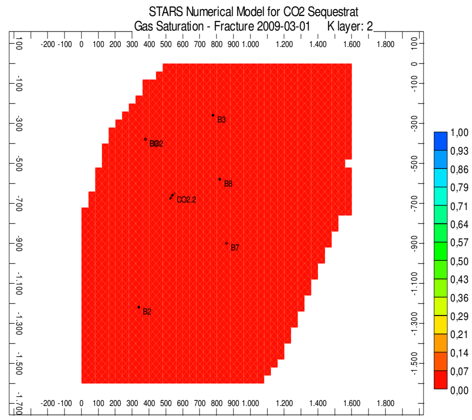

Layer 2-case 25

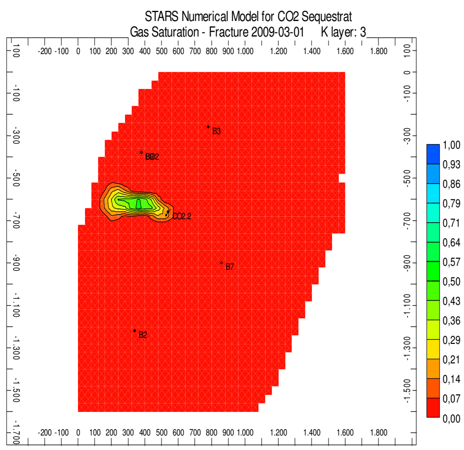

Layer 3 case 25

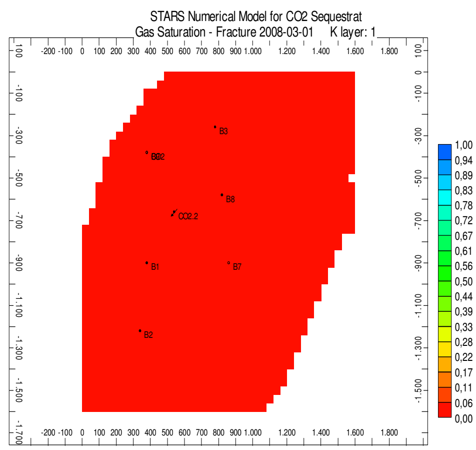

Layer 1 case 26

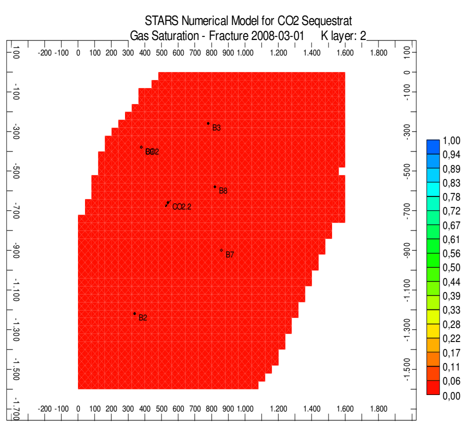

Layer 2 case 26

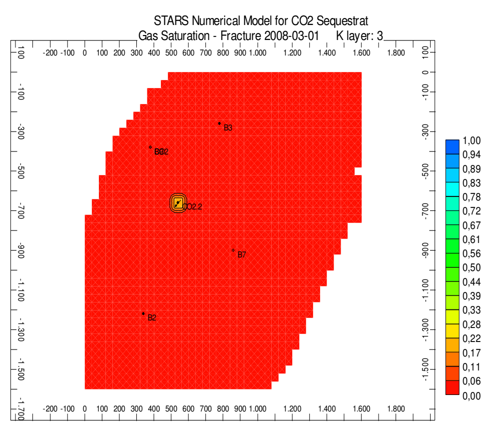

Layer 3 case 26

Figure 6.21 Different gas saturation section views for injections in optimum location

Since the oil zone is the second and first zone, it is expected that the injection will take place in either the top or the bottom zone. However, the above figures recall this fact better when compared to each other. (Figures 6.22 and 6.23) show the oil recovered and CO_2 stored for each layer.

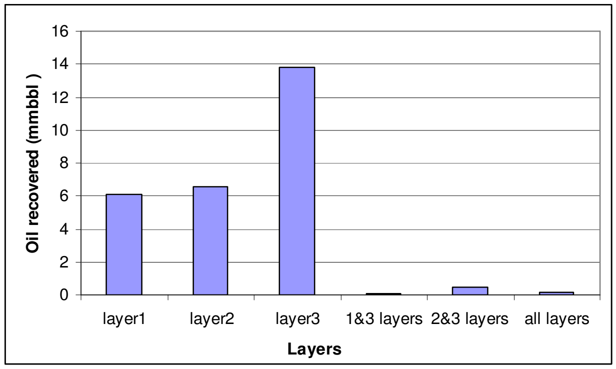

Figure 6.22 Injection depth effect on oil recovery

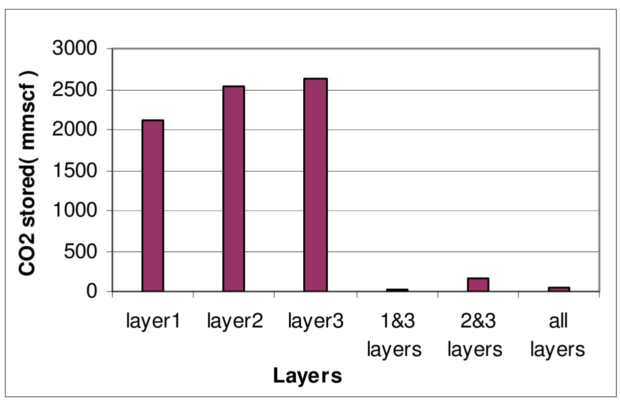

Figure 6.23 Injection depth effect on CO_2 stored

When injected from layer 3(bottom layer), (Figure 6.24) explains the effect of gas saturation on different injection layers such that a higher amount of gas in total and instantly is sequestered. Again, highest oil rate for the high injection cases , was found as case 23 and case 18 (The oil rate is 1000 bbl/day for case 23 and 1020 bbl/day for case 18).

Hence, so far we could optimize injection location, rates and depth as (CO2.2), 350Mscf/day and layer 3.

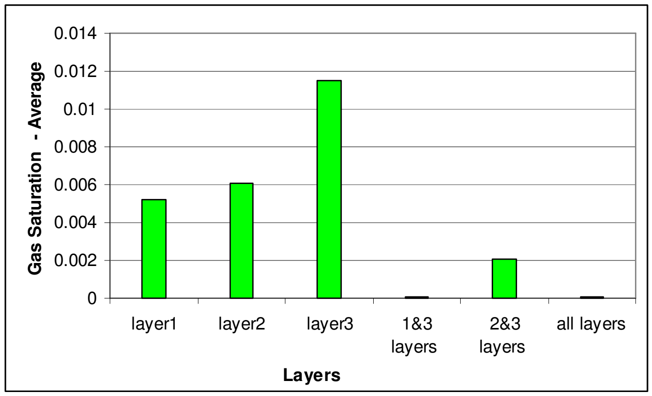

Figure 6.24 Injection depth effect on gas saturation (total run time)

6.2.2.4 Effect of injection pressure

Injection pressure is thought to have a positive effect on the amount of CO_2 injected and oil recovered. To verify the validity of this claim, simulation runs were done using different injection pressures. Injection pressures for the run in concern assumed the minimum pressure for preserving the supercritical state of CO_2 which is 7373kpa. The effect of injection pressure was more pronounced in high pressures. The denser gas in supercritical state should have a higher recovery as the injection pressure proceeds up. Simulation run results are listed in (Table 6.6).(Figures 6.22-23) show the Gas saturation for hydro-dynamical favored the increase in pressure. (Table 6.6) shows the injection pressures that are used for sensitivity analysis.

Table 6.6 injection pressure optimization

Case #	Pressure (Kpa)	Oil recovered (mmbbl)	CO2 stored (mmscf)	Duration (day)
Base case (no gas injection)	-	7.34	-	7300
Case27	4000	9.14	2550	8760
Case28	6000	13	2550	13140
Case 29	8000	7.11	2472.4	7081
Case 30	9000	7.12	2476.1	7081
Case 31	12000	7.31	2553.6	7358.4
Case 33	18000	7.22	2553.6	7329.2
Case 18	18900	13.80	2630	13505
Constraints	Maximum gas injection rate 9900 rbbl/day. Maximum gas injection pressure changes with case but does not exceed 18900kpa.Minimum bottom hole pressure is 1070 psi for production wells			

From (Table 6.6) we can see that we have (27,28and 18) three cases of better sequestration for the field in concern.

(Table 6.6) clearly explains positive effect of pressure on oil recovered. The injection pressure helps energizing the reservoir. However after a certain extent it can also cause fracture from which the sequestration will be negatively affected. Such fractures may provide a path for the CO_2 to retaliate back to the atmosphere. When examining the results, the formation is thought to have the highest production potential whereas the field has a small potentiality (injection of low pressure, may mean that the low injection pressures can prove to be sufficient to extract most of the oil).

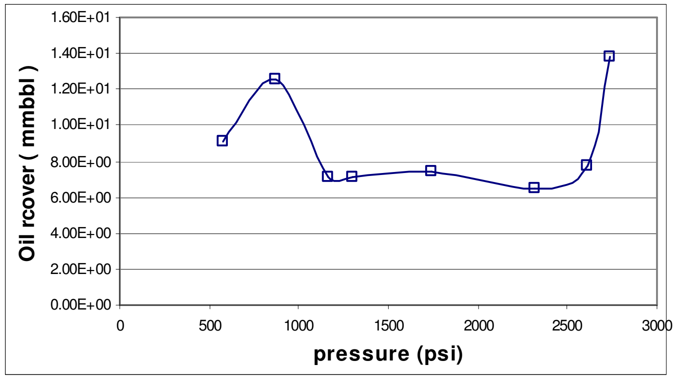

Figure 6.25 Pressure effect on Oil recovered

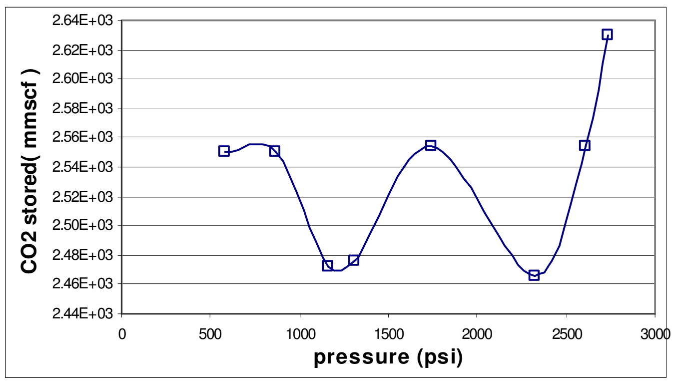

Figure 6.26 Injection Pressure effect on CO_2 injected

When trapping types are considered , it was found that for free gas saturation increasing the pressure will lead more of the gas to migrate up dip or displacing the oil in the capillary to be residually trapped (see Figure (6.27).

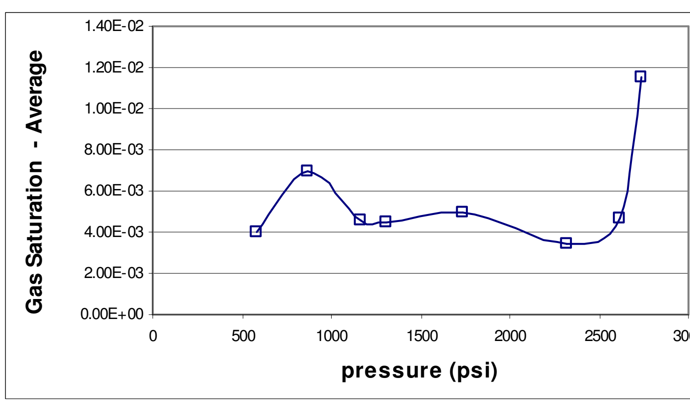

Figure 6.27 Pressure effect on Gas saturation average

From the diagrams it was noticed that an unusual increase in the overall recovery and storage amounts occurs, when injection pressure was 2320 psi or 16000kpa. This can be attributed to threshold pressure (flow in the opposing capillarity). That is to say that after 16000kpa or (2320psi) using higher injection pressure will force the gas to be dissolved in oil and CO_2 will not be visible in the free gas phase anymore.

6.2.2.5 Impact of relative permeability curves

The effect of matrix relative permeability on CO_2 sequestration was examined by the use of three different relative permeability curves for the gas- oil system. A base case and then two other cases [51] were considered.

Doughty and Pruess [51] suggested that the growing CO_2 shape can aid in determining the type of relative permeability that exists between different components for sandstone reservoirs. When CO_2 is injected, the plume does not migrate as far up dip as for generic characteristic curves, but remains localized near the injection well [See Appendix C]. However, when injection stops the plume begins to spread and it does not take long for the gas saturation to decrease to the residual value, making the plume immobile [51].

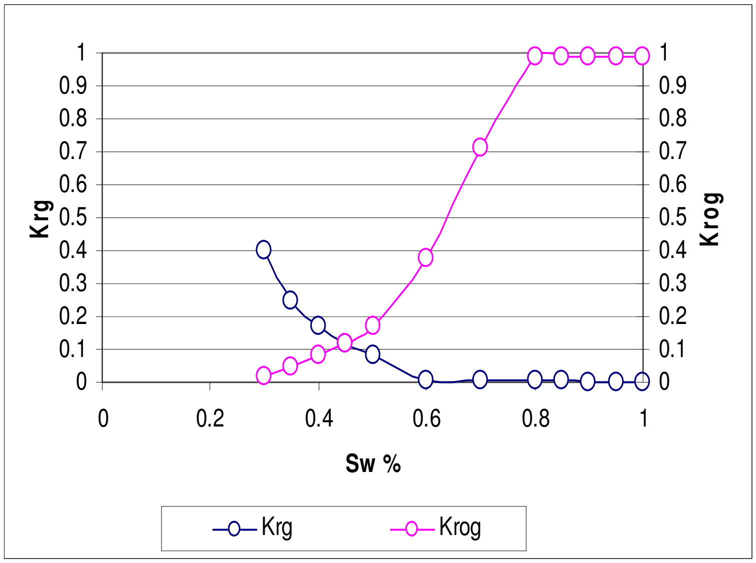

Figure 6.28 Generic like modified gas-oil relative permeability curves

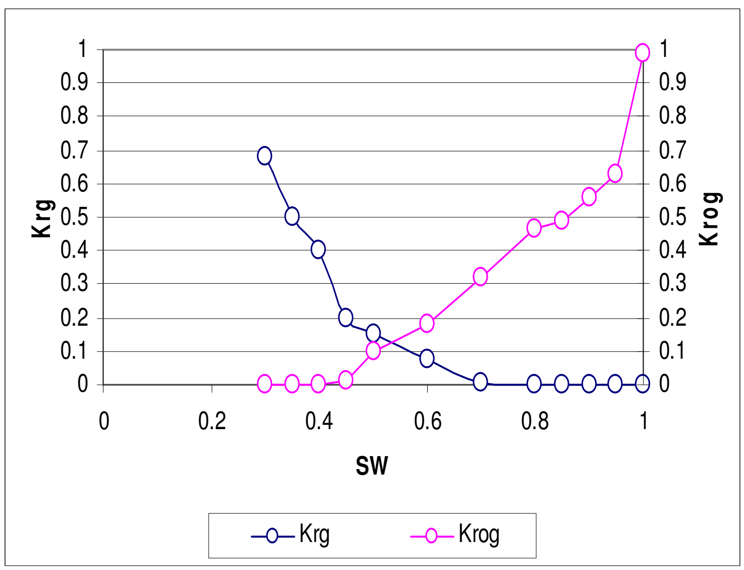

Figure 6.29Frio like modified gas-oil relative permeability curves

The example curves are exhibited in Figures (6.28– 6.29). For generic-like case the oil relative permeability is higher, whereas for Frio- like relative permeability the gas relative permeability is higher. The proposed modifications of oil-gas relative permeability curves resulted in more oil recovered and CO_2 sequestered in the reservoir due to relative permeability's of gas and liquid (see Figures 6.30-31) .

The trapping methods associated with the change of end point relative permeability were studied by finding the different trapping parameters at the timestep of (4775days). In (Figure 6.32), trapped gas saturation for Frio-like case is less than that of generic, for gas saturation at the common time but higher for gas saturation at total time(Figure 6.33).

Table 6.7 Effect of relative permeability end points

Case #	Relative perm curve used	Oil recovered (mmbbl)	CO2 stored (0mmscf)	duration (day)
Case 18	Default STARS	13.8	2630	13505
Case 38	Frio	14.1	2400	14600
Case 39	Generic	4.74	794.76	4745
constraints	Maximum gas injection rate 9900 rbbl/day . Maximum gas injection pressure 18900 kpa Minimum bottom hole pressure is 1000psi for production wells			

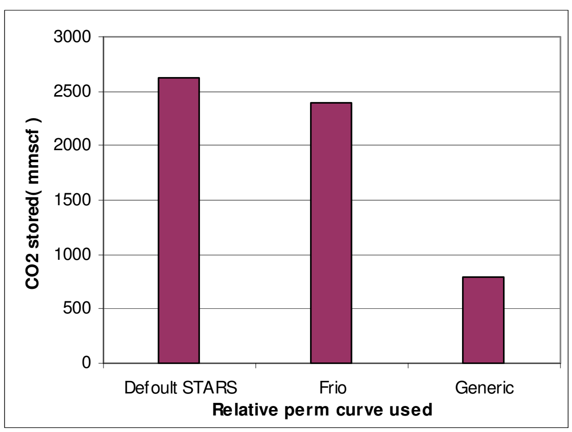

Figure 6.30 Effect of relative permeability curve on CO_2 injected

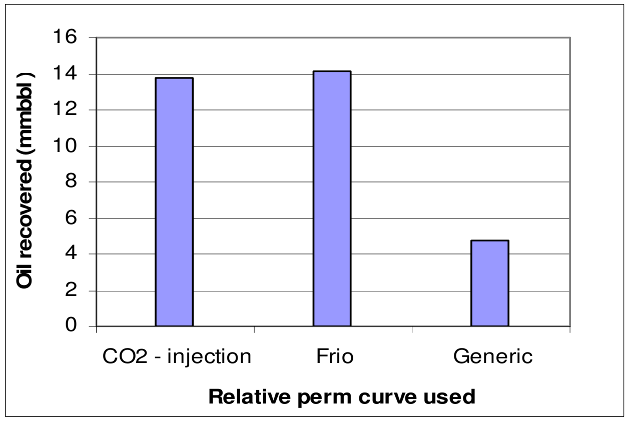

Figure 6.31 Effect of relative permeability curve on oil recovered

The Frio like relative permeability curves resulted in less gas saturation. That is because of the localization process which will be for a Frio like curve less visible and for a Generic like curve spreading easier. However in the long run, Frio like curves do not tend to cause gas breakthrough or up dip migration ,instead the increased saturation will make help the oil dissolve at a certain pressure and oil to be more ready to flow.

Therefore a Frio like relative permeability in B Field resulted in a higher overall gas saturation.

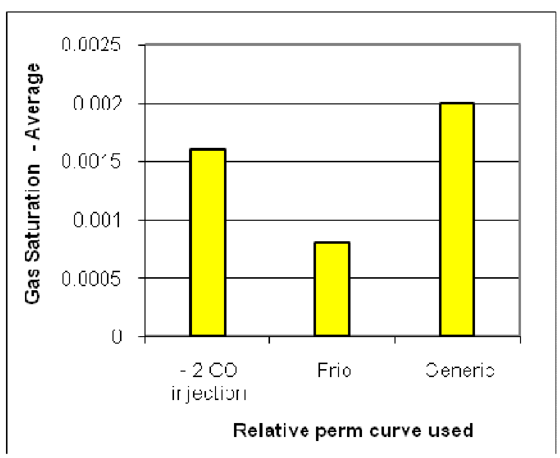

Figure 6.32 Effect of relative permeability curve on Gas saturation average (latest common time)

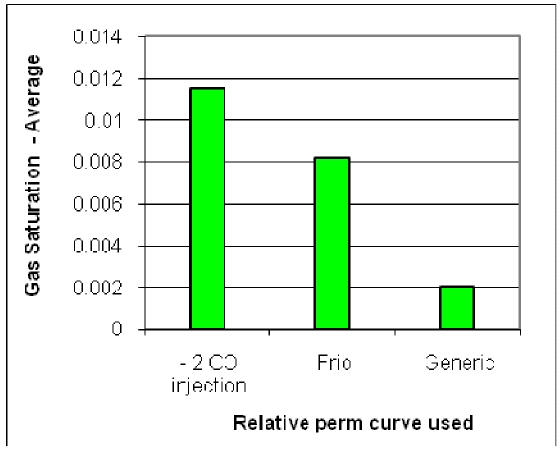

Figure 6.33 Effect of relative permeability curve on Gas saturation average (total run time)

6.2.2.6 Impact of relative permeability hysteresis

Hysteresis effects are observed in both relative permeability and capillary pressure functions. Once injection stops, the CO_2 phase continues to migrate upwards due to the density difference between CO_2 and oil. At the leading edge of the CO_2 plume, the CO_2continues to displace oil in a drainage-like process, while at the tail of the plume the voidage in the pore space created as a result of this CO_2 migration is filled by water, resulting in an imbibition type process [9]. There are several mechanisms by which water can displace CO_2 during imbibition [52]. Of these, snap-off is the dominant mechanism in water-wet rocks [53], which leads to the trapping of the CO_2 phase. These physical phenomena result in hysteresis.

The relative permeability hysteresis between drainage and imbibitions for the non-wetting phase is illustrated in (Figure 6.34).

During the drainage process, the CO_2 saturation (*Sg*) increases and oil saturation decreases and the relative permeability of the non-wetting phase follows the O-B-A curve. The oil saturation at A is the irreducible saturation *Swi*. If the drainage process is then followed by gravity segregation and the imbibing water phase replaces the gas phase, the relative permeability now follows the A-D curve. The water does not completely displace the gas and we have some CO_2 trapped in the pore space. This saturation (Sgtmax) corresponds to the CO_2 saturation at point D on the curve.

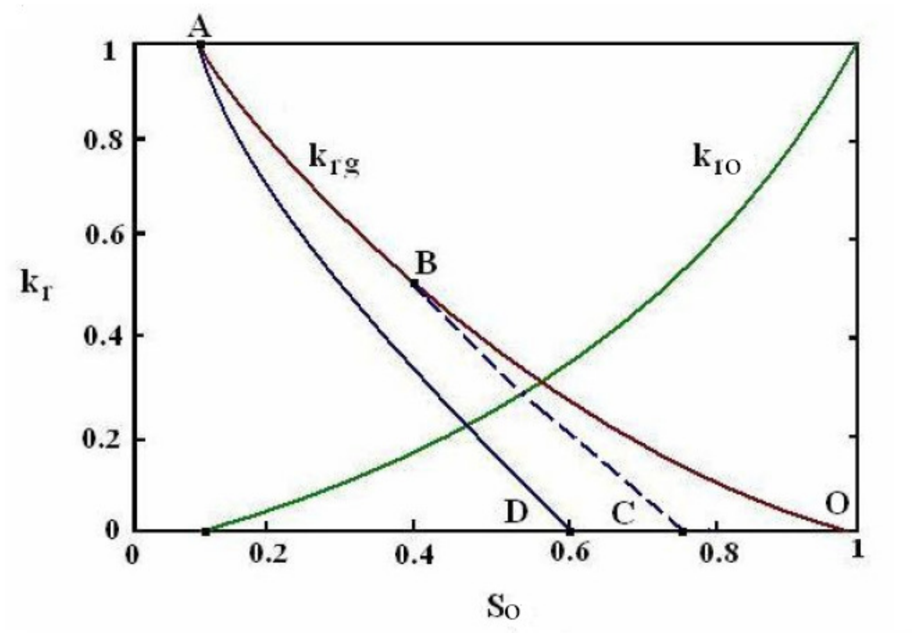

Figure6.34Relative permeability hysteresis between drainage and imbibition

Carlson hysteresis

Although the simulation run did not last more than 1390 days, the percentage of gas trapped residually was twice as that without hysteresis.

Average gas saturation in the fracture was 0.0079, whereas the optimized single well injection was 0.0036. The dissolved gas will be stored in the matrix (see page 31). This value has changed as the value of maximum trapped gas(stgmax) was changed from 0.4 to 0.2 and 0.1.When Stgmax was 0.2, the average gas saturation was almost the same, however when stgmax was 0.1, average gas saturation is 0.0009.

For the dissolved gas, it was highest in the matrix when the degree of hysteresis was in it is lowest (see Figure 6.39). However, the effect of hysteresis when Sgtmax was

0.4 and 0.2 , was the same ,indicating the threshold in value of hysteresis after the entrapment value of 0.2.

Killough hysteresis

To do the sensitivity analysis using Killough's model, the curvature or position number (the power of equation 5.6(page 39) (HYEXG) was assumed to be 1.5. Average gas saturation in the matrix was the same as Carlson's results (see Table 6.8).

Average gas saturation in the fracture was 0.0079 for optimized single well injection without hysteresis. However, when hysteresis was enabled the average gas saturation in the matrix was 0.0036. As the dissolved gas was stored in the matrix (page 31), this value has changed as the value of curvature power (HYEXG) was changed from 1.5 to 0.75 then to 0.375. When HYEXG was 0.75, the average gas saturation was almost the same, however when stgmax was 0.1, average gas saturation was 0.0009.

For the dissolved gas in the matrix it was highest when the degree of hysteresis was lowest (see Figures 6.39). However, the effect of hysteresis between when (Sgtmax is 0.4 and 0.2) , was the same ,indicating a threshold in value of hysteresis after the entrapment value of 0.2.

Hysteresis is thought to have a negative effect on CO_2 trapping and oil recovery provided that all other factors are constant. The overall analysis of both oil recovery and CO_2 injectivity (Figures 6.35And 6.36), showed a negative influence of the hysteresis on these amounts. This was again approved when average gas saturation is studied.

The effects of hysteresis are significant in that they provide a clear view of the outcome of a natural phenomenon. At the least common time (1095days), deviation from the drainage path resulted in higher oil recovery but lower CO_2 storage both for Carlson's and Killough's model for all sensitivity runs.

The cumulative results for both Carlson's and Killough's models are as in (Figures 6.35-6.36).

For gas saturation, the same trend was noticed. At the latest common time step, showed a high percentage of gas remained as free gas when the hysteresis was on it is smallest value. The migration of gas updip as was proved at the beginning of the scenarios for single well locations was this time influenced by the hysteresis in relative permeability that trapped the gas before reaching upper layers. Thus, a small trapping value of Stgmax for Carlson's and (HYEXG) for Killough's model resulted in the highest gas saturation value. This was evidenced in Figures (6.37 and 6.38).

On the other hand when it comes to gas mole fraction a clear tendency towards more dissolved gas moles was observed when the hysteresis entrapment factor was lower. The dissolved gas and the entrapment factor for Carlson and Killough s' models depicts reciprocal relationship between the amount trapped due to hysteresis as a free gas and the amount dissolved in oil and water. (See Figure 6.39) This can be due to the path effect (or residence time) that prohibits the CO_2 from being exposed to a larger volume after being residually trapped.

Table 6.8 Hysteresis effect

Case #	Hystersis effect	Days	Oil recovered (mmbbl)	CO2 stored (mmscf)
Case 39	Carlson hys.Stgmax 0.4	1390	1.93	568.8
Case 41	Carlson hys.Stgmax 0.2	1372	1.92	561.6
Case 44	Carlson hys.Stgmax 0.1	1095	1.69	468.4
Case 40	Killough hys.curveture power 1.5	1390	1.93	568.8
Case 43	Killough hys.curveture power 0.75	1372	1.93	568.8
Case 45	Killough hys.curveture power 0.375	1095	1.69	468.4

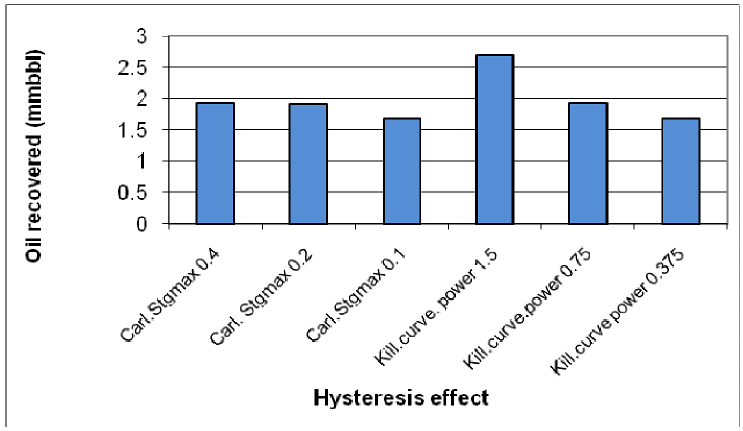

Figure 6.35 Effect of relative permeability hysteresis on oil recovered

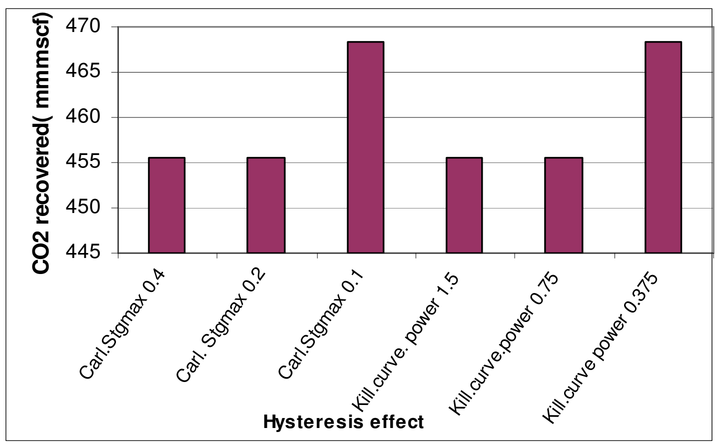

Figure 6.36 Effect of relative permeability hysteresis on amount of CO_2 stored

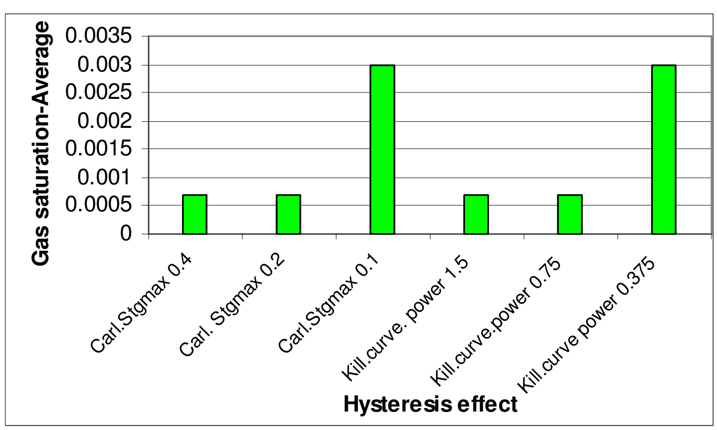

Figure 6.37 Effect of hysteresis on gas saturation (total run time)

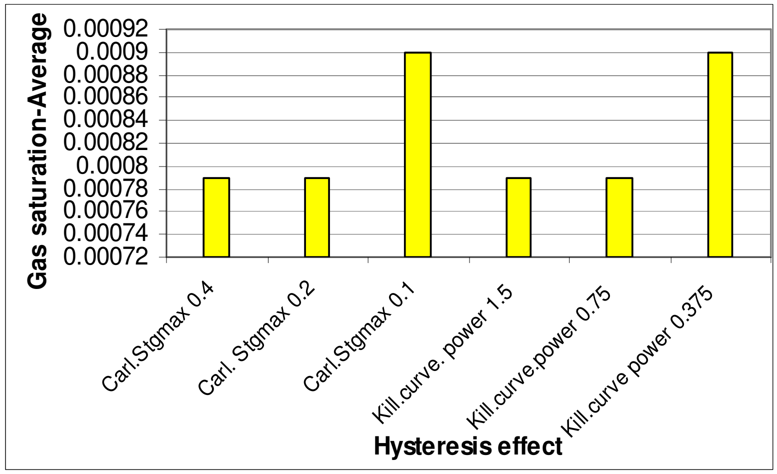

Figure 6.38 Effect of hysteresis on gas saturation (latest common time)

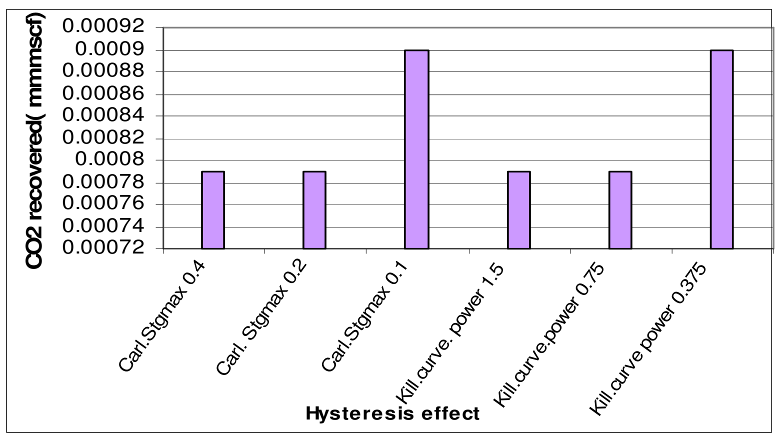

Figure 6.39 Effect of hysteresis on gas mole fraction (water)in matrix (latest common time)

The effect of hysteresis on relative permeability curve is most visible when the curve for Gas- oil relative permeability is sketched for Carlson model at 0.4 as Stgmax.

In (Figure 6.40) the red line resembles the original gas relative permeability while the blue line shows gas relative permeability. In addition, for oil the black line resembles the original oil relative permeability and the purple line shows.the decrease due to hysteresis, which will result in less recovery.

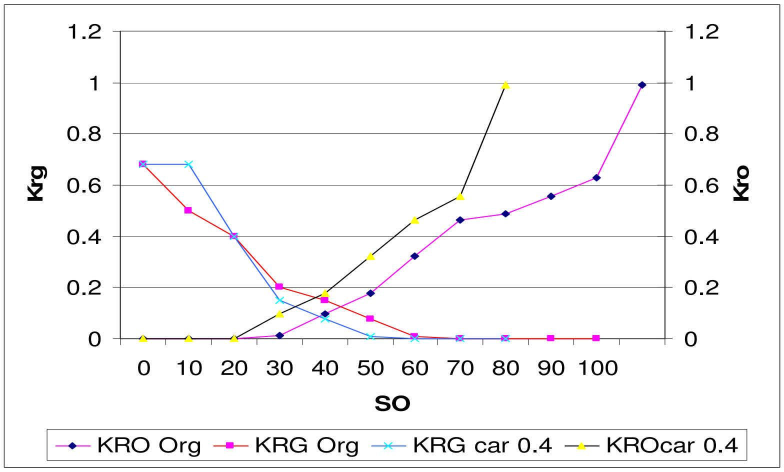

Figure 6.40 Hysteresis in relative permeability values Carlson model gas entrapment maximum value at0.4

6.2.2.7 Fracture spacing effect

Fracture spacing (or density) is a major parameter that could affect CO_2 sequestration efficiency [54]. A sensitivity analysis was carried out to analyze the effect of fracture spacing. Five different cases were considered: base case (5 x 5 x 5 m), horizontal fracture dominant case (1 x 1 x 20 m) and vertical fracture dominant case (20 x 20 x 1 m) and (20*20*20) fine spaced case. In all comparisons, there are more fractures compared to the base case. We compare the fracture heterogeneity, where there are fine fractures and homogenous fractures. The fine spaced fractures (optimum injection case) tend to act like a matrix system. That is to say, the flow is easy when fractures are more connected. Results depicted in (Figures 6.41 -6.42) reveal the change on oil recovery. The amount of CO_2 trapped enlarged due to less fracture spacing which leads a better flow and dissolution in the fracture.

It was observed that oil recovery has increased and CO_2 storage has decreased when more spaced system was used. When vertical fracture spacings dominated the reservoir , oil recovery was affected positively and caused a better hydrodynamical and residual trapping, as the gas will use these paths due to gravity.

When horizontal fractures dominated the reservoir a lower recovery lower recovery and CO_2 storage was observed. This is because of the tendency of gas to migrate in upward direction instead of using the path effect towards injection wells.

In these runs the only case that manages to compete with fine (or equal fracture density is the case with higher fracture spacing; this is because of the better chance for the gas to become immobile in the presence of high density fractures. But, the kind of trapping that happens at these finely distributed fractures needs further investigation and beyond the scope of this work.

Table 6.9 Fracture spacing effect

Case #	Fracture Spacing (m)	Oil recovered (mmbbl)	CO_2 stored (mmscf)	duration (days)
Case18	homogenous	13,8	2630	13505
Case 36	vertical	10.2	1230	9855
Case 37	horizontal	6.09	1021.1	6205
Case 38	higher values homogenous	13.1	1230	13505
Constraints	Maximum gas injection rate 9900 rbbl/day . Maximum gas injection pressure 18900 kpa Minimum bottom hole pressure is 1000psi for			

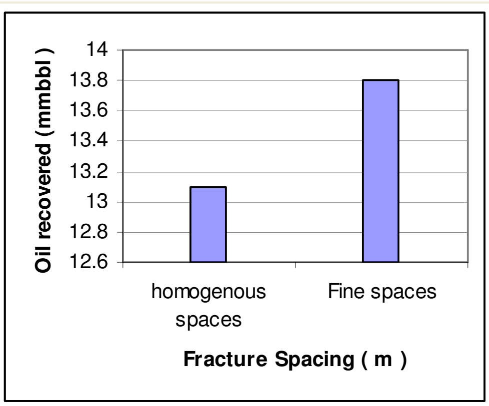

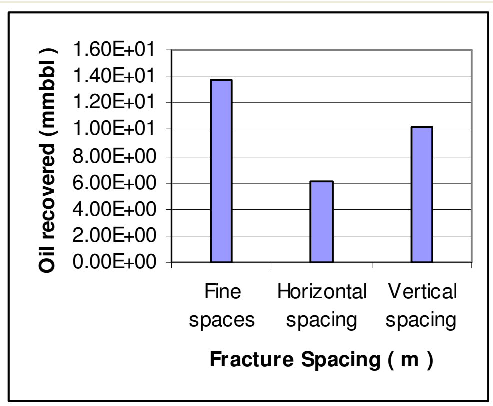

a b

Figures 6.41 Fracture spacing effect on oil recovered: a) spacing magnitude b) fracture orientation

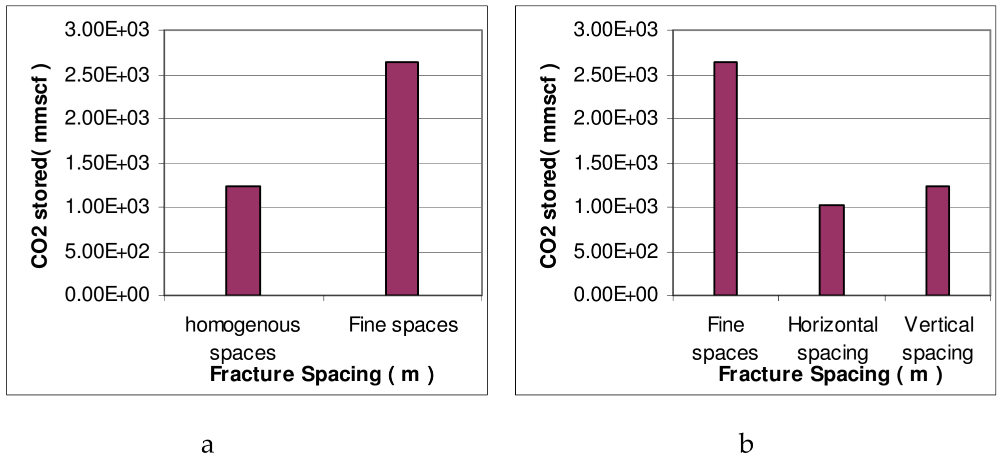

Figure 6.42 Fracture spacing effect on CO_2 stored: a) spacing magnitude b) Fracture orientation

The amount of gas saturation that might be stored as free gas in uppermost layer and other layers has increased when fracture spacing is fine as gas follows paths for the vertical migration. Similarly, at vertical fracture dominancy case gas can travel between vertically spaced fractures better than horizontally placed ones. Hence, gas saturation will be higher for finely spaced and vertically spaced systems as in (Figure 6.43).

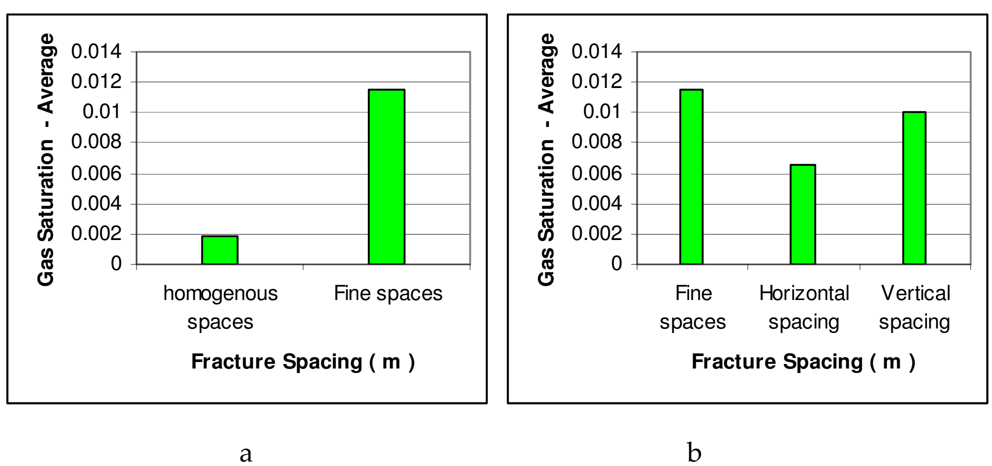

Figure 6.43 Fracture spacing effect on average gas saturation (total run time): a) spacing magnitude b) fracture orientation

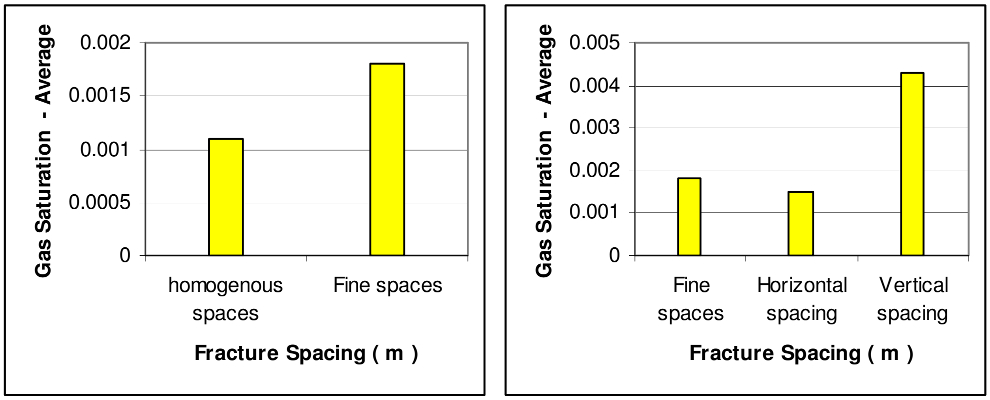

a b

Figure 6.44 Fracture spacing effect on average gas saturation (latest common time): a)spacing magnitude b) fracture orientation

For solubility trapping, fine and densely spaced fractures were compared. Having higher capacity (when other factors are considered constant), fine fracturing resulted in the trapping of a higher amount of CO_2. When comparing vertical and horizontal spacing systems (Figures 6.43-a,b and 6.44-a,b), as it is related to many factors including grid permeability and/or pressure, it is hard to know if (for the same time step), solution trapping mechanism was dominant in any kind of spacing to another. However, since the gas whether supercritical or subcritical had a tendency towards migrating upward, the total amount of trapping provided that was most likely linked to vertical migration. Thus, vertical fracture spacing is the most suitable type for such a trapping system.

6.2.2.8 Impact of injected gas impurity

Despite its importance in reducing the minimum miscibility pressure, as it was delivered from the sweetening power plant, an 80% purity of CO_2 with a 20 mol% of an additive was tested. These additives are Hydrogen Sulfide (H_2S) and Carbon Monoxide (CO). An increase in oil recovery was expected when decreasing minimum miscibility pressure. In the meantime in the case of H_2S a chemical reaction is expected to take place (i.e. precipitation of hydrogen sulfide). To be able to remove one of the toxic emissions by the power plant, as is the case with hydrogen sulfide (H_2S), a percentage of carbon monoxide (CO) is released into the atmosphere from the power plant. When CO is injected it can it can react with formation water forming CO_2 using the infamous (water gas reaction)[44] .

$$CO + H_2O \xleftrightarrow{400°f} CO_2 + H_2 \tag{6.1}$$

Even though CO is far more toxic than CO_2, it is thought that CO will react with water to produce carbon dioxide. The gas will lower the viscosity in the reservoir [50] making it more ready to flow to production wells.

Table 6.10 injected gas impurity effect

Case #	Impurity	Oil recovered (mmbbl)	CO2 stored (mmscf)	Duration (day)
Case 18	CO_2 injection	13.8	2630	13505
Case 46	CO 20%	1.84	225.97	1825
Case50	CO 10 %	1.48	185.96	1503.8
Case 51	CO 5%	1.53	533.33	1576.8
Case 47	H2S 20%	0.94	114.2	1095
Case 48	H2S 10 %	0.79	99.21	1182.6
Case 49	H2S 5%	1.14	398.45	1182.6
Constraints	Maximum gas injection rate 9900 rbbl/day . Maximum gas injection pressure 18900 kpa Minimum bottom hole pressure is 1000psi for production wells			

The effects of these additives to the gas stream are shown in (Figures 6.45-6.46). Due to numerical instabilities these cases did not continue more than a small period of time (in some cases as short as 1095 days) .Assuming this as an acceptable period, the following results are concluded from this study.

It was found that, H_2S may have a positive effect on oil recovery as it's mole fraction was increased from 5% to 10% and then to 20% percent. Bachu [33] concluded that the increase in sour gas mole fraction helps achieving miscibility in an easier fashion. For CO_2 storage, when H_2S was injected, it showed a positive impact on the storage (Figure 6.45). When the impurity was 10%, an increase in storage occurred: which can be considered as an approximate proof of minimum enrichment concentration at this percentage.

However, in the case of CO, higher CO concentration has negatively influenced oil recovery. For water and gas reaction, Hyne and Tyrer [44] concluded that unless the reservoir temperature is above 260°F or 126°C, the reaction will continue at very slow rates that will render the whole process unbeneficial regardless of amount of CO injected(See Appendix C for comparing optimum case with CO addition case).

Unlike, H_2S when CO was injected it showed a clear negative impact on the amount of CO_2 stored and oil recovery. This is because the injected CO which occupied the pores that might be used by CO_2.This was evidenced in (Figures 6.45-46).

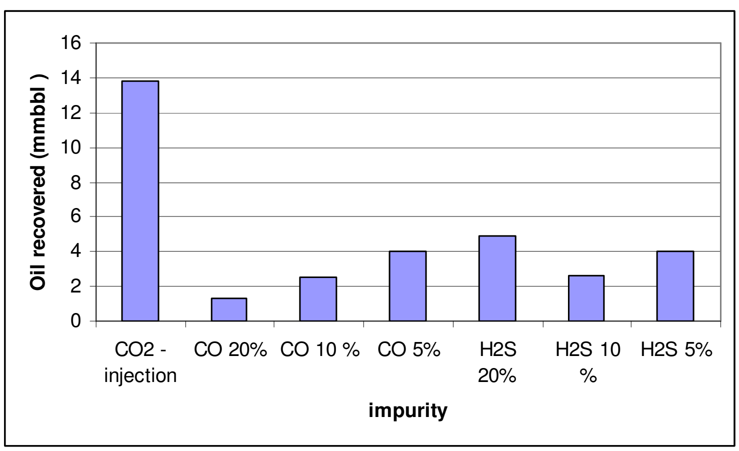

Figure 6.45 Impurity effect on oil recovery

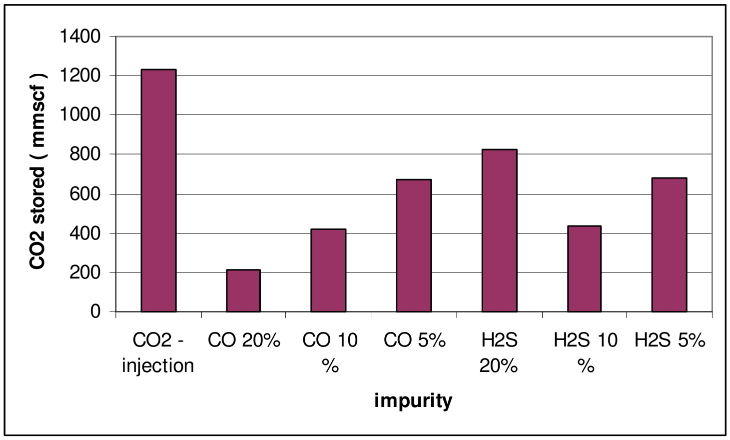

Figure 6.46 Impurity effect on CO_2 stored

For hydrodynamical trapping, in case for H_2S addition, we notice the least amount of gas saturation at the 20% of H_2S addition. A good evidence that is this point the CO_2 and oil became miscible. In other words, MMP is decreased with the addition of H_2S (provided that other variables are constant), CO_2 and oil will become miscible, and free CO_2 saturation will be reduced as shown in (Figures 6.47-6.48). This can be explained with the minimum enrichment concentration previously explained in (page15). To prove this we need to compare it with another total time property and/or another case that is close to it. The same diagram for the total gas saturation reveal that H_2S is indeed close to required additive concentration. Furthermore, since in case 47 (20%) and case 49(5%) a total of 7.1cubic meters (a fraction of total grid size which is (40*40*67) cubic meters was observed at the given time step. It can be concluded that required enrichment concentration of H_2S is at least 10%. At this step, experimental data is needed to validate this conclusion.

For CO addition to CO_2, CO reacts with water, some of it should have produced CO_2 which then migrate updip. However, this was not neatly visualized as the simulator gave combined data of both the CO that was stagnant and that which formed CO_2. Handful evidence to this fact was that when the total injected gas plotted, the graph yielded a very similar graph to the instantaneous injection case.

Thus, this process continued until the material balance error exceeded the required accuracy level.

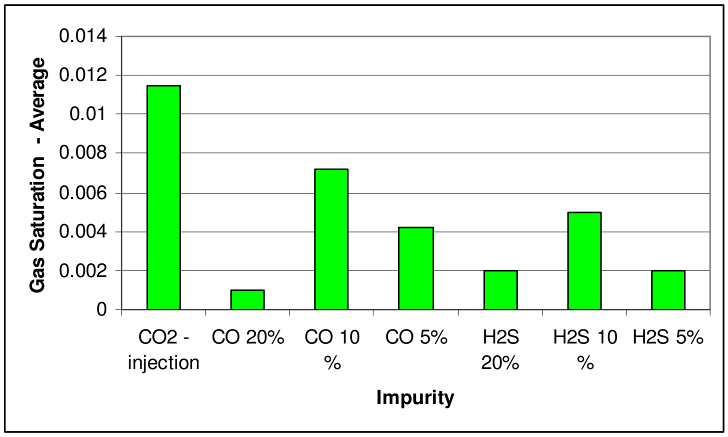

Figure 6.47 Impurity effect on gas saturation (total run time)

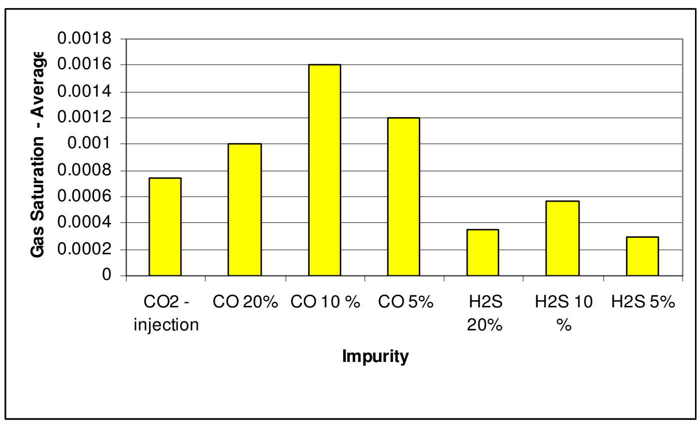

Figure 6.48 Impurity effect on gas saturation (latest common time)

6.2.3 Interpreting the successful cases

Six of the simulation runs were found to perform better than the base case in oil production values. Cases numbered 18, 19, 27, 28, 34 and 38 are profitable (see Table 6-2).

For the cases that have a centered injection well (i.e. injection in B7), we see low injection pressures (see cases 27, 28, case 28 a Frio like relative permeability end and larger fracture spacing). The following figures represent the outcome of these cases.

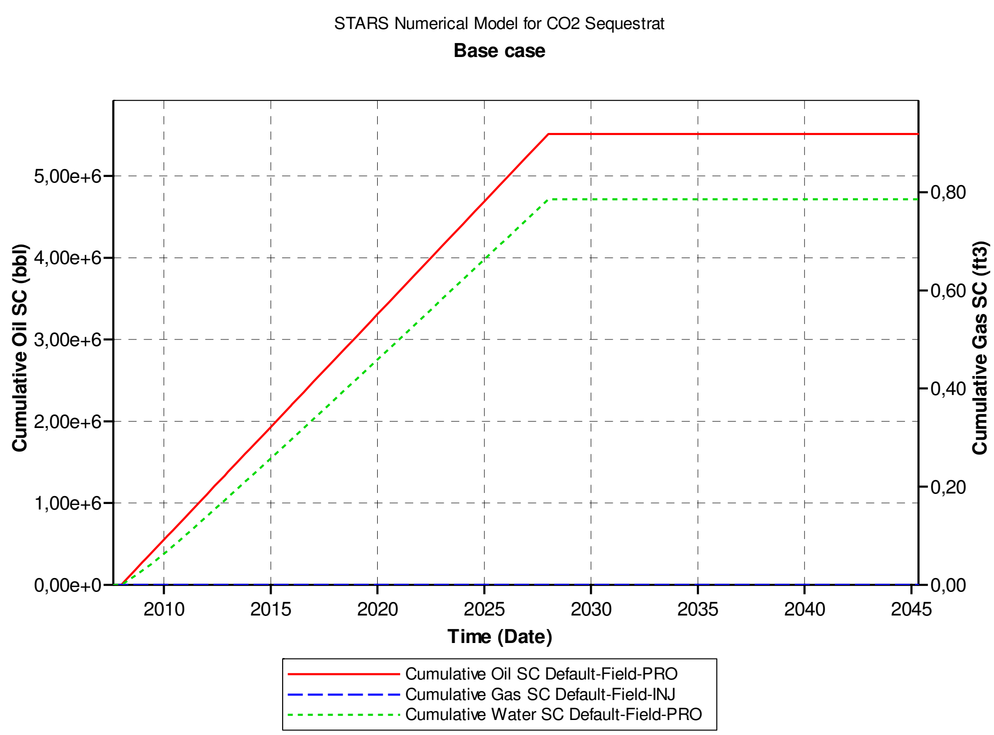

Figure 6.49 Base case, without gas injection, cumulative oil and water produced

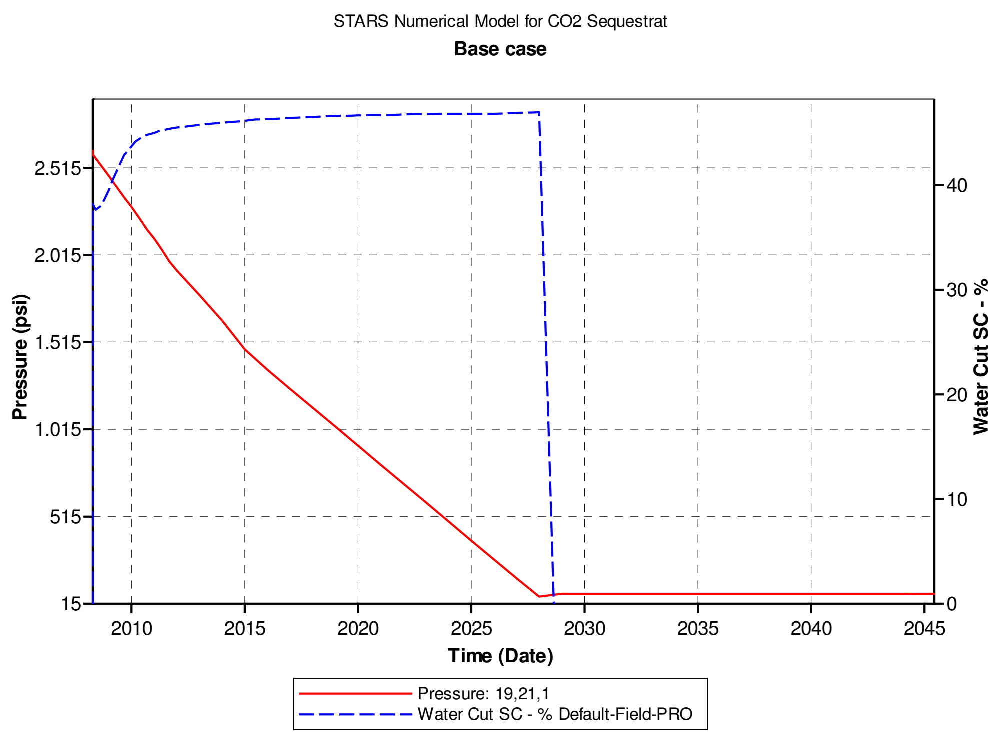

Figure6.50 Base case, Average pressure and water cut

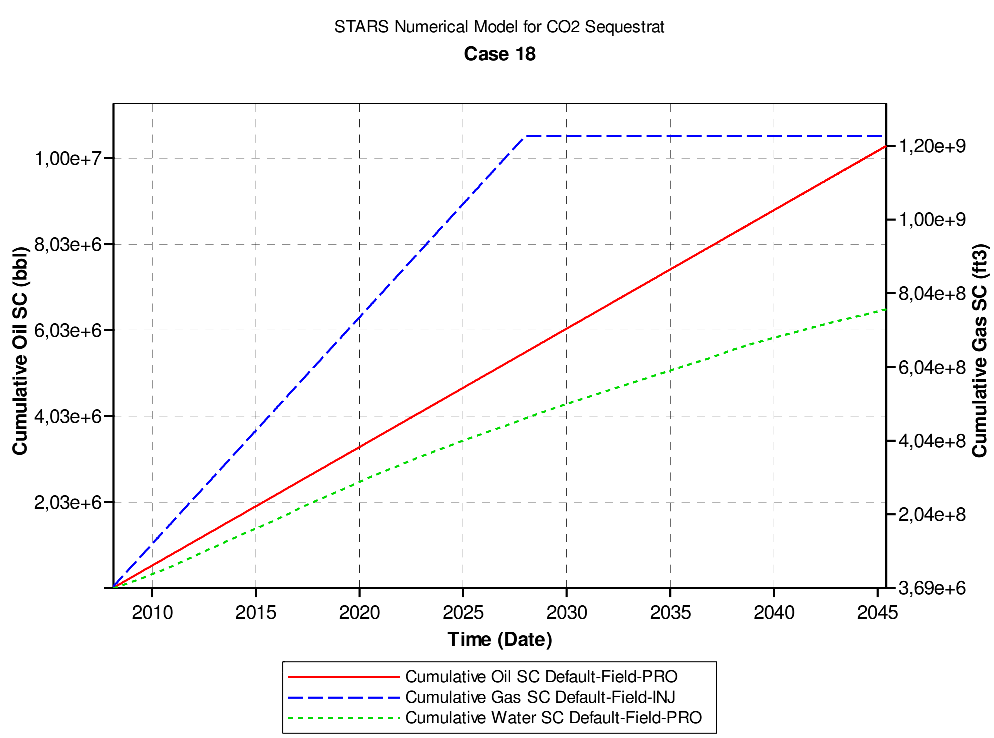

Figure6.51 Case18, Cumulative oil and water produced

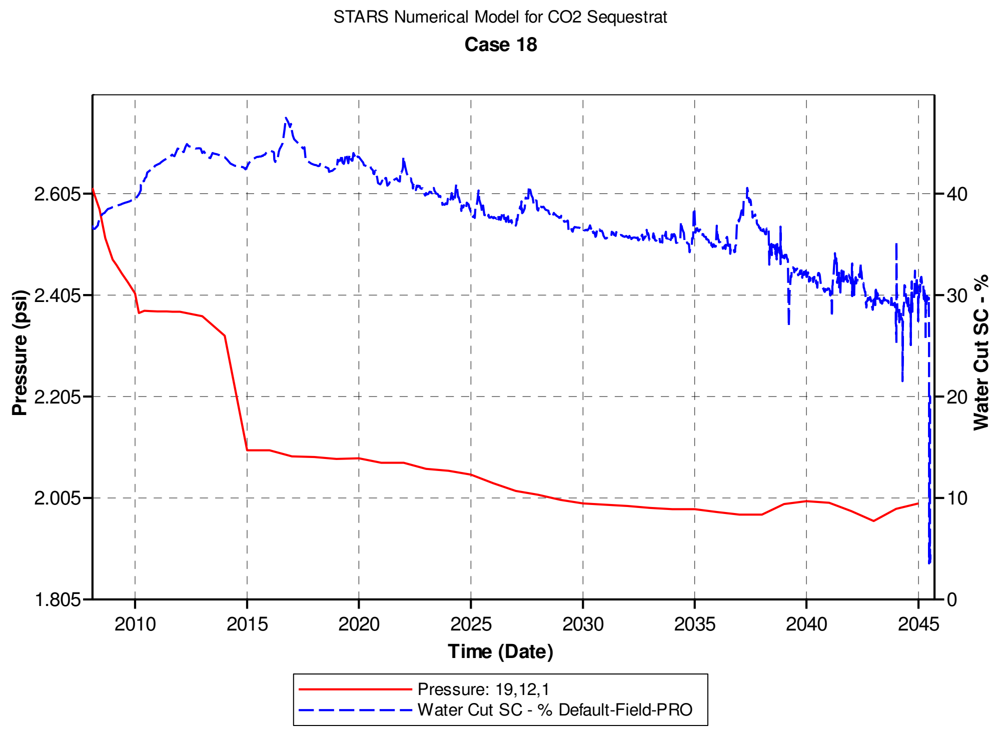

Figure6.52 Case 18, Average pressure and water cut

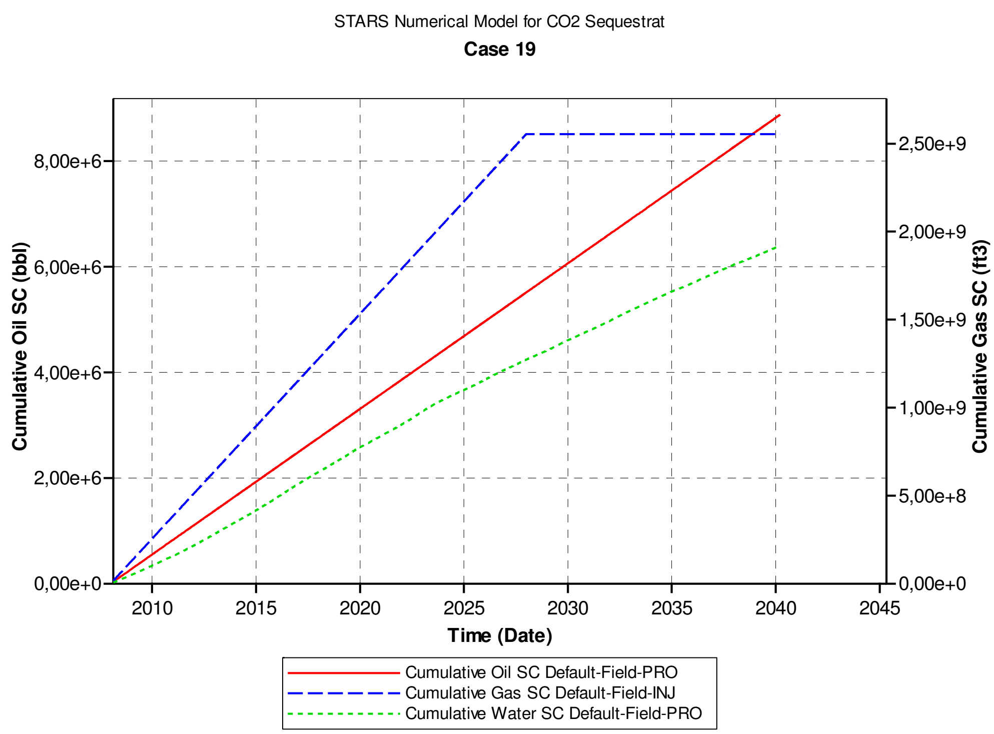

Figure6.53 Case19, Cumulative oil and water produced

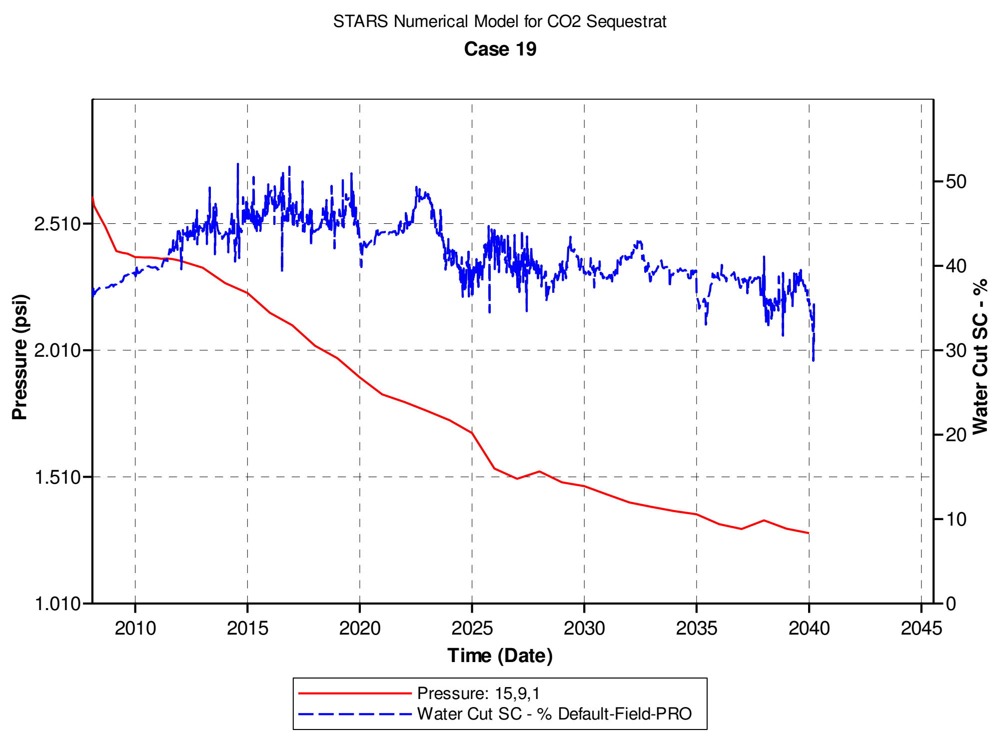

Figure6.54 Case 19, Average pressure and water cut

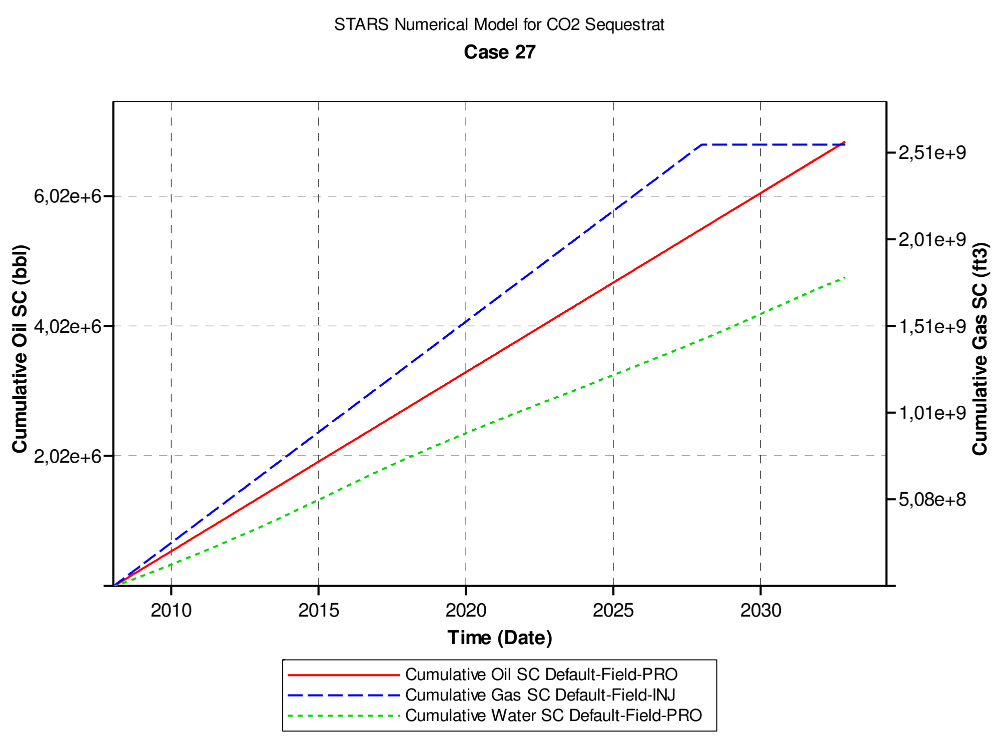

Figure6.55Case19, Cumulative oil and water produced

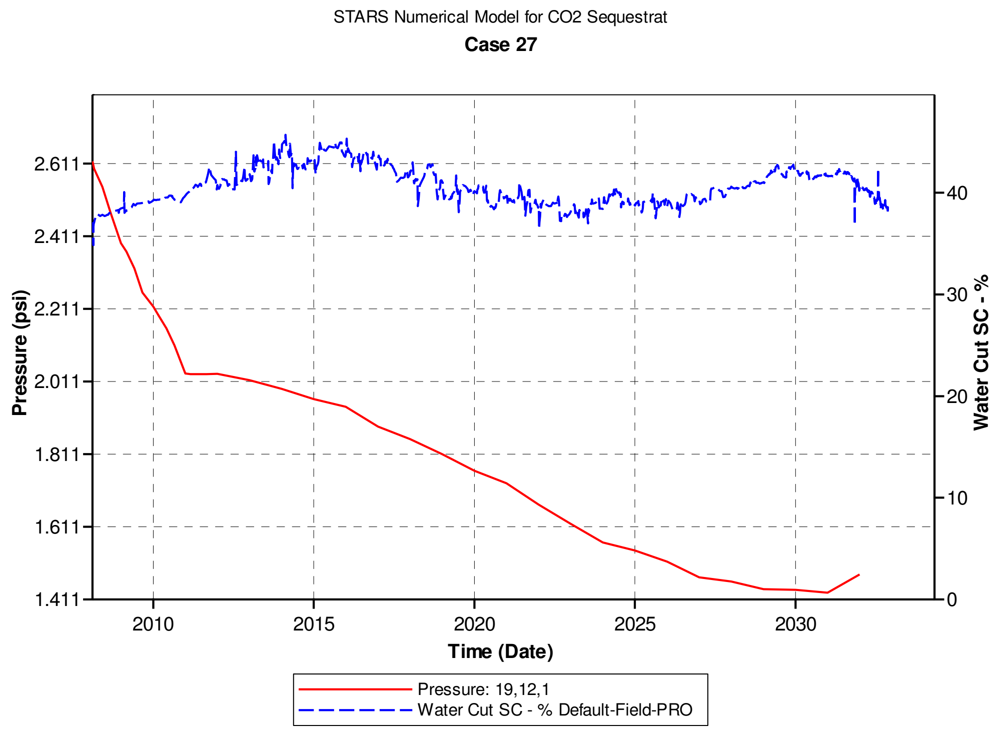

Figure6.56 Case 27, Average pressure and water cut

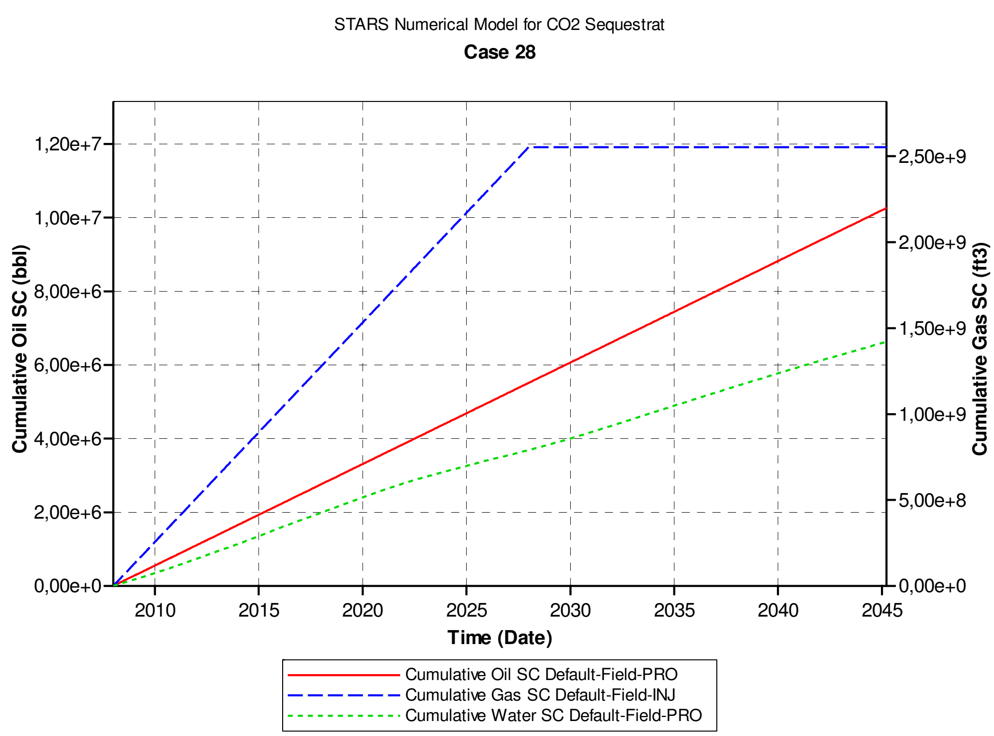

Figure6.57 Case18, Cumulative oil and water produced

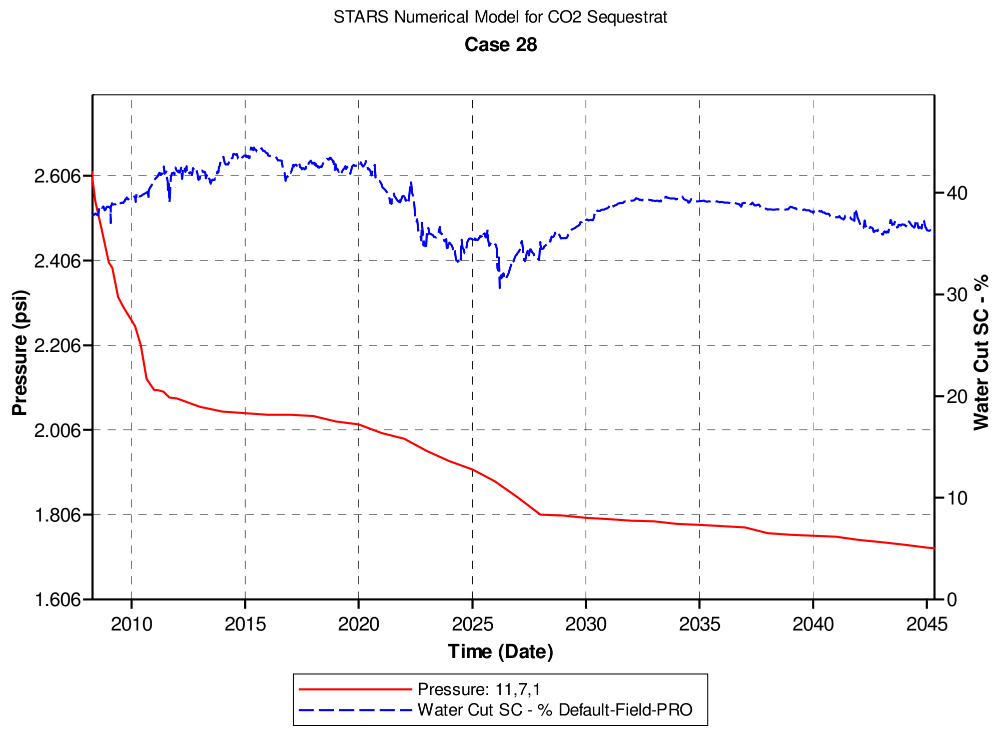

Figure6.58 Case 28, Average pressure and water cut

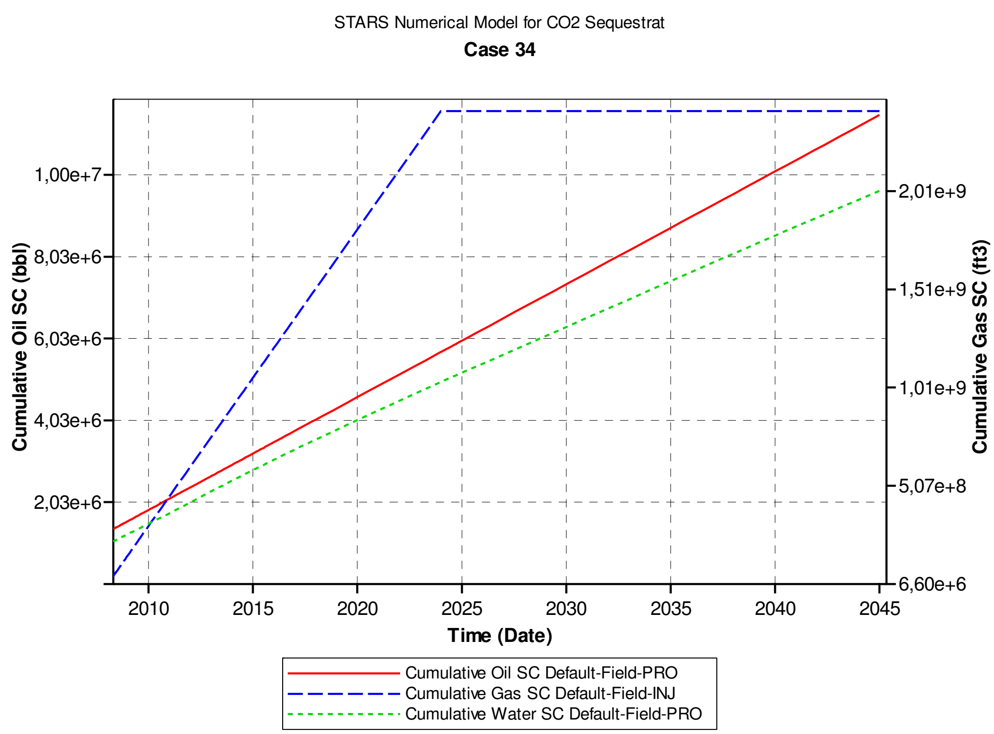

Figure6.59 Case34, Cumulative oil and water produced

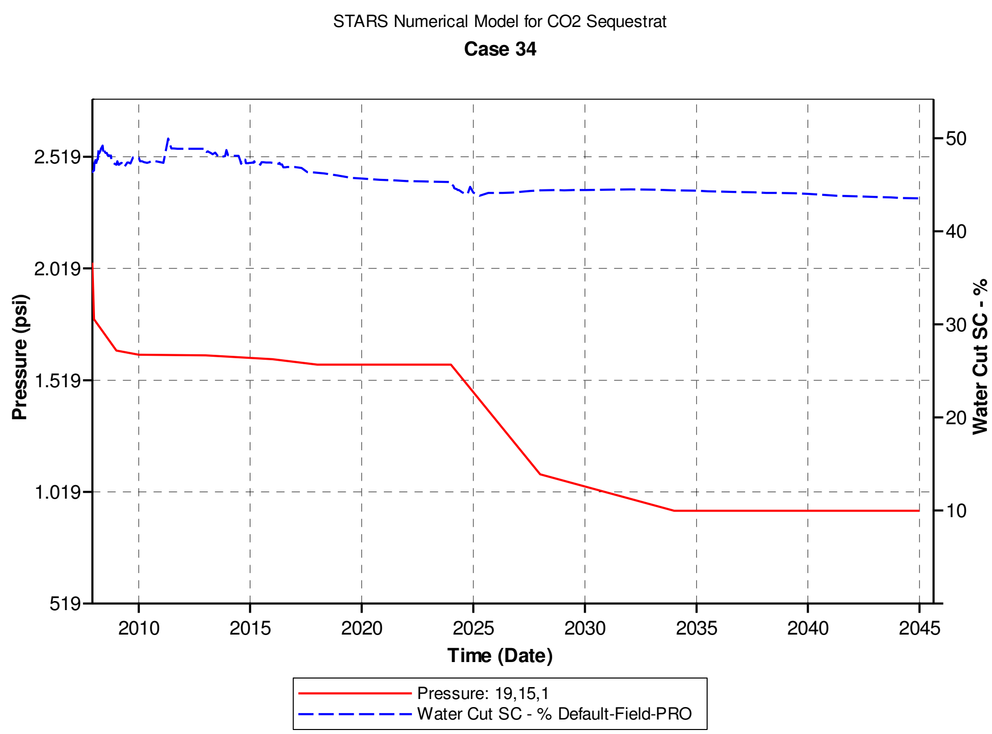

Figure6.60 Case 34 , Average pressure and water cut

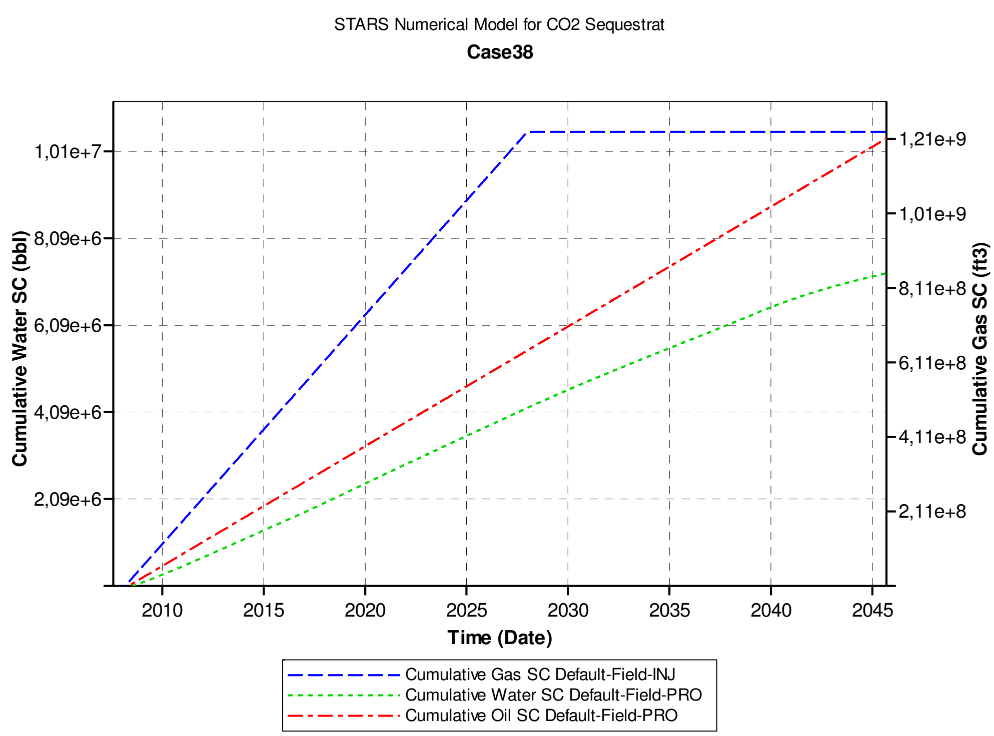

Figure6.61 Case38, Cumulative oil and water produced

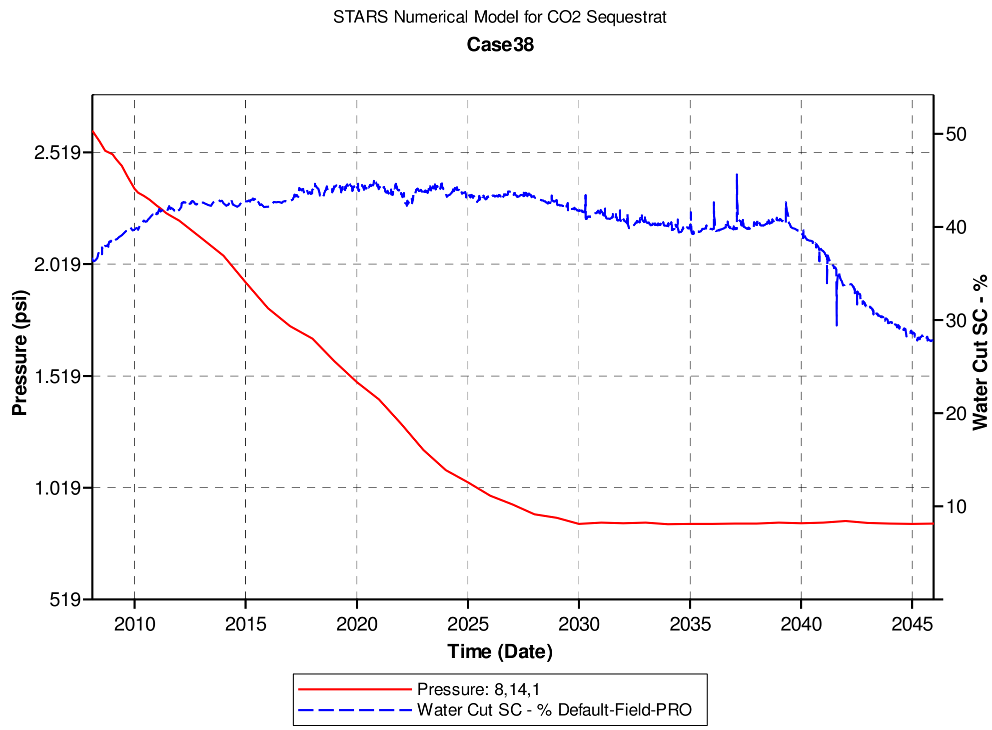

Figure6.62 Case 38, Average pressure and water cut

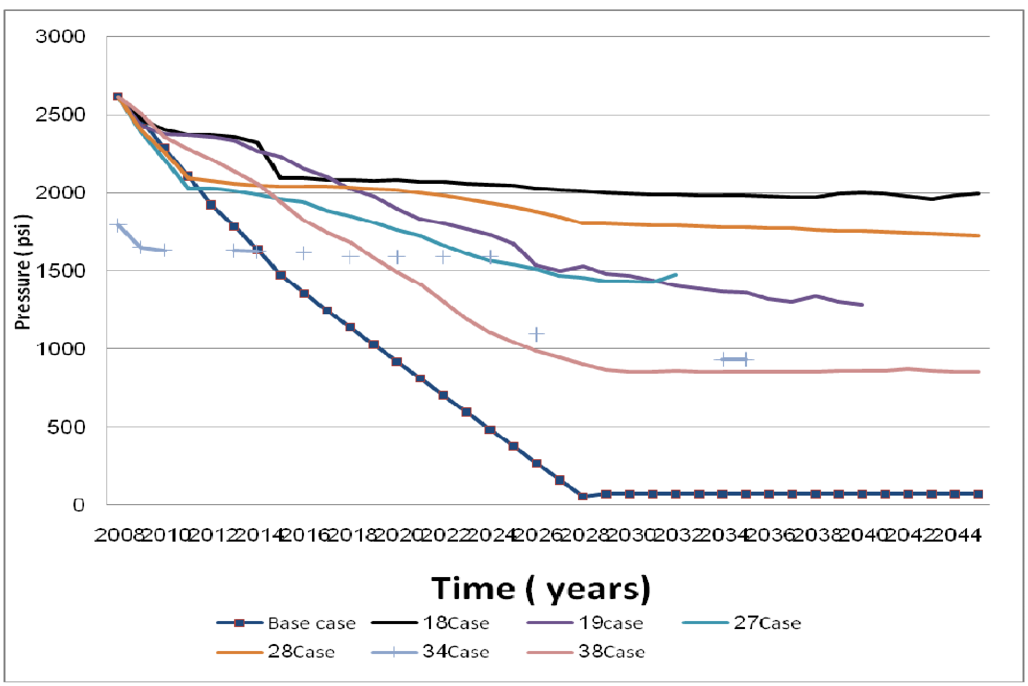

Figure6.63 Comparison between different pressures for cases with higher oil recovery

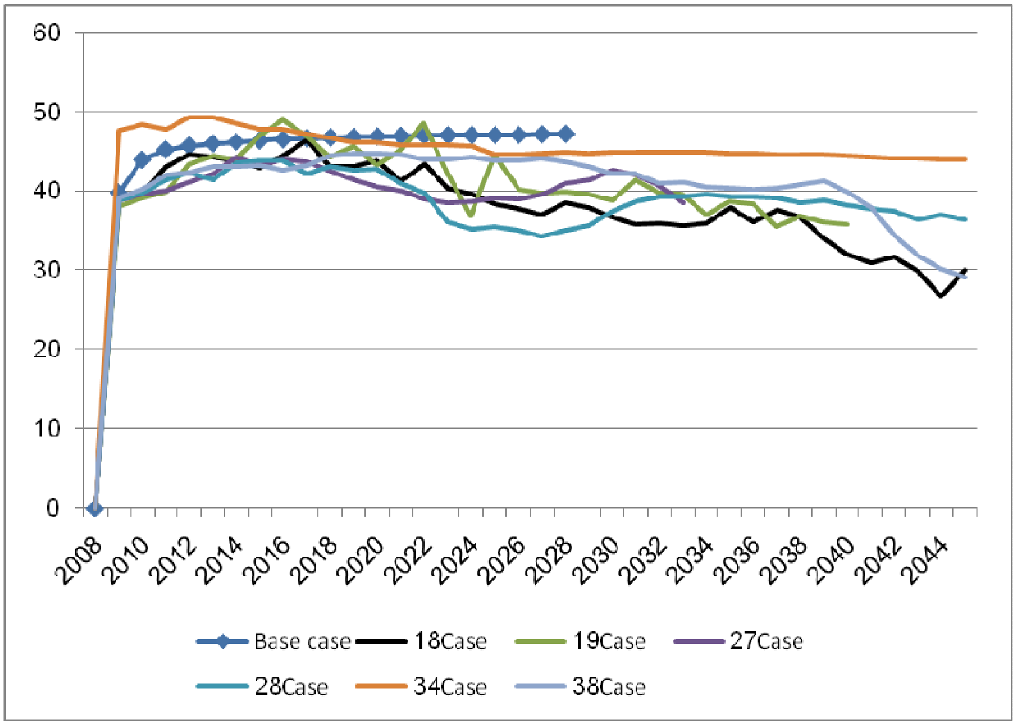

Figure6.64 Comparison between different water cuts for cases with higher oil recovery

6.2.3 The economical feasibility of the project

6.2.3.1 The economical model

For the sake of finding the maximum net present value (NPV) and comparing it among different sequestration cases, the study included an economical feasibility part. First, a cost overview is explained using the best cases. Analysis included NPV calculations using both current cases and carbon credited cases.

6.2.3.2 The costs of the sequestration process:

The costs of the sequestration can be divided in to four parts [45].These are capture, compression, transportation and storage costs. Any of these costs should not be directly compared, for they involve variation about fuel price and discount rate [55]. The following is a brief description of each section of the process.

The capture and processing contribute a good deal to overall cost of the sequestration process. Compression costs are higher for slow flows than for higher ones [55]. The costs according to Ecofys [56] range from 7.4-12.4US$/ton of CO_2.

An important factor is the capture cost. It constitutes about 75% of the total costs for CO_2 sequestration. Capture cost depends on the CO_2 concentration and stream, amount of CO_2 to be captured and pressure in the stream of emission source.

Van Bergen et al [55] suggested that, high capture costs are due to the equipments used for adsorbing carbon dioxide from sources where it's concentration is low.

Chances are there for minimizing the capture and compression costs. For example taking CO_2 from industrial process with high concentrations will need less energy for the effect of high concentration.

In our case, the hypothetical B field is nearby a thermal plant. With an annual amount of emissions of 3.12 MM Mt from plant A, and 2.91 MM Mt (52507MMcf) from the adjacent plant B, CO_2 concentration is assumed to be 70 %.

The cost of transportation was assumed to be so small as the field is assumed to be very close (<1 km) to the plant. Another assumption is the operating cost which was assumed to be 4US$/mt CO_2.

The storage cost varies from reservoir to another. Factors include injection costs, reservoir depth, and temperature [45]. However, for the sake of simplicity we will consider the injection costs only.

6.2.3.3 The assumptions of the project

Production scenarios were conducted before the corporate tax was deduced. Therefore, depreciation was not considered. The discount rate was taken as 12%. Royalty tax is assumed to be 12% [45]. No annual gas price escalation was assumed. Finally an assumed carbon credit of 5 US$/Mt CO_2 was used.

Capital expenditures and Operating expenditures:

Operating expenditures, for the well to be drilled and equipped the costs are assumed as in the following:

Compression cost = 0.06 US$ /McfCO_2, including compression and storage costs

However the capital expenditures (CAPEX) are as follows [45]:

Cost of drilling a new well = 1 MM US$

Investment in capture = 6 MMUS$

Investment in compression = 3 MMUS

Investment in storage = 3 MMUS$

Total Capex = 13MMUS$

Finally, the taxes that are associated are royalties' of12%. Severance tax of 8% is assumed.

These parameters are then put in an economical model proposed by Gasper et al [45]. The model was previously used in a mature Brazilian oil field. Since, some of the terms in the equation vary from place to another, the simplified yet still effective form of the equation was written as in equation 6.1

$$NCF = \left(R + C_{CO2} - Roy - OPEX - IW - D\right) * \left(1 - T\right) + D - CAPEX \qquad (6.1)$$

Leakage percentage was assumed as 5%of the injected CO_2 during the compression and storage processes. NCF is net cash flow. C_{CO2} is the assumed carbon credit, royalties is 12% and operating expenditure can be divided into four parts that are mentioned above, IW are drilling and completion expenditures.

Since it will have a positive effect, the depreciation factor was not considered. The simplified form of the equation was used as shown below:

$$NCF = \left(R + C_{CO2} - Roy - OPEX\right) - CAPEX \tag{6.2}$$

Economical analysis reveals that the more CO_2 was injected the more profits were gained. Such as Case 18 where the injection is from (CO2.2). Type relative permeability curves have the highest income among these cases.

6.2.3.3 Net Present Value results

When the simulation runs are compared, the NPV values revealed as in (Table 6.11) ,that the higher oil produced the better the outcome will be. However, a fundamental concept is the time value of money. When considering the successful cases. The following three concepts should be thoroughly controled:

1-The amount of oil produced: As the oil will be the only possible way to pay for the expenses of the project; and to provide an evacuated space for the carbon to sequester, oil recovery is highly important that only the cases exceeded the base case (without CO_2 injection) managed to a have a break even amount of money.

2-The amount of CO_2 injected: In the cases with high values of CO_2 sequestration two other things were important: The cost value of every cubic feet injected and the amount of oil produced which can compensate for the cost of the process.

3-The time value of money: Many of the cases that lasted for long period winded up uneconomical because of the value of money that was represented by the discount rate or opportunity cost after say 30 years. Thus, taking the total oil recovery as the basis for our analysis, six cases have produced higher amounts of oil than the base case. Those cases are able had the nearest NPV values to base case. Only two of the cases managed to be profitable with the costs of sequestration included. On the other hand, when a value was assigned for carbon credits, many of the cases that seemed unbeneficial turned out to be more profitable than the most profitable case without credits. Nineteen cases are higher than the base case. This time the equally important thing to oil recovery is the amount of carbon sequestered. This can be most vividly noticed in cases that lasted for only three of 4 years and were able to exceed the value of base case that lasted for twenty years.

Despite the role that carbon credits play in this process, carbon credits regulations are not widely used. Hence, we will rely on the cases that have exceeded in the amount of oil recovered, the base case since that and time are only sources to meet the project's expenses. The six cases that exceeded the base are plotted in (Figures 6.65-70).

Table 6.11 NPV Value comparisons for all runs.

Case #	NPV (MMUS$)	NPV with C. Cr(MMUS$)	Case #	NPV (MMUS$)	NPV with C. Cr(MMUS$)
Case 1	224.02	-	Case 27	201.69	334.15
Case 2	68.64	126.04	Case 28	213.41	355.22
Case 3	85.35	133.51	Case 29	190.85	326.69
Case 4	72.81	95.18	Case 30	190.93	326.78
Case 5	69.80	103.35	Case 31	192.95	334.17
Case 6	73.22	152.22	Case 32	186.07	318.57
Case 7	112.21	155.92	Case 33	195.36	360.39
Case 8	42.01	75.05	Case 34	208.11	373.24
Case 9	74.81	143.18	Case 35	200.69	294.96
Case 10	76.81	150.18	Case 36	220.89	335.34
Case 11	170.07	301.57	Case 37	197.60	290.90
Case 12	94.68	176.71	Case 38	230.40	296.56
Case 13	78.57	144.35	Case 39	73.90	137.97
Case 14	75.80	133.62	Case 40	73.90	137.97
Case 15	22.22	39.52	Case 41	117.90	155.30
Case 16	64.63	120.74	Case 42	73.19	136.62
Case 17	45.93	56.55	Case 43	73.94	138.01
Case 18	235.76	295.86	Case 44	133.85	249.81
Case 19	212.46	344.54	Case 45	192.98	198.18
Case 20	149.77	256.41	Case 46	77.58	102.09
Case 21	142.13	243.28	Case 47	59.52	73.29
Case 22	182.24	311.96	Case 48	129.43	170.35
Case 23	165.77	374.19	Case 49	166.68	219.41
Case 24	6.17	10.55	Case 50	127.47	167.74
Case 25	32.14	55.03	Case 51	166.10	218.68
Case 26	9.32	15.97			

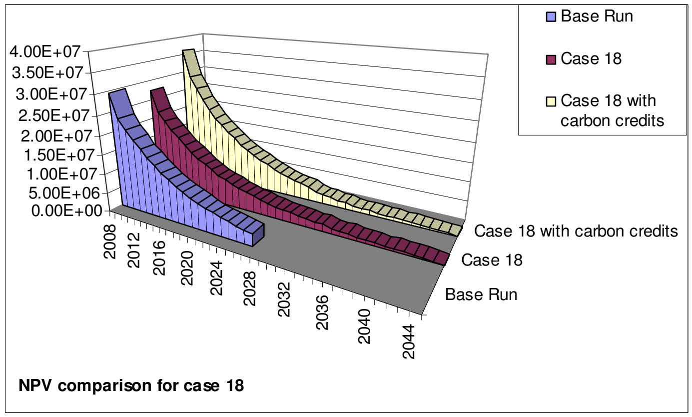

Figure6.65 NPV comparison for case 18

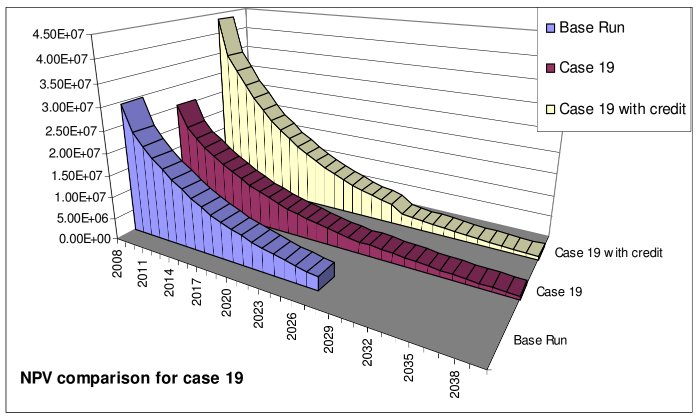

Figure6.66 NPV comparison for case 19

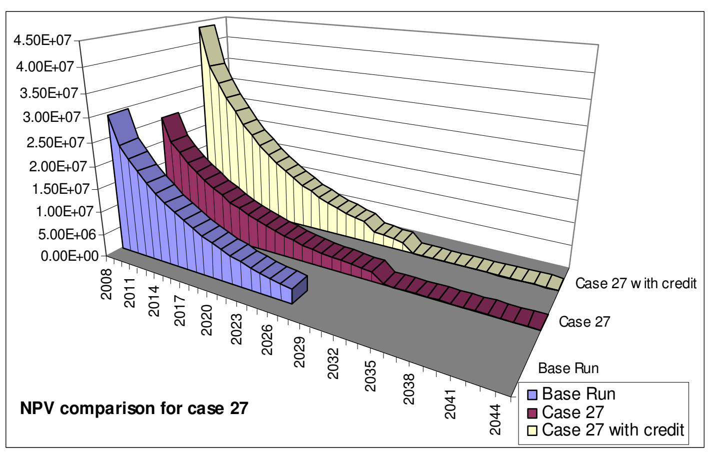

Figure6.67 NPV comparison for case 27

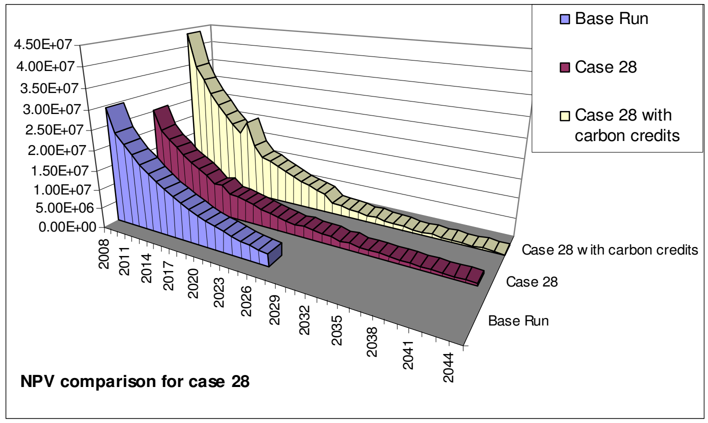

Figure6.68 NPV comparison for case 28

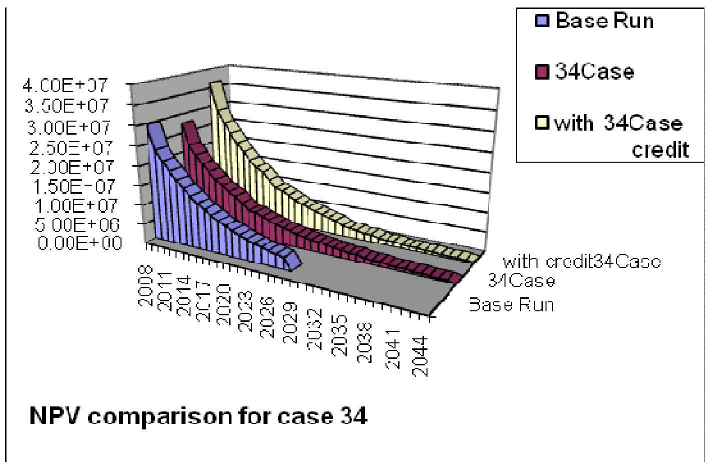

Figure6.69 NPV comparison for case 34

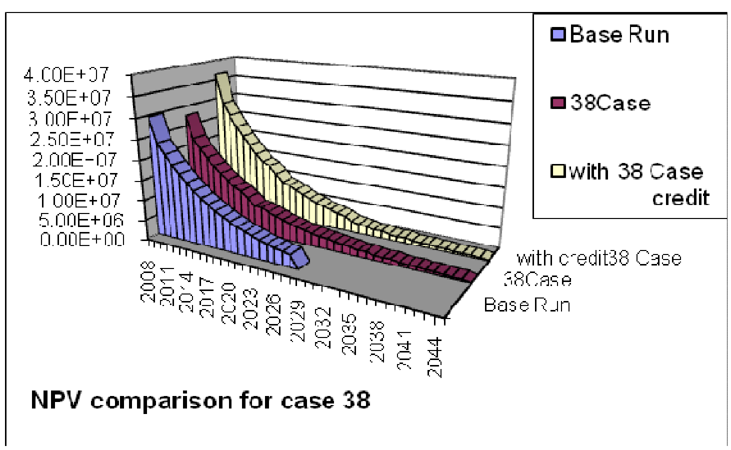

Figure6.70 NPV comparison for case 38

To have a more realistic view that compares the six cases all together (Figure 6.71) – was plotted. In this figure we are able to see the two cases that exceeded the base

NPV value without credit. When carbon credits added, all six cases are more profitable with the one that most CO_2 storage as the largest.

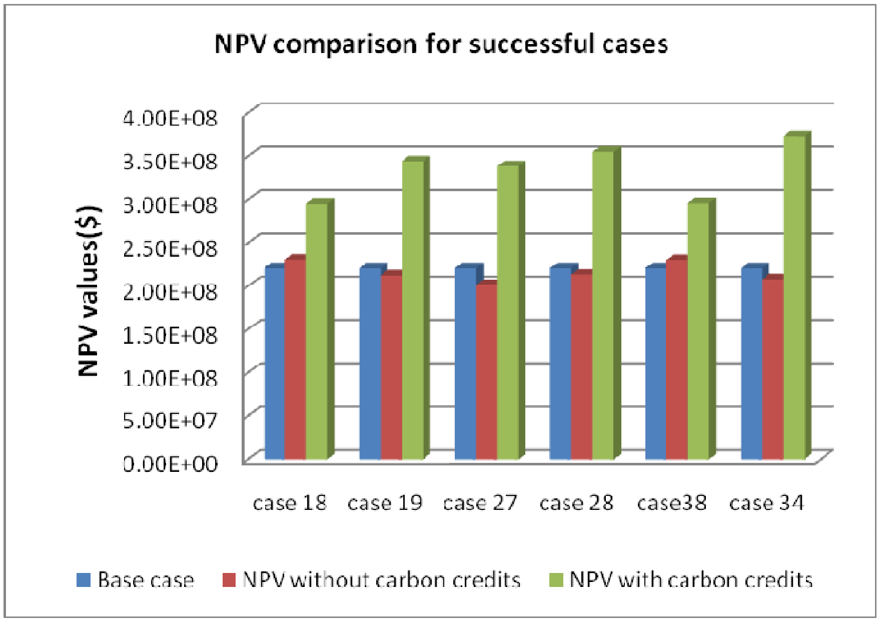

Figure 6.71Comparison between the base case, successful prediction cases and predictions cases with carbon credit

CHAPTER 7

CONCLUSIONS

7.1 Conclusions

The study explores the feasibility of CO_2 sequestration in a mature carbonate field. The first part of the study is history matching, where the production, bottom hole pressure and water cut data were matched. This match was achieved using.CMG STARS. After that, factors and late fate of the type of trapping is studied. Finally, an economical analysis is provided for the successful cases. During this study the following were concluded**:**

1-Applying sum of square residual analysis is accurate and resulted in acceptable water cut and production history matching.

2- For the field of concern, injection into a low permeability region proved to be more productive than high injection permeability regions.

3- Large distances between injection and production well locations are required to avoid early breakthroughs. In our case, well location (CO2.2) proved to be at approximately equal distance from production wells and highly permeable regions (to avoid channeling).

4-Although, in general it is wise to inject gas in supercritical state from the reservoir crest to use gravity forces and have pressure support. It was found that the highest recovery and CO_2 sequestration obtained by injecting from the bottom layer since supercritical CO_2 has a density less than oil and water, and will have a tendency to migrate upwards.

5- Injection rate is found to be one of the main controlling features for a successful sequestration. When injection was from more than a single point the production was negatively affected yielding the whole process unbeneficial.

6-Injecting from the bottom layer was found to be the only feasible way to keep the pressure. and injection from more than one layer forced the CO_2 from the lower layer to combine and increase the pressure or cause cooling that resulted in time step cuts and eventually, erratic answers. Therefore, it was found that injection from a single injection well located at the center of the reservoir provides longer injection period with no gas breakthrough and no pressure violation.

7-High injection pressures lead to dissolution of CO_2 in water at a higher rate. Mineral deposition of carbonate calcium is influenced negatively as the flowrate gets higher that leads to smaller residence time and renders the chemical reactions incomplete.

8- The effect of end point relative permeability change is important. A change in relative permeability end points may result in either a production improvement or reduction. The hydrodynamical trapping when generic curves are used is higher at the beginning is higher. Since flow is not localized (less compact plume). But the overall hydrodynamical trapping result is better for Frio like relative permeabilities relative where relative permeability is higher. For solubility trapping, the total solubility in Frio case is higher; and both curves did not improve the storage amount but did improve oil recovery.

9-Hysteresis effect can render the gas trapped which is an effective cause of immobile free gas trapping. Carlson and Killough models are compared and both cases resulted in less gas being stored. Changing saturation path for the gas enlarged the amount of oil recovered but CO_2 stored was less.

10- Fracture spacing effect was explained by five contemporary systems. Fine spaced systems produced more oil. The gas saturation for hydrodynamical and structural trapping was better in fine and vertical spacing types. For vertical, horizontal and homogenously fractured systems, oil recovery is positively affected by vertical spacing since better hydrodynamic and residual trappings was achieved . Horizontal fracture dominated runs resulted in a lower recovery and CO_2 storage. This is because of the gas tendency to migrate upwards instead of using the path effect towards injection wells, and thus results in late gas breakthrough to production wells, which is a favorable result for sequestration. For hydrodynamical trapping, vertical fracturing is more favored as the gas can travel vertically more than horizontal fracturing. For solubility trapping, again the gas will prefer horizontal flow paths and will dissolve on the way to production wells. However once injection stops the gas starts migrating to the upper layers. And thus vertical trapping will dominate the flow again.

11- H_2S addition to CO_2 has a positive effect on oil recovery by decreasing the minimum miscibility pressure. For solubility trapping the minimum enrichment time was effective when the H_2S concentration was higher than 10%. In the case of adding CO to the CO_2, the hydrodynamical trapping was good, as the simulator gave combined results of both the free CO and that which formed CO_2 by reaction . The overall performance was that, CO additive affected the storage badly.

12- The NPV values of a CO_2 storage project depends on many factors like oil price, capital expenditures, operating expenditures, royalties, number of injection/production wells …etc. It was observed that oil produced, CO_2 injected and injection time are the major parameters for a successful CO_2 sequestration project.

13 -Having six high recovery cases for this field does not guarantee that each one of them is applicable, nor that any high gas storage value cases will necessarily mean

that each high storage case will be a profitable case. However, the three should be balanced. It was noticed that moderate storage rate and high recovery rate are the characteristics of the profitable case.

7.2 Recommendations

Automated history matching may improve the time spent in history matching.

Smart wells may be used to control the amount of gas injected.

Advanced process like acid gas effect on increasing ph and sulfide reaction could result in more realistic simulations. Adding the sour gas may help to recover oil. This will need additional data and experiments to show the rate and represent the reaction in a realistic manner.

Risk analysis to calculate economical facts independently can yield to erroneous results. These can better represented by encountering a group of factors simultaneously with a software.

REFERENCES

1- Houghton J.T., Ding Y., Griggs D.J., Noguer M., van der Linden P.J. and Dia X. :"Climate Change 2001: The Scientfic Basis", Cambridge University Press,2001.

2- Bolin B. : "Key Features of the Global Climate System to be considered in analysis of the Climate Change issue".Association of Environmental Resourses Economists,Tilburg,Sweden ,June, 1997.

3-Fact sheet US Delegation to the 3rd Conference of the Parties: "Sixgreenhouse gases", United Nations Committee on Climate Change, Kyoto, December 5, 1997.

4- Rose A.: "Burden Sharing and Climate Change Policy Beyond Kyoto: Implications for Developing Countries", Penn. State University, University Park, PA16802, U.S.A.

5-Pearce D.W. "Economic Development and Climate Change", University College London, Gower St, London WCIE 6BT, UK.

6- Hourcade J., Ch., : "The Thin Pathway for reconciling development and climate change mitigation",Research Director (Cnrs) 94736Nogent sur Marne Cedex,France.

7- Hendriks C. A. and Blok K. : "Underground Storage of Carbon Dioxide", Energy Conversion and Management, 34(9-11),949-957,1993.

8- Herzog H., Eliasson B. and Kaarstad O. : "Capturing Greenhouse Gases", Scientific American,P72,Feb,2000.

9- Jarrell P.M., Fox C.E Stein, M.H. and Webb, S.L.:"Practical Aspects of CO_2 Flooding", SPE Monograph series, Volume 22, Richardson, TX, 2002.

10- Al-Dliwe A., and Asghari K.: "Reservoir Characterization and Simulations Studies in a Heterogeneous Pinnacle Reef for CO_2 Flooding Purposes: A Case Study", Middle East Gas and Oil Show, Bahrain, March, 2005.

11- Mo S. and Akervoll I.:"Modelling Long term CO_2 storage in aquifer with a black oil reservoir simulator", 2005.

12- Juanes R. Spireti E, J., Orr Jr. F. M.: "Scaling analysis of the migration of CO_2 in saline Aquifers".SPE paper 102796, Annual Technical Conference and Exhibition San Antonio, TX.

12- Kumar D.: "Optimization of well testing to maximize residually trapped CO_2 in Geologic Carbon Sequestration", M.Sc thesis, Department of Energy Resourses Engineering ,Stanford University,California, USA, June,2007.

13- Izgec O., Demiral B., Bertin H., Akin S.: " CO_2 injection into carbonate aquifer formations II: Comparison of Numerical Simulations to Experiments", Transp.Porous.Med, 73:57-74, DOI 10.1007/s 11242-007-9160-1, 2008.

14- Pruess K., Xu T .,Apps J.: numerical modeling of aquifer disposal of CO_2 paper SPE 66537 prepared for a presentation at the SPE/EPA/DOE exploration and production environmental conference held in San Antonio ,Texas,26-28 February,2001.

15- Nguyen T .A, Farouq A., S.M.: Effect of Nitrogen on solubility and Diffusivity of carbon Dioxide into oil Recovery by the Immiscible WAG process.

16- Juanes,R. and MacMinn C.W.: " Upscaling of capillary trapping under gravity override :application to CO_2 Sequestraion in Aquifers", SPE paper 113496, presented at the 2008 SPE/DOE improved oil recovery Symposium held in Tulsa Oklahoma, 19-23 April 2008.

17- Asgarpour S.: "An overview of miscible Flooding" journal of Canadian petroleum Technology, February 1994, Volume 33 No. 2, pp 13-15

18- Kovscek A.R.:" Screening Criteria for CO_2 Storage in Oil Reservoirs". Department of Petroleum Engineering, Stanford University, Stanford, CA, U.S.A, January, 2002.

19- Thambimuthu K.V., McMullan P., Wright J., Wilson M., and Seckington B.:"Capture & Storage of CO_2," annual report, IEA GHG, Stoke Orchard, United Kingdom Nov, 2002.

20- Bromeyer R.J., Borling D.C., Pierson W.T.: " lost soldier Tensleep CO_2 Tertiary Project, performance Case History; Bairoil, Wyoming" paper SPE 35191 presented at the premium Basin oil & Gas recovery conference held in Midland, TX, USA., March 27-29 1996.

21- Hadlow R.E.:"Update of industry experience with CO_2 injection," paper SPE 24928 presented at the 6th Annual technical conference in Washington D.C, October 4-7, 1992.

22- Bellavence J.F.R.: "Dollarhide Devonian CO_2 Flood: project performance review 10 years later," paper SPE 35190 presented at the SPE premium Basin Oil & GAS Recovery conference held in midland , TX,U.S.A, March 27-29, 1996

23- Taber J.J, Martin S., Seright R.:"EOR Screening Criteria Revisited-part1: introduction to screening criteria and enhancement recovery Field projects " SPE Reservoir engineering, August 1997,pp 189-198.

24- Howes J.B." Enhancement oil recovery in Canada success in progress," Journal of Canadian Petroleum Technology, November-December 1988, volume 27, No. 6, pp 80-88

25- Laieb K., Tiab D.: "Design and performance of miscible Flood displacement" paper SPE 70021 presented at the SPE Permian Basin Oil and Gas conference held in Midland, Texas, May 15-17, 2001.

26- Malik Q. and Islam M.: "CO_2 injection in the Weyburn field of Canada optimization of enhanced oil recovery and Greenhouse Gas storage with Horizontal wells" paper SPE 59327 presented at the 2000 SPE/DOE Improved Oil recovery Symposium held in Tulsa Oklahoma, April 3-5.

27- Bachu S. and Shaw M.: "Evaluation of the CO_2 sequestration capacity in Alberta's oil and Gas reservoirs at the depletion and at the effect of the underlying aquifers," journal of Canadian petroleum Technology, September 2003, volume 43 No 9, pp 51-61.

28- Pletcher J.L.: "Improvements to reservoir Material –Balance methods", SPE Reservoir Evaluation & engineering February 2002, pp 49-59.

29- Dumore J.M.: Stability consideration in downward miscible displacement, SPE paper 961 presented at the 39th SPE annual fall meeting held in Houston, October 11-14, 1964.

30- Lee J.E., Niven R.G., and Cochrane J.T.H.: "the effect of rate on recovery for Canadian Carbonate Reservoir," paper SPE 5128 was prepared at for the 49th Annual Fall Meeting of society of petroleum engineering of AIME to be held in Houston, Texas, October 6-9, 1974.

31- Zhang P.Y., Huang S., Sayegh S., Zhou X.L.: "Effect of CO_2 Impurities on Gas-injection EOR process," paper SPE 89477 presented at the 2004 SPE/DOE Fourteenth Symposium improved oil Recovery held in Tulsa, Oklahoma , U.S.A., April 17-21.

32- Mungan N., and Johansen R.T.:"Fundamental Aspects of Carbon Dioxide Flooding", World Oil, August, 1981.

33-Bachu S.: "sequestration of CO_2 in geological media in response to climate change: road map for site selection using transform of the geological space in to the CO_2 phase space, "energy conversion and management, , volume 43, pp 87-102, 2002.

34-Gunter W.O. , Chalatrunyk R.J. and Scott J.D. : "Monitoring of aquifer disposal of CO_2 : Experience from underground Gas Storage and Enhanced Oil Recovery" ,Greenhouse gas control technologies , p151-153.

35- Karaoguz K.O.,Topguder N.N.,Lane R.H., Kalfa U. and Celebioglu D. : "Improved Sweep In Bati Raman Heavy- Oil CO_2 Flood: Bulhead Flowing Gel Treatments Plug Natural Fractures ,SPE paper 89400, SPE Reservoir Evaluation & Engineering, April 2007.

36- Sengul. M: "CO2 sequestration a safe transition technology", SPE paper 98617, AbuDHABI, April 2-4 , 2006.

37- Doughty Ch., Freifeld B.M. and Trautz R.C. : “ Site characterization for co2 geoloic storage and vice versa : the frio brine pilot , Texas , USA as a case study”, Environ. Geol. (2008), DOI 10/1007/s—254-007-0942-0, July ,2007.

38- Hovorka S.D., Benson S.M., Doughty Ch., Freifeld B.M., Sakurai S., Daley T.M., Kharaka Y.K., Holtz M.H., Trautz R.C., Nance H.S., Meyer L.R.and Knauss K.G.: “Measuring permanence of CO2 storage in saline formations—the Frio experiment”. Environ Geosci., 13(2):105–121, 2006.

39-Alberta geological survey,

http://www.ags.gov.ab.ca/co2_h2s/means_of_storage.html

Last online accestion on 30.10.2008.

40- TNO Built Environment and Geosciences, "CO_2 storage pressure in finite saline aquifers”, Gelogical survey of Natherlands, 2007.

41 –Land C.S.:"Calculation of relative permeability of two and three phase flow properties, Soc.Pet.eng journal. pp 243149-156, 1968.

42- Killough J.E.:”Reservoir simulation with history dependent saturation functions”, petrol Trans, AIME; 261:37-41, 1973.

43- Bachu S. &. Gunter W.D.:"Acid-gas injection in the Alberta basin, Canada: a CO_2-storage experience, Alberta Geological Survey & Alberta Research Council, Canada, 2004.

44- Hyne J.B. and Tyrer D.: "Use of hydrogen free carbon monoxide with steam in recovery of heavy oil at low temperatures".United states patent, 1982.

45- Gasper A.T.F.S., Suslick S.B., Ferreira D.F. and Lima G.A.C.: " Economic Evaluation of Oil Production Project with EOR: CO_2 Sequestration in Depleted Oil Field".Paper SPE 94922, Presented at the American and Caribbean Petroleum Engineering Conference, Rio de Janeiro, Brazil, June, 2005.

46- Computer Modeling Group (CMG): STARS users guide, Computer modeling group LTD, Calgary ,Alberta,Canada,2007.

47- Mungan, N., and Johansen, R.T.: "Fundamental Aspects of Carbon Dioxide Flooding", World Oil, August, 1981.

48- Sengunduz,N.: " Reservoir Characterization and Modeling",TPAO, Bozova ,SE,Turkey,May,2006.

49-Parlaktuna M. and Gud-mundsson J.: "Phsical Properties of Natural Gases Computer program and subroutines".University of Trondheim and Norwegian Institute of Technology, November, 1991, pp21, Trondheim.

50-Janssen P. H., and Bossie-Codreanu D., 2005, "The Impact of Shale Barriers and Injection Strategy on CO2-Flooding and Sequestration Performance," paper SPE 95468 presented at the 2005 SPE Annual Technical Conference and Exhibition, Dallas, October 9-12.

51- Doughty Ch., and Pruess K.,"Modeling Supercritical Carbon Dioxide Injection in Heterogenous Porous Media", Earth Science Division, E,O.,Lawrence Berkeley National Laboratory, #1 Cyclotron Rd., MS 90-1116, Berkeley, CA, 94720,USA, January,2004.

52-Lenormand R., Zarcone C., and Sarr A.: "Mechanisms of the Displacement of One Fluid by Another in a Network of Capillary Ducts," J. Fluid Mechanics, 135, 123-132, 1983.

53- Valvatne P. H., and Blunt M. J.: "Predictive Pore-Scale Modeling of Two-Phase Flow in Mixed Wet Media," Water Resource. Res., 40, W07, 406, DOI: 10.1029/2003WR002, 627, 2004.

54- Dastan A., Gursel T.M., Karahan Y. and Akin S. "Carbon Sequestration in High Temperature Liquid Dominated Geothermal Reservoirs", World Geothermal Congress, Antalya, 24-29, April 2005.

55- Van Bergen F., Wildenburg T., Gale and J., Damen K.:" World wide selection of early opportunities of CO_2-EOR", Netherlands institute of applied geosciences TNO, National Geological Survey, 2002.

56- Ecofys and TNO –NITG:"Global Carbon dioxide Storage Potential and Costs", report, n EEP-02001, 2004.

APPENDICES

Appendix A

History matching runs

Table A.1 Manual changes in relative permeability around wells

case #	Permeablity over all	Layer 1 nearwell perms.(md)	Layer2 nearwell perms.	Layer 3 nearwell perms.
perm6		Grids perm (Distant, Closer)	Grids perm (Distant, Closer)	Grids perm (Distant, Closer)
B1	100	100,300	100,300	100,300
B2	100	100,500	100,700	200,800
B3	100	150,500	100,800	800 ,1200
B8	100	250,300	500,800	500 ,1200
B9	100	100,300	250,400	250,500

case #	Permeablity over all	Layer 1 nearwell perms.(md)	Layer2 nearwell perms.	Layer 3 nearwell perms.
perm4 ,j,kequal i		Grids perm (distant, Closer)	Grids perm (distant, Closer)	Grids perms (distant, Closer)
B1	100	100, 100	100,100	100,100
B2	100	100, 100	100,100	100,100
B3	100	100, 100	100,100	100,100
B8	100	100,100	100,100	100,100
B9	100	100,100	100,100	100,100

Table A-1 Continued

case #	Permeablity over all	Layer 1 nearwell perms.(md)	Layer2 nearwell perms.	Layer 3 nearwell perms.
perm8		Grids perm (Distant, Closer)	Grids perm (Distant, Closer)	Grids perm (Distant, Closer)
B1	200	200,350	200,350	200,350
B2	200	1600, 1200	1600, 1400	200,500
B3	200	1600 ,1000	1600 ,800	1600 ,500
B8	200	2400 ,1200	2000 ,2400	200 ,2400
B9	200	200 ,1200	1200 ,1600	1000 ,500

case #	Permeablity over all	Layer 1 nearwell perms.(md)	Layer2 nearwell perms.	LAYER 3 nearwell perms.
perm 4		Grids perm (distant, Closer)	Grids perm (distant, Closer)	Grids perms (distant, Closer)
B1	100	100,100	100, 100	100,100
B2	100	100,200	100, 200	100, 200
B3	100	100 , 150	100,150	100,150
B8	100	100 , 500	100 , 500	100 , 500
B9	100	100 , 250	100 , 250	100 , 250

Table A-1 Continued

case #	Permeablity over all	Layer 1 nearwell perms.(md)	LAYER 2 nearwell perms.	LAYER 3 nearwell perms.
perm7		Grids perm (distant, Closer)	Grids perm (distant, Closer)	Grids perms (distant, Closer)
B1	200	200 ,350	200 , 350	200 , 350
B2	200	800 ,600	800 , 700	200,250
B3	200	800 ,500	800 , 400	800 , 250
B8	200	1200, 600	1000 ,1200	200 , 1200
B9	200	200,600	800 , 600	500 , 250

case #	Permeablity over all	Layer 1 nearwell perms.(md)	LAYER 2 nearwell perms.	LAYER 3 nearwell perms.
perm9		Grids perm (distant, Closer)	Grids perm (distant, Closer)	Grids perms (distant, Closer)
B1	200	200,350	200 , 350	200 , 350
B2	200	5000, 4800	4000 , 5000	200 , 5000
B3	200	5000, 4000	5000 , 4000	5000 , 4000
B8	200	5000, 4000	4000 , 5000	200 , 2400
B9	200	200, 5000	200 , 5000	5000 , 4000

Table A-1 Continued

case #	Permeablity over all	Layer 1 nearwell perms.(md)	Layer2 nearwell perms.	Layer 3 nearwell perms.
perm9		Grids perm (Distant, Closer)	Grids perm (Distant, Closer)	Grids perm (Distant, Closer)
B1	200	200,350	200,350	200,350
B2	200	1600, 1200	1600, 1400	200,500
B3	200	1600 ,1000	1600 ,800	1600 ,500
B8	200	2400 ,1200	2000 ,2400	200 ,2400
B9	200	200 ,1200	1200 ,1600	1000 ,500

case #	Permeablity over all	Layer 1 nearwell perms.(md)	LAYER 2 nearwell perms.	LAYER 3 nearwell perms.
perm 5		Grids perm (distant, Closer)	Grids perm (distant, Closer)	Grids perms (distant, Closer)
B1	500	500,500	500,500	500,500
B2	500	500,500	500,500	500,500
B3	500	500,500	500,500	500,500
B8	500	500,500	500,500	500,500
B9	500	500,500	500,500	500,500

Table A-2 History match trails

					Solid densities							
Case number	kmat j	kmatk	Kfrac j	Kfrack	CaCO3	CaCHO3	NaBr	dep. reac for	dep. reac back	Numeric. Assump	Isothermality	Perms around wells
1	15	15	1200	1200	2.71	2.11	3.2	56	300	y	y	change by Multiplier
2	4	4	50	30	2.71	2.11	3.2	56	300	y	y	change by Multiplier
3	15	15	1200	1200	2.71	2.11	3.2	168	900	y	y	change by Multiplier
4	4	4	50	30	271.1	211.46	320. 0	56	300	y	n	change by Multiplier
5	4	4	200	200	2.71	2.11	3.2	56	300	y	y	change by Multiplier
6	15	15	1200	1200	2.71	2.11	3.2	3500	550	y	y	change by Multiplier
7	4	4	50	30	271.1	211.46	320. 0	0	0	n	n	change by Multiplier
8	4	4	200	200	271.1	211.46	320. 1	0	0	n	n	change by Multiplier
9	4	4	50	30	271.1	211.46	320. 3	0	0	n	n	change by Multiplier
10	15	15	200	200	271.1	211.46	320. 8	56	300	n	n	change by Multiplier
11	15	15	200	200	271.1	211.46	320. 0	56	300	n	n	change by Multiplier
12	4	4	100	100	271.1	211.46	320. 1	56	300	n	n	change by Multiplier
13	4	4	50	50	271.1	211.46	320. 2	56	300	n	n	change by Multiplier
14	15	15	1200	1200	2.71	2.11	3.2	168	900	y	y	Manual & Multiplier change
15	15	15	1200	1200	2.71	2.11	3.2	168	900	y	y	Manual & Multiplier change
16	15	15	1200	1200	2.71	2.11	3.2	168	900	y	y	Manual & Multiplier change
17	15	15	1200	1200	2.71	2.11	3.2	168	900	y	y	Manual & Multiplier change
18	15	15	1200	1200	2.71	2.11	3.2	168	900	y	y	Manual & Multiplier change
19	15	15	1200	1200	2.71	2.11	3.2	168	900	y	y	Manual & Multiplier change
20	15	15	1200	1200	2.71	2.11	3.2	20	50	y	y	Manual & Multiplier change

APPENDIX B

Table B.1 Prediction simulation runs

Base run

Wells in Production/Date	Wells in Injection and abandonment /Date	CO_2 injection Rates, rbbl/day /well	Factors & Constraints	Duration in (days)
OPEN B1-1-1-2008 OPEN B2-1-1-2008 OPEN B3-1-1-2008 OPEN B8-1-1-2008	No gas injection	0	-	7300

Case 2

Wells in Production/Date	Wells in Injection and abandonment /Date	CO_2 injection Rates, rbbl/day /well	Factors & Constraints	Duration in days
OPEN B9-1-2-2008 OPEN B2-1-2-2009 OPEN B3-1-2-2010 OPEN B8-1-2-2011	OPEN B7-1-2-2008 OPEN B1-1-2-2009 OPEN CO2-1-2-2010 SHUTİN B7-1-1-2028 SHUTİN B10-1-1-2028 SHUTİN CO2-1-1-2028	3300	3 injection wells- B7, B1&and CO2 Constraints: injection started in all of the nj. Wells in 2008. But stopped in B10 in 2009 and resumed in other wells	1752

Case 3

Wells in Production/Date	Wells in Injection and abandonment /Date	CO_2 injection Rates, rbbl/day /well	Factors & Constraints	Duration in days
OPEN B1-1-2-2008 OPEN B2-1-2-2009 OPEN B3-1-2-2010 OPEN CO2.2-1-2-2011 OPEN B8 in 1-1-2015	OPEN B7-1-2-2008 OPEN B1-1-3-2008 OPEN B8-1-3-2008 SHUTIN B7-1-1-2028 SHUTIN B10-1-1-2028 SHUTIN B80-1-1-2012:	3300	3 injection wells B7 , B1 and B8 Constraints: injection started in all of the nj. Wells in 2008. But stopped in B8 in 2009 and resumed in other wells	2190

Case 7				
Wells in Production/Date	Wells in Injection and abandonment /Date	CO2 injection Rates, rbbl/day /well	Factors & Constraints	Duration in days
OPEN B1-1-22008 OPEN B8-1-2-2009 OPEN B9-1-2-2010 OPEN B7.2-1-2-2008	OPEN B2-1-2-2009 OPEN B3-1-2-2009 OPEN CO2.2-1-2-2008 SHUTIN B2 1-9-2011 SHUTIN B3 1-9-2011 SHUTIN CO2.2 1-9-2011	3300	3 injection wells B2 ,B3, & CO2.2 Constraints : simulation stopped due to pressure violation in 2017.in blocks 2,6,3 4,53	3036.8
Case 8				
Wells in Production/Date	Wells in Injection and abandonment /Date	CO2 injection Rates, rbbl/day /well	Factors & Constraints	Duration in days
OPEN B1-1-2-2008 OPEN B2-1-2-2008 OPEN B3-1-2-2008 OPEN B8-1-2-2008	OPEN B7-1-2-2008 OPEN CO-1-2-2008 OPEN CO-1-2-2008 SHUTIN B7-1-1-2028 SHUTIN CO-1-1-2010 SHUTIN CO2.2-1-1-2028	3300	3 injection wells B7 , CO2.2 ,& CO2. Constraints : simulation stopped due to pressure violation in 2017.in blocks 2,6,3 4,53	730
Case 3				
Wells in Production/Date	Wells in Injection and abandonment /Date	CO2 injection Rates, rbbl/day /well	Factors & Constraints	Duration in days
OPEN B1-1-1-2008 OPEN B2-1-1-2008 OPEN B3-1-1-2008 OPEN B8-1-1-2008	OPEN CO2-1-1-2008 SHUTIN CO2-1-1-2028 OPEN B7-1-2-2008 SHUTIN B7-1-1-2028	4950	2 injection wells B6 , B7 Constraints : simulation stopped due to pressure violation in 2017.in blocks 2,6,3 4,53	1547.6

Case 13				
Wells in Production/Date	Wells in Injection and abandonment /Date	CO2 injection Rates, rbbl/day /well	Factors & Constraints	Duration in days
OPEN B1-1-2-2008 OPEN B2-1-2-2008 OPEN B3-1-2-2008 OPEN B8-1-2-2008	OPEN B7-1-2-2008 OPEN B10-1-2-2008 OPEN CO2-1-2-2008 SHUTIN B7-1-1-2028 SHUTIN B10-1-1-2028 SHUTIN CO2-1-1-2028	3300	3 injection wells- 2nd layer injection Constraints : simulation stopped due to pressure violation in 2017.in blocks 2,6,3 4,53	2058.6

Case 14				
Wells in Production/Date	Wells in Injection and abandonment /Date	CO2 injection Rates, rbbl/day /well	Factors & Constraints	Duration in days
OPEN B1-1-2-2008 OPEN B2-1-2-2008 OPEN B3-1-2-2008 OPEN CO2.2-1-2-2008	OPEN B7 1-2-2008 OPEN B10 1-3-2008 OPEN B80 1-3-2008 SHUTIN B71-1-2024 SHUTIN B10-1-1-2025 SHUTIN B80-1-1-2026	3300	3injection wells- 2nd layer injection Constraints : simulation stopped due to pressure violation in 2017.in blocks 2,6,3 4,53	1460

Case 15				
Wells in Production/Date	Wells in Injection and abandonment /Date	CO2 injection Rates, rbbl/day /well	Factors & Constraints	Duration in days
OPEN B1-1-2-2008 OPEN B2-1-2-2008 OPEN B3-1-2-2008 OPEN B8-1-2-2008	OPEN B7-1-2-2008 OPEN CO2-1-2-2008 OPEN CO2.2-1-2-2008 SHUTIN B7-1-1-2028 SHUTIN CO2-1-1-2010 SHUTIN CO2.2-1-1-2028	3300	3 injection wells- 2nd layer injection Constraints : simulation stopped due to pressure violation in 2017.in blocks 12,6,3 14,2,3	328.5

Case 16				
Wells in Production/Date	Wells in Injection and abandonment /Date	CO2 injection Rates, rbbl/day /well	Factors & Constraints	Duration in days
OPEN B1-1-1-2008 OPEN B2-1-1-2008 OPEN B3-1-1-2008 OPEN B8-1-1-2008	OPEN CO2.2-1-1-2009 SHUTIN CO2.2-1-1-2028	9900	1injection wells- 2nd & 3rd layer injection Constraints : simulation stopped due to pressure violation in 2017.in blocks 2,6,3 4,53	1182.6

Case 17				
Wells in Production/Date	Wells in Injection and abandent /Date	CO2 injection Rates, rbbl/day /well	Factors & Constraints	Duration in days
OPEN B1-1-2-2008 OPEN B2-1-2-2008 OPEN B3-1-2-2008 OPEN B8-1-2-2008	OPEN B20-1-1-2009 OPEN B30-1-1-2009 OPEN CO2.2-1-2-2008 SHUTIN B20-1-9-2011 SHUTIN B30-1-9-2011 SHUTIN CO2.2-1-9-2011	3300	3injection wells- 2nd & 3rd layer injection Constraints : simulation stopped due to pressure violation in 2017.in blocks 12,9,3	846.8

Case 18				
Wells in Production/Date	Wells in Injection and abandonment /Date	CO2 injection Rates, rbbl/day /well	Factors & Comments	Duration in days
OPEN B1-1-1-2008 OPEN B2-1-1-2008 OPEN B3-1-1-2008 OPEN B8-1-1-2008	OPEN CO2.2-1-1-2008 SHUTIN CO2.2-1-1-2028	9900	Single Injection well location optimization Comments: simulation run smoothly , to the end of the required period	13505

Case 19				
Wells in Production/Date	Wells in Injection and abandonment /Date	CO_2 injection Rates, rbbl/day /well	Factors & Constraints	Duration in days
OPEN B1-1-1-2008 OPEN B2-1-1-2008 OPEN B3-1-1-2008 OPEN B8-1-1-2008	OPEN B7-1-1-2008 SHUTIN B7-1-1-2028	9900	Single Injection well location optimization Constraints : simulation stopped due to pressure violation in 2017.in blocks 24,23,3	11680

Case 20				
Wells in Production/Date	Wells in Injection and abandonment /Date	CO_2 injection Rates, rbbl/day /well	Factors & Constraints	Duration in days
OPEN B1-1-1-2008 OPEN B2-1-1-2008 OPEN B3-1-1-2008 OPEN B8-1-1-2008	OPEN CO2-1-1-2008 SHUTIN B6-1-1-2028	9900	Single Injection well location optimization Constraints : simulation stopped due to pressure violation in 2017.in blocks 3,16,3	3650

Case 21				
Wells in Production/Date	Wells in Injection and abandonment /Date	CO_2 injection Rates, rbbl/day /well	Factors & Constraints	Duration in days
OPEN B1-1-1-2008 OPEN B2-1-1-2008 OPEN B3-1-1-2008 OPEN B8-1-1-2008	OPEN B20-1-1-2008 SHUTIN B20-1-1-2028	9900	Single Injection well location optimization Constraints : simulation stopped due to pressure violation in 2017.in blocks 5,17,3	3285

Case 22				
Wells in Production/Date	Wells in Injection and abandonment /Date	CO_2 injection Rates, rbbl/day /well	Factors & Constraints	Duration in days
OPEN B1-1-1-2008 OPEN B2-1-1-2008 OPEN B3-1-1-2008 OPEN B8-1-1-2008	OPEN CO2.2-1-1-2008 SHUTIN CO2.2-1-1-2028	9900	Optimum location –layer optimization Constraints : simulation stopped due to pressure violation in 2017.in blocks 9,18,3	6073.6

Case 23				
Wells in Production/Date	Wells in Injection and abandonment /Date	CO_2 injection Rates, rbbl/day /well	Factors & Constraints	Duration in days
OPEN B1-1-1-2008 OPEN B2-1-1-2008 OPEN B3-1-1-2008 OPEN B8-1-1-2008	OPEN CO2.2-1-1-2008 SHUTIN CO2.2-1-1-2028	9900	Optimum location –layer optimization Constraints : simulation stopped due to pressure violation in 2017.in blocks 11,17,2	6570

Case 24				
Wells in Production/Date	Wells in Injection and abandonment /Date	CO_2 injection Rates, rbbl/day /well	Factors & Constraints	Duration in days
OPEN B1-1-1-2008 OPEN B2-1-1-2008 OPEN B3-1-1-2008 OPEN B8-1-1-2008	OPEN CO2.2-1-1-2008 SHUTIN CO2.2-1-1-2028	9900	Optimum location –layer optimization Constraints : simulation stopped due to numerical instability	116.8

Case 25				
Wells in Production/Date	Wells in Injection and abandonment /Date	CO2 injection Rates, rbbl/day /well	Factors & Constraints	Duration in days
OPEN B1-1-1-2008 OPEN B2-1-1-2008 OPEN B3-1-1-2008 OPEN B8-1-1-2008	OPEN CO2.2-1-1-2008 SHUTIN CO2.2-1-1-2028	9900	Optimum location –layer optimization Constraints : simulation stopped due to numerical instability	481.8

Case 26				
Wells in Production/Date	Wells in Injection and abandonment /Date	CO2 injection Rates, rbbl/day /well	Factors & Constraints	Duration in days
OPEN B1-1-1-2008 OPEN B2-1-1-2008 OPEN B3-1-1-2008 OPEN B8-1-1-2008	OPEN CO2.2-1-1-2008 SHUTIN CO2.2-1-1-2028	9900	Optimum location –layer optimization Constraints : simulation stopped due to numerical instability	146

Case 29				
Wells in Production/Date	Wells in Injection and abandonment /Date	CO2 injection Rates, rbbl/day /well	Factors & Constraints	Duration in days
OPEN B1-1-1-2008 OPEN B2-1-1-2008 OPEN B3-1-1-2008 OPEN B8-1-1-2008	OPEN CO2.2-1-1-2008 SHUTIN CO2.2-1-1-2028	9900	Optimum location – pressure optimization Constraints : simulation stopped due to pressure violation in 2017.in blocks 16,19,3	7081

Case 30				
Wells in Production/Date	Wells in Injection and abandonment /Date	CO_2 injection Rates, rbbl/day /well	Factors & Constraints	Duration in days
OPEN B1-1-1-2008 OPEN B2-1-1-2008 OPEN B3-1-1-2008 OPEN B8-1-1-2008	OPEN CO2.2-1-1-2008 SHUTIN CO2.2-1-1-2028	9900	Optimum location – pressure optimization Constraints : simulation stopped due to pressure violation in 2017.in blocks 14,15,3	7081

Case 31				
Wells in Production/Date	Wells in Injection and abandonment /Date	CO_2 injection Rates, rbbl/day /well	Factors & Constraints	Duration in days
OPEN B1-1-1-2008 OPEN B2-1-1-2008 OPEN B3-1-1-2008 OPEN B8-1-1-2008	OPEN CO2.2-1-1-2008 SHUTIN CO2.2-1-1-2028	9900	Optimum location – pressure optimization Constraints : simulation stopped due to pressure violation in 2017.in blocks 14,18,3	7358.4

Case 32				
Wells in Production/Date	Wells in Injection and abandonment /Date	CO_2 injection Rates, rbbl/day /well	Factors & Constraints	Duration in days
OPEN B1-1-1-2008 OPEN B2-1-1-2008 OPEN B3-1-1-2008 OPEN B8-1-1-2008	OPEN CO2.2-1-1-2008 SHUTIN CO2.2-1-1-2028	9900	Optimum location – pressure optimization Constraints : simulation stopped due to pressure violation in 2017.in blocks 14,22,3	6467.8

Case 33				
Wells in Production/Date	Wells in Injection and abandonment /Date	CO2 injection Rates, rbbl/day /well	Factors & Constraints	Duration in days
OPEN B1-1-1-2008 OPEN B2-1-1-2008 OPEN B3-1-1-2008 OPEN B8-1-1-2008	OPEN CO2.2-1-1-2008 SHUTIN CO2.2-1-1-2028	9900	Optimum location – pressure optimization Constraints : simulation stopped due to pressure violation in 2017.in blocks 18,18,3	7329.2

Case 10				
Wells in Production/Date	Wells in Injection and abandonment /Date	CO2 injection Rates, rbbl/day /well	Factors & Constraints	Duration in days
OPEN B1-1-1-2008 OPEN B2-1-1-2008 OPEN B3-1-1-2008 OPEN B8-1-1-2008	OPEN CO2.2-1-1-2008 OPEN CO2.2-1-1-2008 SHUTIN B7-1-1-2028 SHUTIN CO2.2-1-1-2028	4950	2 injection wells Constraints : simulation stopped due to Fatal error	2555

Case 11				
Wells in Production/Date	Wells in Injection and abandonment /Date	CO2 injection Rates, rbbl/day /well	Factors & Constraints	Duration in days
OPEN B2-1-1-2008 OPEN B3-1-1-2008 OPEN B8-1-1-2008 OPEN B9-1-1-2008	OPEN CO2.2-1-1-2008 OPEN B10-1-1-2008 SHUTIN CO2.2-1-1-2028 SHUTIN B10-1-1-2028	4950	2 injection wells-2nd layer injection comments : simulation stooped due to time step cuts at 2022 (pressure warnings)	5475

Case 37				
Wells in Production/Date	Wells in Injection and abandonment /Date	CO2 injection Rates, rbbl/day /well	Factors & Constraints	Duration in days
OPEN B1-1-1-2008 OPEN B2-1-1-2008 OPEN B3-1-1-2008 OPEN B8-1-1-2008	OPEN CO2.2-1-1-2008 SHUTIN CO2.2-1-1-2028	9900	Fracture spacing Horizontal comments : simulation stooped due to time step cuts at 2022 (pressure warnings)	6205

Case 9				
Wells in Production/Date	Wells in Injection and abandonment /Date	CO2 injection Rates, rbbl/day /well	Factors & Constraints	Duration in days
OPEN B2-1-1-2008 OPEN B3-1-1-2008 OPEN B7-1-1-2008 OPEN B9-1-1-2008	OPEN B10-1-1-2008 OPEN B80-1-1-2008 OPEN CO2.2-1-1-2008 OPEN B10-1-1-2028 OPEN B80-1-1-2028 OPEN CO2.2-1-1-2028	3300	3 injection wells-2nd layer injection comments : simulation stooped due to time step cuts at 2020 (pressure warnings)	4015

Case 34				
Wells in Production/Date	Wells in Injection and abandonment /Date	CO2 injection Rates, rbbl/day /well	Factors & Constraints	Duration in days
OPEN B1-1-1-2008 OPEN B2-1-1-2008 OPEN B3-1-1-2008 OPEN B8-1-1-2008	OPEN CO2.2-1-1-2008 SHUTIN CO2.2-1-1-2028	9900	Rel. perm optimization-Frio Comments: simulation run smoothly , to the end of the required period	13505

Case 3				
Wells in Production/Date	Wells in Injection and abandonment /Date	CO2 injection Rates, rbbl/day /well	Factors & Constraints	Duration in days
OPEN B1-1-1-2008 OPEN B2-1-1-2008 OPEN B3-1-1-2008 OPEN B8-1-1-2008	OPEN B7-1-1-2008 OPEN B6-1-1-2008 SHUTIN B7-1-1-2028 SHUTIN B7-1-1-2028	4950	2 injection wells Constraints : simulation stopped due to numerical instability	1547.6

Case 4				
Wells in Production/Date	Wells in Injection and abandonment /Date	CO2 injection Rates, rbbl/day /well	Factors & Constraints	Duration in days
OPEN B7-1-1-2008 OPEN B8-1-1-2008 OPEN B3-1-1-2008 OPEN B1-1-1-2030 OPEN B2-1-1-2030	OPEN B1-1-1-2008 OPEN B2-1-1-2008 SHUTIN B1-1-1-2028 SHUTIN B2-1-1-2028	4950	2 injection wells simulation stooped due to time step cuts at (pressure warnings)	1752

Case 5				
Wells in Production/Date	Wells in Injection and abandonment /Date	CO2 injection Rates, rbbl/day /well	Factors & Constraints	Duration in days
OPEN B7-1-1-2008 OPEN B8-1-1-2008 OPEN B2-1-1-2008 OPEN B1-1-1-2030 OPEN B3-1-1-2030	OPEN B1-1-1-2008 OPEN B3-1-1-2008 SHUTIN B1-1-1-2028 SHUTIN B3 1-1-2028	4950	2 injection wells simulation stooped due to time step cuts at (pressure warnings)	1241

Case 35				
Wells in Production/Date	Wells in Injection and abandonment /Date	CO_2 injection Rates, rbbl/day /well	Factors & Constraints	Duration in days
OPEN B1-1-1-2008 OPEN B2-1-1-2008 OPEN B3-1-1-2008 OPEN B8-1-1-2008	OPEN CO2.2-1-1-2008 SHUTIN CO2.2-1-1-2028	9900	Rel. perm optimization-Generic Constraints : simulation stopped due to pressure violation in 2017.in blocks 14,16,3	13870

Case 39				
Wells in Production/Date	Wells in Injection and abandonment /Date	CO_2 injection Rates, rbbl/day /well	Factors & Constraints	Duration in days
OPEN B1-1-1-2008 OPEN B2-1-1-2008 OPEN B3-1-1-2008 OPEN B8-1-1-2008	OPEN CO2.2-1-1-2008 SHUTIN CO2.2-1-1-2028	9900	Hysteresis Carlson – max trap of 0.4 comments: simulation stopped after mole fractions normalized at2012	1460

Case 40				
Wells in Production/Date	Wells in Injection and abandonment /Date	CO_2 injection Rates, rbbl/day /well	Factors & Constraints	Duration in days
OPEN B1-1-1-2008 OPEN B2-1-1-2008 OPEN B3-1-1-2008 OPEN B8-1-1-2008	OPEN CO2.2-1-1-2008 SHUTIN CO2.2-1-1-2028	9900	Hysteresis Killough – max curve of 1.5 comments: simulation stopped after mole fractions normalized at2012	1460

Case 46				
Wells in Production/Date	Wells in Injection and abandonment /Date	CO_2 injection Rates, rbbl/day /well	Factors & Constraints	Duration in days
OPEN B1-1-1-2008 OPEN B2-1-1-2008 OPEN B3-1-1-2008 OPEN B8-1-1-2008	OPEN CO2.2-1-1-2008 SHUTIN CO2.2-1-1-2028	9900	Impurity injection 0.2CO comments: simulation stopped after mole fractions normalized at2014	1825

Case 50				
Wells in Production/Date	Wells in Injection and abandonment /Date	CO_2 injection Rates, rbbl/day /well	Factors & Constraints	Duration in days
OPEN B1-1-1-2008 OPEN B2-1-1-2008 OPEN B3-1-1-2008 OPEN B8-1-1-2008	OPEN CO2.2-1-1-2008 SHUTIN CO2.2-1-1-2028	9900	Impurity injection 0.1CO comments: simulation stopped after mole fractions normalized at2013	1503.8

Case 51				
Wells in Production/Date	Wells in Injection and abandonment /Date	CO_2 injection Rates, rbbl/day /well	Factors & Constraints	Duration in days
OPEN B1-1-1-2008 OPEN B2-1-1-2008 OPEN B3-1-1-2008 OPEN B8-1-1-2008	OPEN CO2.2-1-1-2008 SHUTIN CO2.2-1-1-2028	9900	Impurity injection 0.5CO comments: simulation stopped after mole fractions normalized at2013	1503.8

Case 47				
Wells in Production/Date	Wells in Injection and abandonment /Date	CO2 injection Rates, rbbl/day /well	Factors & Constraints	Duration in days
OPEN B1-1-1-2008 OPEN B2-1-1-2008 OPEN B3-1-1-2008 OPEN B8-1-1-2008	OPEN CO2.2-1-1-2008 SHUTIN CO2.2-1-1-2028	9900	Impurity injection 0.2H2S comments: simulation stopped after mole fractions normalized at2011	1095

Case 48				
Wells in Production/Date	Wells in Injection and abandonment /Date	CO2 injection Rates, rbbl/day /well	Factors & Constraints	Duration in days
OPEN B1-1-1-2008 OPEN B2-1-1-2008 OPEN B3-1-1-2008 OPEN B8-1-1-2008	OPEN CO2.2-1-1-2008 SHUTIN CO2.2-1-1-2028	9900	Impurity injection 0.1H2S comments: simulation stopped after mole fractions normalized at2011	1182.6

Case49				
Wells in Production/Date	Wells in Injection and abandonment /Date	CO2 injection Rates, rbbl/day /well	Factors & Constraints	Duration in days
OPEN B1-1-1-2008 OPEN B2-1-1-2008 OPEN B3-1-1-2008 OPEN B8-1-1-2008	OPEN CO2.2-1-1-2008 SHUTIN CO2.2-1-1-2028	9900	Impurity injection 0.05H2S simulation stooped due to time step cuts at (pressure warnings)	1182.6

Case 36				
Wells in Production/Date	Wells in Injection and abandonment /Date	CO2 injection Rates, rbbl/day /well	Factors & Constraints	Duration in days
OPEN B1-1-1-2008 OPEN B2-1-1-2008 OPEN B3-1-1-2008 OPEN B8-1-1-2008	OPEN CO2.2-1-1-2008 SHUTIN CO2.2-1-1-2028	9900	Fracture spacing vertical Constraints : simulation stopped due to pressure violation in 2017.in blocks 6,18,3	9855

Case 42				
Wells in Production/Date	Wells in Injection and abandonment /Date	CO2 injection Rates, rbbl/day /well	Factors & Constraints	Duration in days
OPEN B1-1-1-2008 OPEN B2-1-1-2008 OPEN B3-1-1-2008 OPEN B8-1-1-2008	OPEN CO2.2-1-1-2008 SHUTIN CO2.2-1-1-2028	9900	Hysteresis Carlson – max trap of 0.2 Constraints : simulation stopped due to pressure violation in 2017.in blocks 17,18,3	1460

Case 43				
Wells in Production/Date	Wells in Injection and abandonment /Date	CO2 injection Rates, rbbl/day /well	Factors & Constraints	Duration in days
OPEN B1-1-1-2008 OPEN B2-1-1-2008 OPEN B3-1-1-2008 OPEN B8-1-1-2008	OPEN CO2.2-1-1-2008 SHUTIN CO2.2-1-1-2028	9900	Hysterias Killough – max curve of 0,75 Constraints : simulation stopped due to pressure violation in 2017.in blocks 16,18,3	1460

Case 45				
Wells in Production/Date	Wells in Injection and abandonment /Date	CO_2 injection Rates, rbbl/day /well	Factors & Constraints	Duration in days
OPEN B1-1-1-2008 OPEN B2-1-1-2008 OPEN B3-1-1-2008 OPEN B8-1-1-2008	OPEN CO2.2-1-1-2008 SHUTIN CO2.2-1-1-2028	9900	Hysterias Killough – max curve of 0.375	13505

Case 44				
Wells in Production/Date	Wells in Injection and abandonment /Date	CO_2 injection Rates, rbbl/day /well	Factors & Constraints	Duration in days
OPEN B1-1-1-2008 OPEN B2-1-1-2008 OPEN B3-1-1-2008 OPEN B8-1-1-2008	OPEN CO2.2-1-1-2008 SHUTIN CO2.2-1-1-2028	9900	Hysteresis Carlson – max trap of 0.1 Constraints : simulation stopped due to pressure violation in 2017.in blocks 6,18,3	1096

APPENDIX C

Gas mole fraction for special cases

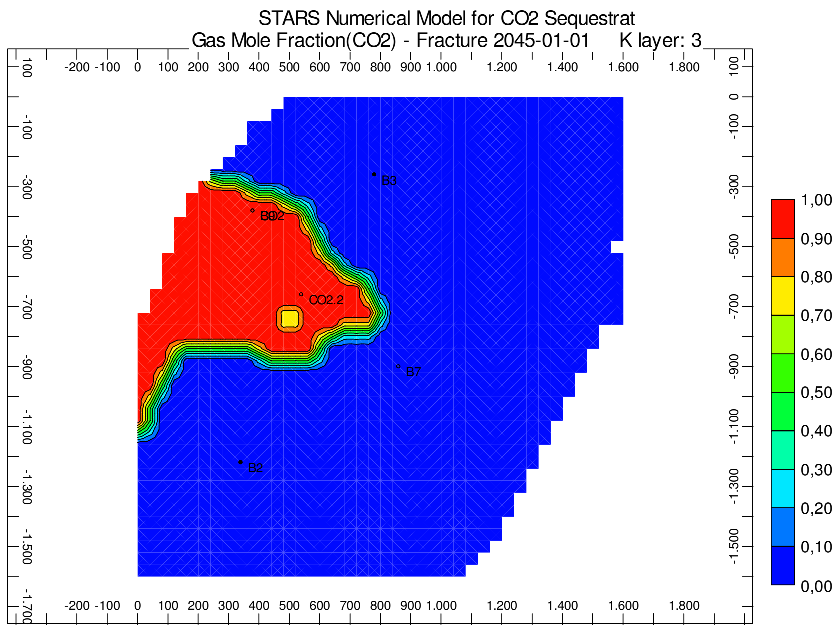

FigureC.1, Gas mole fraction for case 18

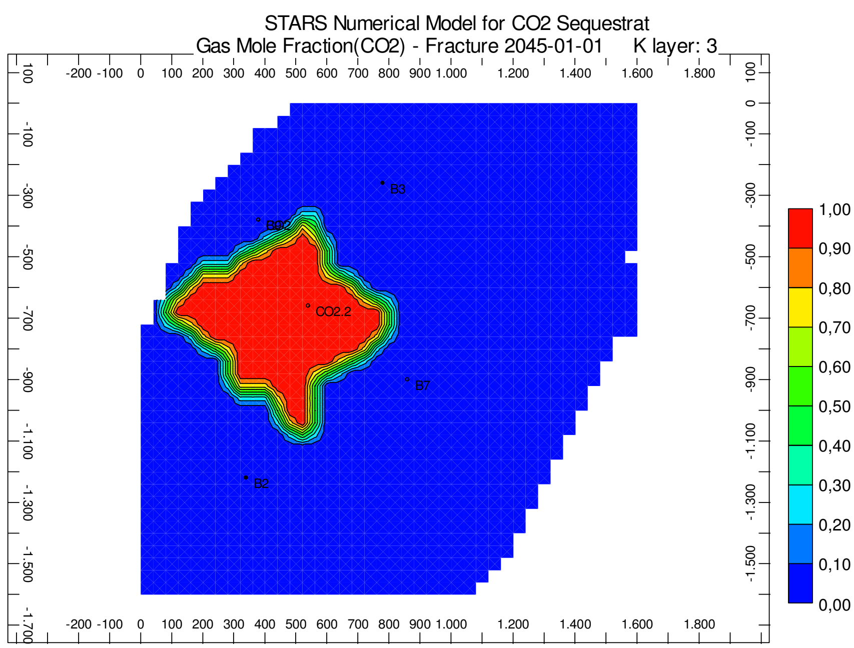

FigureC.2,Gas mole fraction for Frio-like gas oil relative permeability

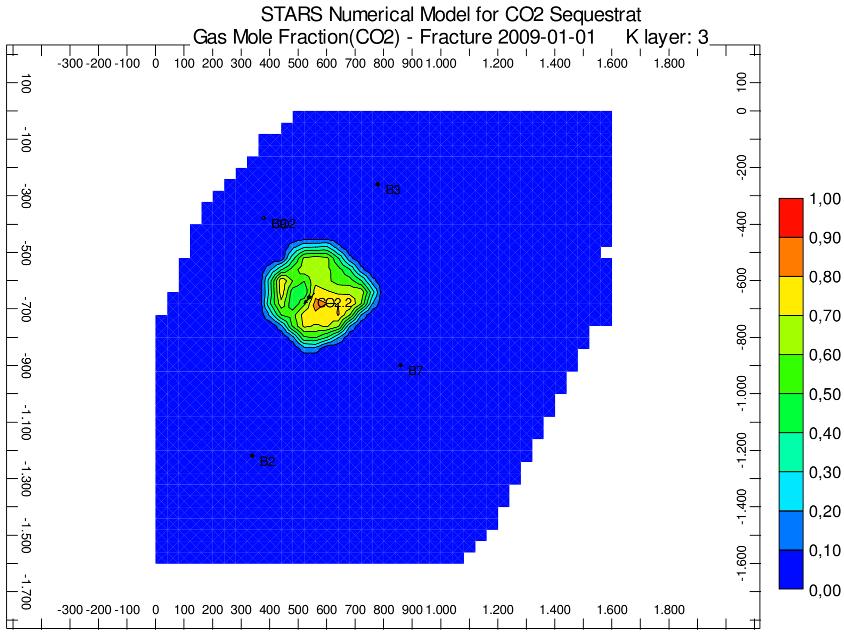

FigureC.3,Gas mole fraction when CO is injected as 10% of the gas stream